

The author(s) shown below used Federal funds provided by the U.S. Department of Justice and prepared the following final report:

**Document Title: Addressing Quality and Quantity: The Role of
DNA Repair and Whole Genome Amplification in
Forensically Relevant Samples**

Author(s): Bruce Budowle

Document No.: 249511

Date Received: December 2015

Award Number: 2010-DN-BX-K227

This report has not been published by the U.S. Department of Justice. To provide better customer service, NCJRS has made this federally funded grant report available electronically.

**Opinions or points of view expressed are those
of the author(s) and do not necessarily reflect
the official position or policies of the U.S.
Department of Justice.**

Federal Agency: Office of Justice Programs, National Institute of Justice, Department of Justice

Federal Grant: Award Number 2010-DN-BX-K227

Project Title: Addressing Quality and Quantity: the Role of DNA Repair and Whole Genome Amplification in Forensically Relevant Samples

Final Report

PI: Bruce Budowle, University of North Texas Health Science Center at Fort Worth, Institute of Applied Genetics, Department of Forensic and Investigative Genetics, Fort Worth, TX 76107
tel: 817-735-2979; email: bruce.budowle@unthsc.edu

Submission Date: May 30, 2013

DUNS Number: 110091808

EIN: 1756064033A1

Recipient Organization: University of North Texas Health Science Center
3500 Camp Bowie Blvd., Fort Worth, TX 76107

Institutional Profile Number: 6108502

Project/Grant Period: 10/01/2010-06/30/2013

Final Progress Report Date: 06/30/2013

Signature: 
Bruce Budowle, Ph.D.

Abstract

Forensic STR analysis is limited by the quality and quantity of DNA. Significant damage or alteration to the molecular structure of DNA by depurination, crosslinking, base modification, and strand breakage can impact typing success. The degree and spectrum of DNA damage depends on the sample source, environmental conditions, and length of exposure time. Previous research on DNA damage (and subsequent repair) has focused on damaging naked cell-line DNA. However, since nuclear DNA in human cells is highly packaged and associated with a variety of other molecules (e.g. histone proteins, phosphoproteins, RNA species), the current study explored methods to damage DNA in its native complexed form. Generation of significantly-damaged samples was challenging and required extensive periods of time and substantial effort to accomplish. The conditions are described so that other researchers may be able to generate sufficiently-damaged DNA for repair studies. The PreCR™ Repair Mix (New England BioLabs) was used to attempt to repair damaged template DNA prior to its use in PCR. Repair was performed on DNA from environmentally-damaged bloodstains, human skeletal remains, and bleach-damaged whole blood. Although the PreCR™ Repair protocol improved the performance of STR profiling of bleach-damaged DNA (and to a lesser extent environmentally-damaged DNA), the results were quite varied and unreliable. A modified PreCR™ protocol outperformed the manufacturer-recommended approach, but still with inconsistent results and only nominal increases in allele peak heights. For bone samples DNA repair showed no improvements, presumably due to the multiple complex lesions that may exist in such samples. Given that forensic samples may be damaged by multiple mechanisms and the quantity available for testing often is limited, the use of PreCR™ should not be considered due to its variable and unpredictable results. As an alternative to repair, whole genome amplification (WGA) was pursued. The DOP-PCR method was selected for WGA because of initial primer design and greater efficacy for amplifying degraded samples. The original DOP-PCR primer was modified by removing the unnecessary restriction site and reducing the required bases on the 3' end of the primer. These modifications allowed for an overall more robust amplification of shorter fragments from damaged samples, contemporary skeletal samples, and even Civil War era bone compared with that obtained by standard DNA typing and a previously described DOP-PCR method. Stochastic artifacts and contamination of DOP-PCR treated samples were nominal and consistent with other LCN typing practices. These new DOP-PCR primers show promise for WGA of degraded DNA.

Table of Contents

	Page
Abstract.....	2
Table of Contents.....	3
Executive Summary.....	5
I. Introduction	
Types of DNA damage.....	10
DNA Repair.....	14
Whole genome amplification (WGA).....	15
Project goals.....	17
II. Materials and Methods	
Generation of damaged/compromised samples.....	18
<i>Oxidative Damage to DNA in Whole Human Blood via Fenton Reaction and Treatment with Potassium Permanganate (KMnO₄).....</i>	18
<i>Depurination of DNA in Human Blood Samples.....</i>	18
<i>Oxidative Damage via Peroxide-based Stain Remover.....</i>	19
<i>DNA Damage in Human Bloodstains via Environmental Exposure.....</i>	19
<i>Oxidative Damage to DNA in Human Blood via Bleach Exposure.....</i>	21
Human Skeletal Remains.....	21
<i>External sanding and surface decontamination of bones.....</i>	21
<i>DNA Extraction Methods for Bones and Teeth.....</i>	22
<i>Amicon® Ultra-4/MinElute® Extraction.....</i>	22
<i>Hi-Flow® Silica Column Extraction.....</i>	22
<i>Phenol-chloroform (Organic) Extraction.....</i>	22
DNA Quantification.....	23
PCR Amplification of Autosomal DNA.....	23

PCR Amplification of Y-chromosome DNA.....	23
DNA detection, separation, and analysis.....	23
DNA Repair with PreCR™ Repair Mix.....	24
Degenerate Oligonucleotide-primed PCR (DOP-PCR).....	25
<i>Primer degeneracy</i>	25
<i>Traditional (original) DOP-PCR amplification</i>	26
<i>dcDOP-PCR amplification</i>	27
III. Results and Discussion	
Generation of damaged/compromised samples.....	28
Human skeletal remains.....	38
PreCR™ repair of compromised samples.....	39
DNA Repair: Implications for forensic casework.....	47
Degenerate oligonucleotide-primed PCR	
<i>Optimization with high-quality DNA</i>	47
<i>Modified DOP-PCR with compromised samples</i>	50
DOP-PCR: Implications for forensic casework.....	77
IV. Conclusions	77
V. References	79
VI. Dissemination of Research Findings	84
VII. Participating Scientists and Project Collaborations	85

Executive Summary

Forensic STR analysis is limited by the quality and quantity of DNA extracted from biological samples. Significant damage or alteration to the molecular structure of DNA by depurination, crosslinking, base modification, and strand breakage can impact typing success. The robustness and reliability of DNA analysis is directly related to the quantity and quality of the template available for testing. Methods are needed that can increase the number of viable template molecules for DNA typing of challenged samples.

The degree and spectrum of DNA damage depends on the sample source, environmental conditions, and length of exposure time. Two approaches were considered to address damaged DNA: 1) Repair damaged DNA and 2) Amplify the limited remaining intact (non-damaged) DNA such that sufficient target DNA is available for STR typing. This project explored protocols to degrade or damage DNA in its native complexed state; determined the best method(s) for generating a pool of compromised samples that would approximate the types of damage encountered in forensic casework samples; evaluated the efficacy of *in vitro* DNA repair and whole genome amplification (WGA) with these intentionally-damaged forensically-relevant samples, as well as with some Civil War era bone samples; compared the effectiveness of *in vitro* DNA repair to WGA, and determined which method would be more successful for improving STR typing results with degraded and/or low-copy (LCN) templates; and sought to identify novel artifacts produced with these methods (e.g. stutter products, allele drop-in, off-ladder alleles, incomplete adenylation), and determine if their presence impacts the ability to interpret resultant STR profiles any differently than encountered with current DNA typing methodology.

The extensive spectrum of DNA damage and the nearly limitless combinations of lesions that can be present in any particular sample pose a unique challenge for forensic analyses. Mechanisms for generating DNA damage were studied. Previous research on DNA damage (and subsequent repair) generally has focused on damaging naked DNA. However, nuclear DNA in human cells is highly packaged and is associated with a variety of other molecules, such as histone proteins, residual proteins, phosphoproteins, RNA species, and lipids. When complexed with these other compounds, DNA is more resilient to the effects of environmental insults. Hence, the manner or degree in which damage occurs to DNA in its native complexed form is likely quite different than in its “naked” counterpart. Aside from the inherent limitations of repair investigations on naked cell-line moieties that arise and are stored in a controlled environment, previous studies often have involved inducing and repairing only a single type of lesion at a time in DNA. Authentic forensic samples, in contrast, likely contain a number of different lesions. Therefore studies were undertaken first to damage DNA in its native complexed form. Single lesions or multiple lesions (the latter more likely to approximate real casework) were generated via the Fenton reaction, treatment with potassium permanganate (KMnO₄), acid/heat treatment, peroxide-based laundry stain remover, bleach immersion, and environmental exposure.

Generation of significantly-damaged samples was challenging and required extensive periods of time and substantial effort to accomplish. For each of the methods employed in this study to degrade DNA, noticeable decreases in RFU peak heights and/or allele dropout (compared to non-damaged controls) were used as rough indicators that damage had occurred. The conditions are described so that other researchers may be able to generate sufficiently-damaged DNA for repair studies. The impact of repair was determined primarily by STR typing success and allele peak height.

After identifying methods that were successful in causing damage to DNA in its native state, repair protocols were investigated to assess their ability to improve obtaining STR profiles from degraded or LCN samples. The PreCR™ Repair Mix (New England BioLabs) was used to attempt to repair damaged template DNA prior to its use in PCR. Research studies by the manufacturer suggested that this enzyme cocktail can repair a broad range of DNA damages/lesions, including those that block or inhibit PCR (e.g. apurinic/apyrimidinic sites, thymine dimers, nicks and gaps) and those that are mutagenic (e.g. deaminated cytosine and 8-oxo-guanine). The PreCR™ Repair Mix also is capable of removing a variety of moieties from the 3' end of DNA leaving a hydroxyl group. In addition, the PreCR™ kit contains bovine serum albumin (BSA), a reagent known to mitigate the effects of several PCR inhibitors. Repair treatment was performed on DNA from environmentally-damaged bloodstains, human skeletal remains, and bleach-damaged whole blood. The PreCR™ Repair protocol did show a trend of improvement of the performance of STR profiling of bleach-damaged DNA (and to a lesser extent environmentally-damaged DNA), although the results were quite varied and unreliable, as well as not significantly different. Bleach [sodium hypochlorite (NaOCl)] primarily generates oxidative damage in DNA. Hence, successful repair of this type of lesion was consistent with previous studies involving repair of a singular, sequestered damage. A modified PreCR™ protocol outperformed the manufacturer-recommended approach for bleach-damaged samples, but still with inconsistent results and only nominal increases in allele peak heights. For environmentally-damaged DNA in bloodstains and bone, the utility of DNA repair was not practical. Lack of successful repair in these types of samples presumably is due to the multiple complex lesions present in such samples and the DNA repair enzyme cocktail's inability to sufficiently overcome those lesions. The PreCR™ Repair Mix does have limitations. It does not repair 8-oxo-7,8-dihydro-2'deoxyadenosines or fragmented DNA (double-strand breaks), nor does it fix DNA-DNA or DNA-protein crosslinks. Additionally, although the ligase present in the mix is very effective at sealing nicks in DNA, it does not successfully ligate blunt ends or nicks near a mismatch.

Results to date indicate that the PreCR™ Repair assay holds some promise for improving STR typing of bleach-damaged DNA, although further studies are needed before its implementation into forensic casework could be considered. One important consideration is that UV-crosslinking and bleaching of laboratory workspaces, instruments, and plasticware are currently the standard practices for destroying exogenous/extraneous DNA molecules prior to DNA extraction or PCR amplification. Since the PreCR™ Repair Mix can repair both UV-crosslinked and bleach-damaged DNA, it also may restore exogenous DNA that was intentionally destroyed during standard decontamination procedures. Thus, extra caution will be needed if repair is used. Furthermore, while standard decontamination methods remove naked DNA, such methods may not be sufficient at decontaminating DNA in cells or DNA complexed with cellular materials. Our studies suggest that a fruitful area of practical research may be effective decontamination practices from all source types of DNA (i.e. native DNA).

The repair assay did not significantly improve DNA profiles from environmentally-damaged bloodstains or bone (and in some cases resulted in lower RFU values for STR alleles), leaving its utility with these types of samples in question. Ultimately, the collective results from studies with environmentally-damaged bloodstains and skeletal remains suggest that the complexity and degree of damage dictates the efficacy of repair. Given that forensic samples may be damaged by multiple mechanisms resulting in a variety of lesions, and since the quantity

available for testing often is limited, the use of PreCR™ should not be considered at this time due to its variable and unpredictable results.

Repair protocols focus on restoring fragmented or otherwise degraded DNA, and because of the possibility that repair protocols may not be able to overcome all lesions, alternate approaches are needed to increase template for typing challenged samples. As an alternative to repair, WGA was pursued. Ideally, WGA targets and copies all intact DNA in an unbiased manner to generate more template DNA. WGA methods were first described in the early 1990s, and a variety of approaches have emerged that tout their ability to amplify microgram quantities of genomic DNA from limited sources. Early WGA methods were used primarily on limited clinical specimens for medical diagnostics, genetic testing, and genomic research, and the amounts of template required were generally much higher than used for forensic analyses. The applicability of WGA methods to forensic analyses would be desirable if the amount of required initial template and the length of template fragments can be reduced.

The amplification of low quantities of DNA can be particularly relevant in forensic DNA analyses, where the availability of sufficient quantities of DNA is critical for the success of STR genotyping and other downstream applications. While early WGA technologies were used primarily on limited clinical specimens for medical diagnostics, genetic testing, and genomic research, interest in the applicability of these methods to forensic analyses has increased and WGA continues to be explored as a tool for improving the possibility of obtaining genetic data from degraded samples.

WGA technology can be divided essentially into two categories: multiple displacement amplification (MDA) and methods involving variations of PCR. MDA has been shown to produce complete genomic DNA amplification with low amplification bias. The high fidelity of the ϕ 29 DNA polymerase used in MDA results in accurate genotyping. However, the success of MDA is highly dependent on the starting quantity and quality of DNA template used in the reaction, which limits the applicability of this method with the types of samples typically encountered in forensic casework. The source and quality of DNA must be considered in the choice of WGA methodology to be used. Therefore, DOP-PCR was selected because of initial primer design and greater efficacy for amplifying degraded samples. The defined sequences at both the 5' and 3' ends of the DOP-PCR primer are important for efficient and successful WGA. The original DOP-PCR method is comprised of two separate cycling stages, a low-stringency phase followed by a high-stringency reaction. Initial low-stringency cycles ensure annealing of the 6-bp 3' defined sequence to complementary sites in the genome. The adjacent random hexamer sequence (that contains all possible combinations of dNTPs) then can bind and start the DOP-PCR-based WGA reaction. The 10-bp 5' defined sequence reportedly permits efficient annealing of primers to previously-amplified DNA, allowing a higher annealing temperature to be used in subsequent (high-stringency) PCR cycles.

The original DOP-PCR primer was modified by removing the unnecessary restriction site and reducing the required bases on the 3' end of the primer. Seven different DOP-PCR primers (six modified and the original published primer) and two different variations in DOP-PCR thermal cycling parameters were tested. Initial results demonstrated that the six modified DOP primers outperformed the original/traditional DOP primer in terms of increased RFU levels, recovery of alleles, and number of artifacts observed (data not shown). For this reason, the study proceeded with focus on three of the modified primers (i.e. the best performing with regard to STR typing). These changes to the primer allowed for an overall more robust amplification of shorter fragments from environmentally-damaged human bloodstains, human skeletal remains,

and even Civil War era bone samples over that obtained by standard DNA typing and a previously described DOP-PCR method.

The re-design of DOP-PCR primers was hypothesized to improve typing success of degraded DNA and the data support that prediction. The original primer (and 10N dcDOP primer) contained a restriction site because cloning of fragments was desired in the original study. Thus, the restriction site in itself does not contribute to the amplification success and can be removed. If removed, there is more flexibility in primer design. In addition, the original primer (i.e. 3' end of the primer) design will identify on average a site in the genome approximately every 4000 bases. Thus, the original primer could be effective for relatively intact DNA; however, forensic samples may be degraded and such long fragments may not be available for DOP-PCR. The newly-designed primers are designed to sit on average approximately every 256 bases and thus could amplify shorter fragments.

The WGA methods employed in the studies herein increased the sensitivity of detection of DNA typing. However, as with any samples with low amounts of template DNA that are subjected to increased sensitivity of detection analyses, exaggerated stochastic effects were observed. These effects manifested as heterozygote allele peak height imbalance, allele dropout, and increased stutter. Also, allele drop-in was observed. These properties are inherent in low template or LCN typing assays and are not novel observations. Importantly, though, no new artifacts were observed. Such effects, however, will impact the ability to interpret results and apply reliable statistical assessments. On the positive side, stochastic artifacts and contamination of DOP-PCR treated samples were nominal and consistent with results from other LCN typing practices. These new DOP-PCR primers could be useful for whole genome amplification of degraded DNA. Statistical models that incorporate uncertain events (e.g., peak area/height, drop-in, dropout, stutter etc.) have been proposed to assess the probability of observed results (for example, see 46). Studies to quantify the uncertain events effectively are needed to employ a statistical model.

Ultimately, forensic samples can experience destructive taphonomic conditions, and thus have often endured extensive microbial and environmental insults. Consequently, the DNA in these environmentally-damaged samples frequently contains multiple complex lesions and may be highly fragmented. Previous studies on repairing DNA focused primarily on damaging extracted or naked DNA. We focused on damaging DNA in its native state. This endeavor entailed extensive studies on conditions to damage DNA while it is still complexed with other cellular molecules. Conditions are described in this report on how to damage such DNA and these can serve as a guide for others who desire to study DNA damage and repair.

The PreCR™ Repair Mix appeared to be challenged by myriad states of DNA damage that may be encountered in forensically-relevant samples. Considering that the amount of sample available in forensic cases is often limited, using 10-20µl of this valuable extract for PreCR™ repair seems to be premature for casework applications, given the assay's varied results. However, additional strategies do exist for potentially improving STR profiles of degraded and/or low-copy templates. Our assessment is that the unpredictable and variable results obtained in our PreCR™ DNA repair experiments indicate that it is more prudent to focus on amplifying existing *intact* template in low-copy or degraded samples as opposed to trying to repair damage.

Our findings suggest that WGA by DOP-PCR is a more fruitful avenue for analyzing challenged samples than attempting DNA repair. DNA repair suffers from the enzyme cocktail's inability to comprehensively address the variety of DNA damage or lesions that may be

encountered in forensic samples. In addition, controls do not exist for monitoring that the enzymes are functional. So DNA repair studies may fail because of quality control issues of reagents. We were successful in using a modified DOP-PCR to improve STR profiling of damaged DNA from environmentally-exposed bloodstains and skeletal remains. Rather than a prior recommendation not to exceed 100pg of input DNA because of observed excessive artifacts, our results (using a different primer design) indicated that up to 1ng of template can be added without production of excessive artifacts in the resultant electropherograms (especially when the candidate samples are severely degraded and have previously produced very low signal or partial profiles). Future investigations might involve comparing results obtained from these DOP-PCR studies to a 2008 Cold Spring Harbor protocol (which involves “re-charging” the low-stringency PCR product with additional reagents before proceeding with high-stringency thermal cycling). It has been purported that addition of a newly-prepared master mix of PCR reagents to the low-stringency WGA product is necessary to provide sufficient resources for subsequent high-stringency cycles (i.e. because some of these reagents may have been depleted/exhausted during the first 5 cycles, thereby limiting the amount of product that can be produced in the second phase of DOP-PCR). Large sample studies will be needed to estimate, if feasible, the rates of drop-in, dropout, and increased stutter if a statistical model is to be applied to WGA treated samples.

I. Introduction

Forensic STR analysis is limited by the quality and quantity of DNA extracted from biological samples. Significant damage or alteration to the molecular structure of DNA is problematic because polymerases stall at damaged/altered sites, preventing amplification (and therefore analysis) of target loci. In order to assess potential strategies for improving STR typing of degraded samples, it is necessary to understand the nature and variety of DNA damage, as well as the conditions that cause it. Although the mechanisms of DNA damage can be divided into four major categories (depurination, crosslinking, base alteration, and strand breakage), the molecular chemistry of the resultant nucleic acid modifications is quite complex and the variety of possible lesions in any given sample is almost limitless. Moreover, the degree and spectrum of DNA damage (as well as its rate of incidence) depends largely on the sample source, the environment to which it was exposed, and the length of exposure time.

Types of DNA damage

A major consideration in understanding DNA's susceptibility to damage is to acknowledge the inherent instability of the DNA molecule itself, which is largely due to the fact that an aqueous environment favors the hydrolysis of polynucleotides. This aqueous environment exists naturally within the cell, and also can be derived from moisture in the external environment. Aside from the molecule's propensity to be hydrolyzed in the presence of water, DNA is subject postmortem to enzymatic and chemical damage by endonucleases and free radicals that are naturally produced by the cell (30,33). These free radicals, known as reactive oxygen species (ROS) and reactive nitrogen species (RNS), are chemical intermediates generated during the course of a cell's normal metabolic activity (i.e. they are a consequence of aerobic metabolism, in which inhaled oxygen is converted to highly reactive intermediates). *In vivo*, the harmful effects of these highly reactive intermediates are mitigated by enzymatic pathways (e.g. superoxidase dismutase, catalase) and by nonenzymatic mechanisms involving antioxidants. However, when a cell dies, these free radicals immediately attack biomolecules such as DNA and can induce significant damage (31,32).

In addition to postmortem damage caused by endogenous enzymes and free radicals, DNA is prone to depurination (and to a lesser extent depyrimidination) when exposed to high temperatures and acidic pH levels. Depurination (or depyrimidination) occurs when the glycosidic bond between a 5-carbon sugar (deoxyribose) and a nitrogenous base is hydrolyzed, leading to the formation of an abasic or apurinic (AP) site (Figure 1). The presence of these AP sites results in loss of primary sequence information, and polymerases stall at these regions during PCR (thereby inhibiting amplification of that region of DNA). Additionally, accumulation of AP sites destabilizes the DNA backbone, leading to strand breaks (35).

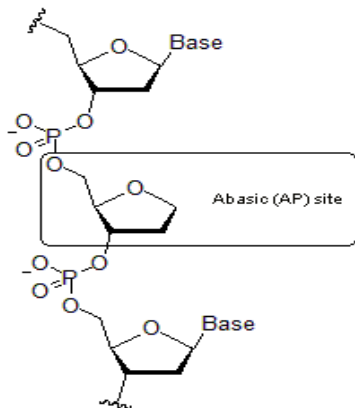


Figure 1: Illustration of an abasic (AP) site, a type of DNA damage caused by cleavage of the glycosidic bond between deoxyribose and the nitrogenous base of a nucleotide. This type of damage occurs when DNA is exposed to high heat/acidic pH conditions. Image modified from (52).

Besides hydrolysis of glycosidic bonds and the subsequent generation of abasic (AP) sites, another type of damage involves cleavage of phosphodiester bonds in the backbone of DNA. The phosphodiester bond is a covalent linkage between the phosphate of one nucleotide and the hydroxyl (–OH) group attached to the 3' carbon of deoxyribose in another nucleotide, forming what is known as the “sugar-phosphate” backbone of DNA. Hydrolysis of phosphodiester bonds results in DNA strand breaks, which can be present only on one strand [single-strand breaks (SSBs)] or adjacently on both strands [double-strand breaks (DSBs)] (Figure 2). These strand breaks can be caused by a variety of factors, including UV radiation, oxygen radicals (ROS), excessive heat, alkylating agents, environmental chemicals, and postmortem endonuclease activity (30,36). DNA in ancient and forensic samples is often highly fragmented, and this fragmentation significantly hinders the success of PCR amplification and restricts the size (length) of target loci that can be examined. For successful amplification to occur, both the target region and its associated primer-binding sites must be intact (2,38).

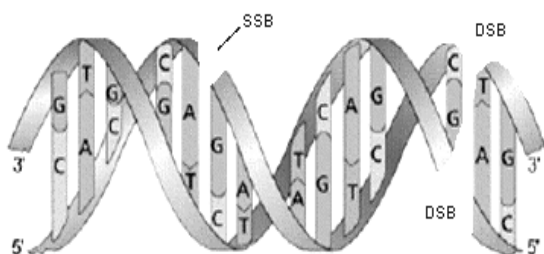


Figure 2: Fragmentation occurs when the phosphodiester bonds are broken in the sugar-phosphate backbone of DNA, resulting in a single-strand break (SSB) or a double-strand break (DSB), as shown in this diagram. Strand breaks are caused by a variety of factors and inhibit successful PCR amplification. Image modified from (51).

Exposure to solar UV radiation can generate several different types of damage in the DNA molecule. Although ultraviolet radiation consists of UV-A, UV-B, and UV-C rays, the latter is absorbed by the atmosphere and therefore is not likely to cause substantial damage to DNA (1,9). The UV-A and UV-B rays cause indirect and direct DNA damage, respectively. UV-A rays create free radicals that then cause indirect damage to the DNA molecule (e.g. bond hydrolysis, base modifications), while UV-B rays result in crosslinking. Crosslinks are covalent linkages between nucleobases on the same DNA strand (intrastrand crosslinks) or between bases on opposite strands (interstrand crosslinks) (Figure 3), and can also form between DNA and proteins.



Figure 3: Graphical representation of an A) interstrand crosslink and B) intrastrand crosslink, two types of DNA damage that can be induced by exposure to sunlight, formalin/formaldehyde, or environmental alkylating agents. Image modified from (53).

The most common types of intrastrand crosslinks induced by UV radiation are cyclopurimidine dimers (CPDs) (e.g. thymine dimers) and 6-4 photoproducts (Figure 4). Regardless of their

origin, the presence of crosslinks can cause a physical deformation or kink in the double helix. Polymerases stall at intrastrand crosslinks, and interstrand crosslinks are problematic because they inhibit denaturation of the double helix (which is the necessary first step in PCR amplification) (30,33,34). It is important to note that there are other causes of crosslinking besides ultraviolet radiation. Exposure to formalin or formaldehyde (e.g. in the case of medical or museum specimens) also can cause crosslinking, as well as exposure to environmental alkylating agents (which are ubiquitous in nature) (30,36,37).

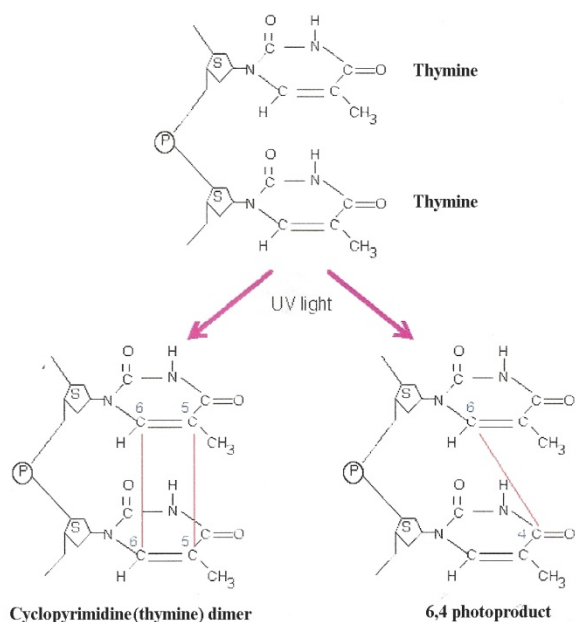


Figure 4: Diagram of the most common forms of intrastrand crosslinks in DNA, induced by exposure to UV radiation (30,43). Image modified from (54).

Finally, in addition to depurination, crosslinking, and strand breakage, there are various mechanisms that can alter or modify DNA nucleobases, including deamination, oxidation, and alkylation. These chemical processes convert standard Watson-Crick nucleobases into modified versions that are unrecognizable by polymerases (thus inhibiting PCR). One of the major types of base modification occurs through a process called deamination, in which the amino group is removed from the base. Some of the most common forms of deaminated bases include conversion of adenine to hypoxanthine, cytosine to uracil, 5-methylcytosine to thymine, and guanine to xanthine (Figure 5) (30,36).

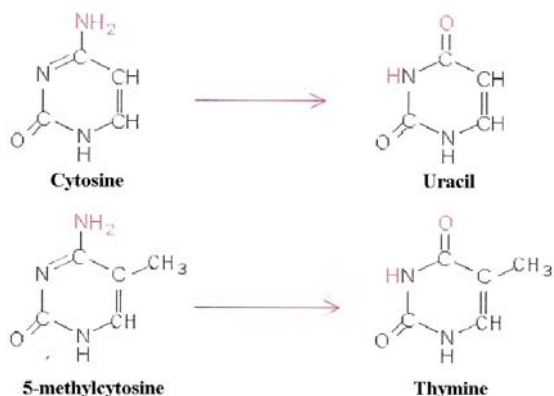


Figure 5: Examples of common base modifications resulting from deamination: conversion of cytosine to uracil (top) and 5-methylcytosine to thymine (bottom). Other examples (not shown) include deamination of adenine to hypoxanthine, and guanine to xanthine. These modified bases are non-coding derivatives that are not recognized by polymerases during PCR. Image modified from (54).

Similar to deamination, oxidative damage can occur to DNA bases, resulting in non-coding derivatives. Generally caused by endogenous ROS, chemicals, or free radicals in the environment, oxidation involves the formation of saturated pyrimidine rings and loss of the double bond between carbons 5 and 6. One of the most common types of oxidative damage in DNA involves conversion of guanine to 8-oxoguanine (Figure 6) (44). Alkylating agents provide another means of base modification, primarily resulting in the attachment of methyl- or other alkyl groups to the N- and O- atoms of DNA bases. These alkylating agents are produced endogenously during cellular metabolism and are ubiquitous in nature (i.e. found in air, water, and food, although generally in small concentrations). Variation exists in alkylation patterns because the exact pattern exhibited depends upon the precise alkylating agent (or agents) involved. Alkylated bases are especially problematic because they are prone to spontaneous depurination and hydrolysis, and secondary damage (e.g. strand breaks, crosslinks) often accompanies the presence of alkylation adducts (30,45).

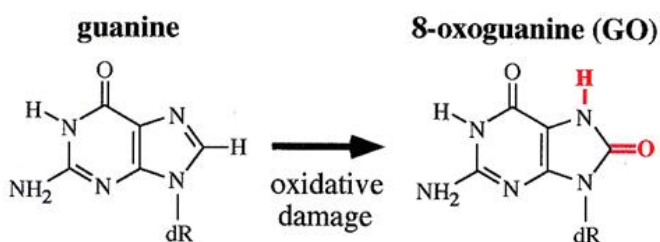


Figure 6: One of the most common modifications to a DNA base via oxidative damage: conversion of guanine to a non-coding 8-oxoguanine derivative. Image modified from (55).

Ultimately, the extensive spectrum of DNA damage and the nearly limitless combinations of lesions that can be present in any particular sample pose a unique challenge for forensic analyses. Table 1 provides a summary of the principal causes/sources of DNA damage and a synopsis of the major types of lesions that occur in forensic and ancient samples. In addition to the challenge of overcoming degradation and low-copy number (LCN), compounds that inhibit PCR amplification can be co-purified with extracted DNA and present further complications for analysis.

Sources of DNA Damage	Types of DNA Damage
"Inherent instability" (aqueous environment) Endogenous cellular enzymes (endonucleases) Excessive heat and humidity Acidic pH levels Exposure to UV light Environmental chemicals Geochemical properties of soil (e.g. humic acids) Microorganism digestion (bacteria, fungi)	Abasic/apurinic (AP) sites (depurination) Single-strand breaks (SSBs) Double-strand breaks (DSBs) Interstrand & Intrastrand crosslinks DNA-protein crosslinks Deaminated bases (e.g. cytosine → uracil) Oxidized bases (e.g. 8-oxoguanine) Alkylated bases

Table 1: Synopsis of the principal sources of DNA damage and major types of DNA lesions.

DNA Repair

Given the prevalence of degradation in forensic and ancient samples, the study of DNA damage and its potential for repair has become an important research topic. Previous research on DNA damage (and subsequent repair) focused on exposing cell-line DNA to a variety of chemical agents in an effort to induce lesions similar to those that might occur in nature. In these studies, cell-line DNA typically is extracted and purified prior to being subjected to conditions in the laboratory that generate damage. In human cells, however, nuclear DNA is not a “naked” molecule. It is a supercoiled structure that is highly “packaged” into chromatin and is always associated with a variety of other molecules (such as histone proteins, residual proteins, phosphoproteins, RNA species, and lipids). Hence, the manner or degree in which damage occurs to DNA in its native complexed form is likely quite different than in its “naked” counterpart. Aside from the inherent limitations of repair investigations on naked cell-line moieties that arise and are stored in a controlled environment, previous studies often have involved inducing and repairing only a single type of lesion at a time in DNA. Authentic forensic samples, in contrast, likely contain a number of different lesions.

There is scant information in the literature on how to effectively damage DNA in a controlled manner when the DNA is complexed with proteins and other materials (i.e. in its native state in a cell). Previous studies on environmental damage to DNA have involved setting blood samples in windowsills or in glass containers that are placed outdoors (1,2). However, these studies have not been very successful in inducing significant DNA damage, which likely is due to several factors. First and foremost, the most common types of glass used in residential and commercial buildings are manufactured with three “architectural” purposes in mind ---- (a) to provide a view, (b) to protect from the outside elements (weather), and (c) to enable visible light transmittance to the interior of the building. According to a 2006 study, clear window glass transmits up to 90% of *visible* light but only allows up to 72% of *ultraviolet* (UV) light to pass through (9). Since UV light is the component of solar radiation that is known to cause DNA damage, the photoprotection afforded by common window glass may explain in part the inability to cause significant damage in bloodstains that are placed behind or underneath such a barrier. Furthermore, when bloodstains are placed in a windowsill behind a glass pane, they are typically only exposed to average room temperatures (18-22°C) and low relative humidity levels (55-65%). However, research has indicated that elevated temperature and humidity increase the degrading effects of UV light on DNA (5).

There are several commercially-available products that have the potential to improve STR typing from degraded or low-copy (LCN) samples. One of the most promising is the PreCR™ Repair Mix (New England BioLabs), an enzyme cocktail formulated to repair damaged template DNA prior to its use in PCR (Table 2).

PreCR™ Repair Enzymes (NEB)
<i>Taq</i> DNA ligase
<i>E.coli</i> Endonuclease IV
<i>Bst</i> DNA Polymerase I
<i>E.coli</i> Fpg (formamidopyrimidine [fapy]-DNA glycosylase)
<i>E.coli</i> Uracil-DNA Glycosylase (UDG)
T4 PDG (T4 Endonuclease V)
<i>E.coli</i> Endonuclease VIII

Table 2: List of the seven DNA repair enzymes contained in New England BioLabs’ PreCR™ Repair Mix.

Research studies by the manufacturer have suggested that this enzyme cocktail can repair a broad range of DNA damages/lesions, including those that block or inhibit PCR (e.g. apurinic/aprimidinic sites, thymine dimers, nicks and gaps) and those that are mutagenic (e.g. deaminated cytosine and 8-oxo-guanine). The PreCR™ Repair Mix also is capable of removing a variety of moieties from the 3' end of DNA leaving a hydroxyl group. In addition, the PreCR™ kit contains bovine serum albumin (BSA), a reagent known to mitigate the effects of several PCR inhibitors. However, despite these extensive repair capabilities, the PreCR™ Repair Mix does have limitations. It does not repair 8-oxo-7,8-dihydro-2'-deoxyadenosines or fragmented DNA. In fact, the ligase present in the mix is very effective at sealing nicks in DNA but does not successfully ligate blunt ends or nicks near a mismatch (28). A few recent studies have evaluated the ability of PreCR™ to repair isolated lesions in DNA (2,4). Although these research findings demonstrated that UV-crosslinks, AP sites, and oxidized bases could effectively be repaired with PreCR™, the samples used in both studies were artificially damaged under controlled conditions in a laboratory. Hence, the utility of the PreCR™ Repair Mix with authentic forensic samples that have been damaged by a variety of environmental insults needs to be further investigated.

Whole Genome Amplification (WGA)

Repair protocols focus on restoring fragmented or otherwise degraded DNA, and because of the possibility that repair protocols may not be able to overcome all lesions, alternate approaches are needed to increase typing capabilities on damaged DNA. Whole genome amplification (WGA) may target and copy any remaining undamaged/intact DNA in a sample. WGA methods were first described in the early 1990s, and a variety of approaches have emerged that tout their ability to amplify microgram quantities of genomic DNA from limited sources (12-14). This amplification of low quantities of DNA is particularly important in forensic DNA analyses, where the availability of sufficient quantities of DNA is critical for the success of STR genotyping and other downstream applications. While early WGA technologies were used primarily on limited clinical specimens for medical diagnostics, genetic testing, and genomic research, interest in the applicability of these methods to forensic analyses has increased and WGA continues to be explored as a tool for improving the possibility of obtaining genetic data from degraded samples.

WGA technology can be divided essentially into two categories: multiple displacement amplification (MDA) and methods involving variations of the PCR (17). MDA has been shown in numerous studies to produce complete genomic DNA amplification with low amplification bias. The high fidelity of the ϕ 29 DNA polymerase used in MDA results in accurate genotyping (14-16). However, the success of MDA is highly dependent on the starting quantity and quality of DNA template used in the reaction, which limits the applicability of this method with the types of samples typically encountered in forensic casework. Established MDA protocols and commercially-available MDA kits (GenomePlex®, GenomiPhi®) recommend input quantities of DNA in the 10-100ng range, and although these reactions are tolerant to mild-to-moderate DNA degradation, the presence of moderate-to-severe degradation significantly affects MDA efficiency. In contrast, PCR-based WGA methods are affected less by DNA quantity or quality, and thus hold more potential as a tool for working with Low copy number (LCN) and degraded templates (12,13,18,19).

Ultimately, the source and quality of sample from which DNA is extracted must be considered in the choice of WGA methodology to be used. Since MDA requires high-quality, high-molecular-weight DNA (usually >2kb) to be successful, it is not a suitable approach to use with forensically relevant samples. Instead, the goal of this project is to evaluate the efficacy of two widely-used PCR-based WGA methods, either degenerate-oligonucleotide-primed PCR (DOP-PCR) or improved primer-extension pre-amplification PCR (iPEP-PCR). These PCR-based WGA methods provide the advantage of efficiently amplifying very short DNA templates and offer the possibility of generating microgram quantities of genome-representative DNA from picogram or nanogram amounts of starting material (17, 20). Thus, PCR-based WGA methods are preferred over MDA for forensic applications. WGA by degenerate-oligonucleotide-primed PCR (DOP-PCR) was selected for further study because of the initial primer design.

DOP-PCR was described first in 1992 as a method that provides complete genome coverage in a single reaction (12). In contrast to the pairs of target-specific primers used in traditional PCR, only a single primer is used in DOP-PCR. The original DOP-PCR primer (5'-CCGACTCGAGNNNNNNATGTGG-3') has defined sequences at both the 5' and 3' ends, with a random hexamer sequence between them. The 10-bp defined sequence at the 5' end of the oligonucleotide contains a 6-bp *XhoI* restriction site that was originally incorporated for use in downstream cloning experiments.

According to Telenius et al. (12), the defined sequences at both the 5' and 3' ends of the DOP-PCR primer are important for efficient and successful WGA (12). The original DOP-PCR method is comprised of two separate cycling stages, a low-stringency followed by a high-stringency reaction. Initial low-stringency cycles ensure annealing of the 6-bp 3' defined sequence to approximately 10^6 complementary sites in the human genome. The adjacent random hexamer sequence (that contains all possible combinations of dNTPs) can bind and start the DOP-PCR-based WGA reaction. The 10-bp 5' defined sequence reportedly permits efficient annealing of primers to previously-amplified DNA, allowing a higher annealing temperature to be used in subsequent (high-stringency) PCR cycles.

A 2009 study investigated the effects of increasing the degeneracy of the original (6N) DOP-PCR primer to 10N and 16N, by removing the first 4 bp of the 5' defined sequence (leaving only the *XhoI* restriction site) and by completely removing the 10-bp 5' defined sequence, respectively (23). Results demonstrated that both the 10N and 16N primers outperformed the original 6N primer in terms of improving the quality of STR profiles obtained from low-copy and degraded samples. However, given the previous assertion that the 5' defined sequence is crucial for efficient annealing of the primer to low-stringency DOP-PCR WGA products --- and because downstream cloning experiments are not a typical part of processing forensic casework samples --- a major goal of the current project is to assess the efficacy of four modified versions of the original DOP-PCR primer that retain at least a portion of the 5' defined sequence and alter the number of bases on the 3' end.

Project Goals

- Explore a variety of protocols that degrade or damage native DNA, and determine the best method(s) for generating a pool of compromised samples that realistically emulate those encountered in forensic casework
- Evaluate the efficacy of *in vitro* DNA repair and whole genome amplification (WGA) with forensically-relevant samples
- Compare the effectiveness of *in vitro* DNA repair to WGA, and determine which method is more valuable to the forensic community for improving STR typing results with degraded and/or low-copy (LCN) templates
- Identify/develop optimal *in vitro* DNA repair and/or WGA approaches for use with degraded and LCN samples
- Monitor artifacts produced during these methods (e.g. stutter products, allele drop-in, off-ladder alleles, incomplete adenylation), and assess how their presence impacts the ability to interpret resultant STR profiles accurately

II. Materials and Methods

Generation of Damaged/Compromised Samples

Oxidative Damage to DNA in Whole Human Blood via Fenton Reaction and Treatment with Potassium Permanganate (KMnO₄)

In the initial Fenton reaction protocol, a 100 μ l working solution of Fe-EDTA (9mM-18mM) was made by diluting 0.5M EDTA and 0.37M iron chloride (FeCl₃) in molecular grade H₂O. 1 ml of 30mM hydrogen peroxide (H₂O₂) was prepared on ice by adding 3.4 μ l of 30% H₂O₂ (~8.8M) stock to 1ml of molecular grade H₂O. 18 μ l of molecular grade water and 5 μ l Fe-EDTA (9mM-18mM) were added to sterile microcentrifuge tubes, followed by the addition of 3 μ l of whole human blood (collected via fingerstick with BD Microtainer contact-activated lancets). The 30mM H₂O₂ solution (4 μ l) was added last to start the Fenton reaction, for a total reaction volume of 30 μ l.

In the second round of Fenton reaction experiments, the concentrations of the Fe-EDTA and H₂O₂ solutions were increased five-fold to 45mM-90mM and 150mM, respectively. 18 μ l of molecular grade water and 5 μ l Fe-EDTA (45mM-90mM) were added to sterile microcentrifuge tubes, followed by the addition of 3 μ l of whole human blood (collected via fingerstick with BD Microtainer contact-activated lancets). The 150mM H₂O₂ solution (4 μ l) was added last to start the Fenton reaction, for a total reaction volume of 30 μ l.

For the potassium permanganate trials, a 100mM KMnO₄ solution was prepared and stored in the dark. 27 μ l of the 100mM KMnO₄ solution and 3 μ l of whole human blood were added to sterile microcentrifuge tubes and vortexed to thoroughly mix the blood with the damaging agent. A more concentrated KMnO₄ solution (500mM) was prepared for additional experimentation using the same 30 μ l total reaction volume (27 μ l of 500mM KMnO₄ and 3 μ l of whole human blood).

All samples were incubated on a heat block at 37°C for various time intervals (60 minutes, 120 minutes, 6 hours, 12 hours, 24 hours, and 48 hours). After each respective exposure period, DNA extractions were carried out using the QIAamp DNA Investigator Kit (Qiagen Cat.#56504).

Depurination of DNA in Human Blood Samples

Depurination buffer (10X) was prepared by combining 0.2ml of 5M sodium chloride, 0.1ml of 1M sodium phosphate, 0.2ml of 0.5M sodium citrate, and 9.5ml of ddH₂O (total volume = 10ml). The pH of the buffer solution was adjusted to 4.8 with hydrochloric acid (HCl). A portion of the 10X stock was diluted to generate a 1X solution. Depurination experiments were conducted both on liquid blood samples and with dried bloodstains.

To depurinate DNA in liquid blood, 47 μ l of each buffer solution were added to sterile microcentrifuge tubes. 3 μ l of whole blood (collected with BD Microtainer contact-activated lancets) were pipetted directly from the donor's finger into tubes containing the respective depurination buffer solutions. The tubes were capped, vortexed, and incubated at 70°C on a VWR digital heatblock for 48 hours, 96 hours, and 120 hours.

For depurination of DNA in dried bloodstains, 3 μ l of whole blood (obtained via fingerstick) were pipetted onto sterile glass microscope slides and allowed to dry in a hood. After drying, 47 μ l of each of the depurination buffer solutions (10X and 1X) were pipetted

directly onto the dried bloodstains. The microscope slides were placed in an incubator at 70°C for 48 hours, 96 hours, and 120 hours. The total reaction volume for both experiments was 50µl. Post-incubation, each sample was extracted using the QIAamp DNA Investigator Kit (Qiagen Cat.#56504).

Oxidative Damage via Peroxide-based Stain Remover

To simulate the manner that this product might be used in a washing machine to eliminate bloodstains from clothing or bedding, two protocols were developed. In the first protocol, 5µl of whole blood were added to 45µl of a 10% OxiClean® solution (50µl total reaction volume) in a microcentrifuge tube and mixed thoroughly. Samples were incubated at room temperature for 30-minute and 60-minute intervals, with periodic vortexing every five minutes. Positive controls consisted of 5µl of whole blood in 45µl of molecular grade ddH₂O (rather than OxiClean®). The second protocol was performed under the same conditions, except at 56°C instead of room temperature (i.e. to simulate the hot water cycle in a washing machine). DNA extractions were performed with the QIAamp DNA Investigator Kit (Qiagen Cat.#56504).

DNA Damage in Human Bloodstains via Environmental Exposure

Four acrylic boxes were constructed to simulate conditions under which DNA degradation would occur at a crime scene. In an effort to differentiate between covered/shaded samples and those that are exposed to sunlight, two different experimental setups were designed. Two boxes were built with black opaque acrylic that blocks UV light, but allows the samples to be exposed to environmental heat and humidity (Figure 7). Another two boxes were constructed of Acrylite® OP-4 acrylic to permit maximum UV light transmission (Figure 8). Acrylite® OP-4 acrylic (Evonik Cyro LLC, Parsippany, NJ) was originally designed for use on indoor sun tanning equipment and in terrariums (6). It offers high levels of UV light transmission and strong resistance to degradation caused by UV light (due to the constituent thermal stabilizers that are introduced during the casting process). The ability of a sheet of Acrylite® OP-4 to resist long-term UV light degradation without loss of physical properties is important in applications such as indoor tanning. If a tanning bed is to produce reliable and rapid tanning results, the acrylic sheet covering the bulbs must maintain consistently high levels of light transmission in the UV-A and UV-B regions during the life of the material. The same rationale was the basis of use of this acrylic for inducing environmental UV damage in dried bloodstains over time.



Figure 7: Black, opaque acrylic box for environmental damage to human bloodstains. Blocks UV light transmission, but ventilation holes allow exposure to heat and humidity. An internal tray that holds the samples is shown here (top) prior to being inserted into the box.

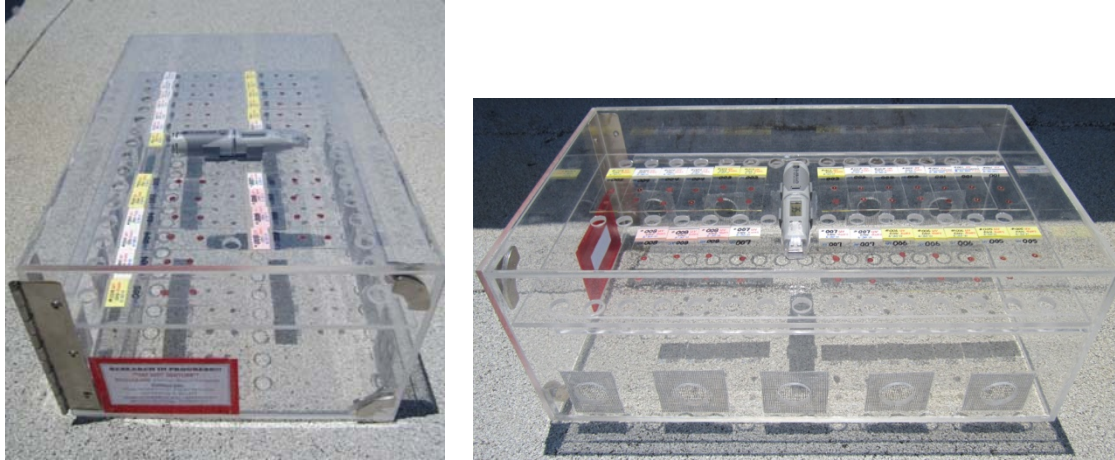


Figure 8: Front and side view of Acrylite® OP-4 acrylic box (maximum UV light transmission). One-inch ventilation holes along the perimeter of the box allow the blood samples to be exposed to variations in heat and humidity. Ventilation holes were covered with rust-resistant, metal screening in an effort to deter insect/animal activity.

Blood samples from 25 different individuals were collected via fingerstick using BD Microtainer contact-activated lancets (1.8mm x 21G). 5 μ l of whole blood were pipetted (in duplicate) directly from the donor's finger onto sterile glass microscope slides. Six slides (each with duplicate spots of blood) were prepared for each individual and placed on the rooftop of the University of North Texas biology building for five different exposure periods (2-weeks, 4-weeks, 8-weeks, 16-weeks, and 24-weeks). Positive controls for each exposure period consisted of spotting the same volume of whole blood (5 μ l) onto sterile microscope slides and storing at room temperature in the laboratory in a dead-air hood.

A total of 300 bloodstains was subjected to environmental exposure/insult. During the various environmental exposure periods, EL-USB-2-LCD data loggers (Lascar Electronics, Erie, PA; Figure 9) were used to collect temperature and humidity readings. These stand-alone USB data loggers collect and store 16,000+ relative humidity (RH) and temperature readings over the 0-100% RH and -35°C to +80°C (-31 to 176°F) measurement ranges at pre-set time intervals. After completion of each of the designated exposure periods, the blood samples were retrieved from the roof, along with the data logger. Sterile cotton swabs were used to collect the entire 5 μ l bloodstain from each microscope slide, and DNA extractions were performed using the QIAamp DNA Investigator Kit (Qiagen Inc., Valencia, CA, Cat.#56504). Data recorded by the EL-USB-2-LCD data loggers were downloaded onto a laboratory computer for analysis, and the data loggers then were returned to the rooftop to collect temperature and humidity readings for the remaining exposure periods.



Figure 9: EL-USB-2-LCD Humidity, Temperature, and Dew Point Data Logger (Lascar Electronics).
*Not shown: plastic cover/cap for moisture protection.

Oxidative Damage to DNA in Human Blood via Bleach Exposure

Bleach-damage protocols were conducted with both liquid (non-coagulated) and coagulated whole human blood samples. Blood was collected via fingerstick using BD Microtainer contact-activated lancets (1.8mm x 21G). Household bleach [6% sodium hypochlorite (NaOCl)] was diluted to produce 10% Clorox® (0.6% NaOCl) and 50% Clorox® (3% NaOCl) solutions.

For experiments with liquid (non-coagulated) blood, 45µl of each of the respective bleach solutions (10% and 50%) were added to sterile microcentrifuge tubes, and 5µl of blood were pipetted directly from the donor's finger into the tubes (for a total reaction volume of 50µl). After vortexing, the samples were incubated at room temperature for 1-hour and 2-hour time intervals.

To investigate the effects of bleach on coagulated blood, 5µl of liquid blood (collected via fingerstick) were pipetted into sterile microcentrifuge tubes and allowed to dry. When coagulation was complete, 45µl of bleach solution (either 10% or 50% Clorox®) were added. The tubes were vortexed to mechanically resolubilize the blood clot, and the samples then were allowed to sit at room temperature for 1-2 hours. After completion of the incubation period, DNA extractions were performed using the QIAamp DNA Investigator Kit (Qiagen Cat.# 56504).

Human Skeletal Remains

DNA extractions were completed on 80 contemporary bone samples from 20 different individuals using two different extraction methods. Four bone powder fractions (0.5g each) from each individual were extracted, two fractions using the Hi-Flow® (Generon) protocol and two via the Amicon® Ultra-4/MinElute® method. Bone powder aliquots used for each extraction method were alternated to eliminate sample bias. In addition to contemporary bones, samples from the 120-year-old skeletal remains of an exhumed Civil War soldier were included as potential candidate samples for DNA repair and whole genome amplification (WGA) assays. These historical remains, obtained from Mercyhurst Archaeological Institute, were a partial skeleton consisting of a femur, both tibiae, and four teeth (2 canines, 1 lateral incisor, 1 premolar).

External sanding and surface decontamination of bones

Prior to extraction, the external surfaces of all bones and teeth were sanded with a Dremel® 4000 High Performance Rotary Tool and individually-sterilized grinding stones. Surface-sanding was conducted under a laminar flow hood in a designated low-copy area of the laboratory. After sanding, the diaphyses of femora and tibiae were sectioned using a Stryker® autopsy saw and individually-sterilized Stryker® sectioning blades. Each resultant bone section was placed in a sterile 50ml polypropylene conical tube. Further surface decontamination procedures were performed on individual bone sections and teeth to remove any remaining exogenous or contaminant DNA. Each bone fragment or tooth was immersed in 50% commercial bleach (3% NaOCl) for 15 minutes, followed by 4-5 washes with molecular grade (nuclease-free) H₂O and brief immersion in 95% ETOH. After the final ETOH rinse, conical tubes containing individual teeth or bone sections were placed in a hood overnight (with lids off) to dry.

Each individual bone or tooth then was placed (along with a stainless steel impactor) in a sterile polycarbonate sample vial flanked by two stainless steel endcaps. Sample vials were submerged in the liquid nitrogen chamber of a SPEX SamplePrep 6750 Freezer Mill® and ground into a fine powder using the following parameters: 10-minute pre-chill, 5-minute grind time, 15-impacts-per-second. Post-grinding, bone powder from each sample was transferred to sterile 15ml polypropylene conical tubes in 0.5-gram aliquots in preparation for DNA extraction.

DNA Extraction Methods for Bones and Teeth

Due to the age and condition of the skeletal remains, several different extraction methods were employed in an effort to maximize DNA recovery. Bone samples were extracted separately in small batches in a designated low-copy area of the laboratory.

Amicon® Ultra-4/MinElute® Extraction

Demineralization was carried out by mixing 0.5g of bone powder with 3ml digestion buffer (0.5M EDTA pH 8.0, 0.5% sodium N-lauroylsarcosinate, 100µg/ml proteinase K), followed by incubation in a hybridization oven at 56°C under constant agitation for 24 hours. After demineralization, bone powder was pelleted via centrifugation, and the supernatant was transferred to an Amicon® Ultra-4 centrifugal filter unit (Millipore Corp., Billerica, MA) for volume reduction. After the volume of each sample was reduced to 100µl, the concentrated supernatant was transferred to a sterile 1.5ml microcentrifuge tube. Final cleanup of the supernatant was performed using MinElute® silica columns (Qiagen MinElute® PCR Purification Kit, Cat.#28004, Valencia, CA), with a 100µl final elution volume.

Hi-Flow® Silica Column Extraction

Demineralization was carried out by mixing 0.5g of bone powder with 3ml digestion buffer (0.5M EDTA pH 8.0, 1% sodium N-lauroylsarcosinate, 100 µg/ml proteinase K), followed by incubation in a hybridization oven at 56°C under constant agitation for 24 hours. After demineralization, bone powder was pelleted via centrifugation, and the supernatant was transferred to a sterile microcentrifuge tube and mixed with five volumes of binding buffer (PB buffer, Qiagen Cat.#19066). This mixture was vortexed thoroughly, transferred to a Hi-Flow® DNA Purification Spin Column (Generon, Berkshire, UK), and centrifuged. With the Hi-Flow® silica column, both cleanup and volume reduction were accomplished with a single device, decreasing the chances of contamination. After discarding the flow-through, the column was washed with 15ml PE buffer (Qiagen Cat.#19065), and the DNA bound to the membrane was eluted with 100µl EB buffer (Qiagen Cat.#19086).

Phenol-chloroform (Organic) Extraction

Demineralization was achieved by mixing 0.5g of bone powder with 3ml digestion buffer (0.5M EDTA pH 8.0, 1% sodium N-lauroylsarcosinate) and 200µl of proteinase K (20mg/ml). Samples were incubated at 56°C under constant agitation for 24 hours. After the incubation period, an equal volume of phenol chloroform isoamyl alcohol (25:24:1) was added to the aqueous extract and the mixture was vortexed for approximately 30 seconds. The bone powder was pelleted via brief centrifugation, the resultant supernatant (aqueous layer) was transferred to an Amicon® Ultra-4 centrifugal filter device (Millipore Corp., Billerica, MA), and a subsequent 10-20 minute centrifugation cycle was performed until all of the sample had passed through the filter. 2 ml of molecular grade H₂O were pipetted into the Amicon® and the column

was centrifuged at maximum speed until the volume of supernatant was reduced to 50 μ l. An additional volume of molecular grade H₂O was added to bring the total volume to 100 μ l, and the entire supernatant was transferred to a sterile microcentrifuge tube. The Amicon® Ultra-4 filter was subsequently rinsed with an additional 100 μ l of molecular grade H₂O, and this extract was added to the same microcentrifuge tube. Five volumes of Buffer PB (Qiagen Cat.#19066) were added to 1 volume of the sample extract, vortexed briefly, and 650 μ l of the mixture were transferred to a QIAquick® spin column that had been placed in a 2ml collection tube (Qiagen QIAquick® PCR Purification Kit, Cat.#28106). After centrifuging and discarding the flow-through, repeated additions and centrifugations of the Buffer PB/DNA extract were carried out until all of the Buffer PB/DNA extract mixture had been filtered through the spin column. The columns were washed with 750 μ l of Buffer PE (Qiagen Cat.#19065), the flow-through was again discarded, and the clean QIAquick® column was transferred to a sterile 1.5ml microcentrifuge tube. DNA bound to the column membrane was eluted with 100 μ l of EB buffer (Qiagen Cat.#19086).

DNA Quantification

The quantity of DNA in each extract was determined using the Quantifiler® Human DNA Quantification Kit (Applied Biosystems Cat.#4343895) and an ABI 7500 Real-Time PCR System. The assay was carried out in a 25 μ l total reaction volume (23 μ l Quantifiler® master mix and 2 μ l DNA extract), with final sample concentrations determined via comparison to a standard curve. This kit amplifies a 62-bp intron of the human telomerase reverse transcriptase (hTERT) gene (59).

PCR Amplification of Autosomal DNA (all sample extracts)

Amplification of autosomal DNA was carried out using the AmpF/STR® Identifiler® Plus PCR Amplification Kit (Applied Biosystems, Cat.#4427368). All extracts were amplified using the ABI GeneAmp® 9700 PCR System, with the following PCR parameters: initial incubation at 95°C for 11 minutes; 28 cycles of (94°C for 20 seconds and 59°C for 3 minutes); final extension at 60°C for 10 minutes. Total reaction volume for each sample was 25 μ l (15 μ l PCR master mix and 10 μ l extract/TE, with a target input of 1ng template DNA). Negative and positive controls consisted of 10 μ l low-TE buffer and 10 μ l 9947A Control DNA (0.1ng/ μ l), respectively.

PCR Amplification of Y-chromosome DNA (*Historical bone samples only*)

Amplification of Y-chromosome DNA was carried out using the AmpF/STR® Yfiler® PCR Amplification Kit (Applied Biosystems, Cat.#4359513). Historical bone extracts were amplified using the ABI GeneAmp® 9700 PCR System, with the following PCR parameters: initial incubation at 95°C for 11 minutes; 30 cycles of (94°C for 1 minute, 61°C for 1 minute, and 72°C for 1 minute); final extension at 60°C for 80 minutes. Total reaction volume for each sample was 25 μ l (15 μ l PCR master mix and 10 μ l extract/TE, with an optimal input of 1ng template DNA). Negative and positive controls consisted of 10 μ l low-TE buffer and 10 μ l 007 Male Control DNA (0.1ng/ μ l), respectively.

DNA Separation, Detection, and Analysis

The amplified DNA samples were size-separated and detected on an ABI 3500xl Genetic Analyzer (Applied Biosystems, Foster City, CA) using 1 μ l PCR product, 8.7 μ l of Hi-Di™

Formamide, and 0.3µl of GeneScan™ 600 LIZ® Internal Lane Size Standard. One microliter of AmpF/STR Identifiler® Plus or Yfiler® allelic ladder was included at least once per injection on the 96-well plate. All samples were denatured at 95°C for 5 minutes and then immediately cooled on ice for 5 minutes. Electrophoresis was performed on a 36-cm capillary array with POP-4™ polymer (Applied Biosystems, Cat.#4393715) using standard (default) injection parameters. The collected STR data were sized and typed with GeneMapper® ID-X Software Version 1.2 (Applied Biosystems, Foster City, CA).

DNA Repair with PreCR™ Repair Mix

A total of 415 repair reactions were performed using the PreCR™ Repair Mix (New England BioLabs). Repair reactions were performed only on samples that exhibited evidence of damage upon STR typing (i.e. samples with marked decreases in RFU levels and/or allele dropout compared with no-damage controls). Since inhibition often cannot be distinguished with degradation, internal PCR control (IPC) values were monitored during the quantification step to assess the potential presence of PCR inhibitors in the extracts used for repair reactions. The volume of DNA template and/or molecular grade H₂O was calculated based upon the initial quantification results for each sample after exposure to a damage-inducing protocol. For purposes of performing post-repair STR analysis, care was taken to maintain the same molar ratio of template DNA:Identifiler Plus reaction components as was used in the pre-repair (damaged) STR typing.

Manufacturer Recommended Protocol

After preparation of a master mix from the reagents in the PreCR™ kit (Table 3), 4.68µl of the master mix were combined with 15.32µl of DNA template/molecular grade water (amount dependent upon original quant value), for a total reaction volume of 20µl.

Volume (per sample)	Reagent	Final Concentration
2 µl	10X ThermoPol Buffer	1X
0.08 µl	25mM dNTPs	100µM
0.2 µl	100X NAD+	1X
2 µl	10X BSA	1X
0.4 µl	PreCR™ Repair Mix	

Table 3:
Manufacturer recommended protocol for DNA repair with PreCR™ Repair Mix

The repair reaction was carried out via incubation on a heat block at 37°C for 20 minutes. After incubation, the samples were immediately placed on ice. Ten microliters of the repair reaction product were added to 15µl of Identifiler® Plus Master Mix/Primer Set, and PCR amplification was performed using the ABI GeneAmp® 9700 PCR System with the following PCR parameters: initial incubation at 95°C for 11 minutes; 28 cycles of (94°C for 20 seconds and 59°C for 3 minutes); final extension at 60°C for 10 minutes.

Modified Repair Protocol

In addition to following manufacturer recommendations, a modified PreCR™ protocol was investigated. In the modified version, damaged DNA extract, PreCR™ Repair mix, and

100X NAD⁺ were added directly to the Identifiler® Plus Master Mix. After preparation of the master mix (shown in Table 4), 10.75µl of the master mix were combined with 10µl of DNA template/molecular grade water (amount dependent upon original quant value), for a total reaction volume of 20.75µl. The tubes were vortexed and then incubated at 37°C for 20 minutes. Immediately after the incubation period, 5µl of the Identifiler® Plus primer set were added, and PCR amplification was performed using an ABI GeneAmp® 9700 PCR System with the following PCR parameters: initial incubation at 95°C for 11 minutes; 28 cycles of (94°C for 20 seconds and 59°C for 3 minutes); final extension at 60°C for 10 minutes.

Volume (per sample)	Reagent
0.25µl	100X NAD ⁺
0.5µl	PreCR™ Repair Mix
10µl	Identifiler® Plus Master Mix

Table 4: Modified protocol for DNA repair with PreCR™

Degenerate-oligonucleotide-primed PCR (DOP-PCR)

Primer Degeneracy

Various different primers were investigated for their efficacy in improving STR profiles of degraded and LCN samples. Table 5 describes the degenerate primers used in the DOP-PCR reactions, including the original DOP-PCR primer (6N), two primers from a 2009 study (by Dawson Cruz, VCU), and four newly-modified primers that retain at least a portion of the 5' defined sequence and alter the number of bases on the 3' end.

	Primer Sequence	Primer Description
6N	5'-CCG ACTCGAG NNNNNNNATGTGG-3'	Original DOP-PCR primer (Telenius et al.1992)
10N	5'- CTCGAG NNNNNNNNNNNATGTGG-3'	Modified dcDOP-PCR primer (Dawson Cruz 2009)
16N	5'-NNNNNNNNNNNNNNNNNNATGTGG-3'	Modified dcDOP-PCR primer (Dawson Cruz 2009)
10N	5'-CCGACTNNNNNNNNNNNATGTGG-3'	CT from <i>XhoI</i> restriction site remaining
12N	5'-CCGANNNNNNNNNNNNATGTGG-3'	Complete removal of <i>XhoI</i> restriction site
12N(2)	5'-CCGACTNNNNNNNNNNNNGTGG-3'	CT from <i>XhoI</i> restriction site remaining; Shortened 3' sequence from 6bp to 4bp
14N	5'-CCGANNNNNNNNNNNNNGTGG-3'	Complete removal of <i>XhoI</i> restriction site; Shortened 3' sequence from 6bp to 4bp

Table 5: Primers used for degenerate oligonucleotide-primed PCR (DOP-PCR). The portion of the 5' defined sequence in **bold (CTCGAG)** represents a *XhoI* restriction site for cloning.

Master Mix Preparation

The DOP-PCR master mix was based on the original Roche DOP-PCR Master Kit (Roche Molecular, Mannheim, Germany). Per sample, the master mix used in this study consisted of 10µl of 10X High Fidelity PCR Buffer (Invitrogen), 4.0µl of 50mM MgSO₄, 5.0µl of dNTPs (4mM each), 5.0µl of degenerate primer (40µM), and 0.5µl of Platinum *Taq* High Fidelity DNA Polymerase 5U/µl (Invitrogen) (Table 6). Using sterile filter tips, 24.5µl of master mix were added to each sample tube, and after addition of 1-50µl of degraded or LCN

template, 25.5-74.5 μ l of TE⁻⁴ buffer were added to bring the total reaction volume up to 100 μ l. 5 μ l of 9947A control DNA (0.1ng/ μ l) and 5 μ l of TE⁻⁴ buffer served as positive and negative controls, respectively. A variety of input DNA template amounts, ranging from less than 100 picograms to one nanogram, were explored to determine the minimum and maximum amounts needed for optimal DOP-PCR results.

Master Mix Component	Volume per sample
10X High Fidelity PCR buffer	10 μ l
MgSO ₄ (50mM)	4 μ l
dNTPs (4mM each)	5 μ l
Degenerate primer (40 μ M)	5 μ l
Platinum Taq High Fidelity DNA Polymerase (5U/ μ l)	0.5 μ l
Total volume	24.5 μ l

Table 6: Preparation of master mix for degenerate-oligonucleotide-primed PCR (DOP-PCR)

DOP-PCR Amplification Parameters

In addition to evaluating seven different DOP-PCR primers, a variation in DOP-PCR thermal cycling parameters was investigated. In particular, the efficacy of the original DOP-PCR method was compared to a 2009 Dawson Cruz protocol (which increases the number of low-stringency cycles from five to twelve) (23).

Optimization with High-quality DNA

Prior to use with damaged and low-copy templates, DOP-PCR reactions were carried out with high-quality (non-degraded) cell-line DNA as a proof-of-concept. 100pg and 500pg of both 9947A (female) and 007 (male) control DNA were amplified separately using each of the seven modified degenerate primers.

Traditional (original) DOP-PCR Amplification

Amplification of the 100 μ l reaction mixture was carried using the ABI GeneAmp[®] 9700 PCR System, with the following PCR parameters: initial incubation at 95°C for 5 minutes; 5 cycles of non-specific amplification (94°C for 1 minute, 30°C for 1.5 minutes, and 72°C for 3 minutes) with a 3-minute ramp to 72°C; 35 cycles of specific amplification (94°C for 1 minute, 62°C for 1 minute, and 72°C for 3 minutes) with a 1-second increase in each subsequent cycle; and a final extension at 72°C for 10 minutes (Table 7).

Denaturation	Non-specific amplification (Low-stringency conditions)	Specific amplification (High-stringency conditions)	Final Extension
95°C 5 min	5 cycles: 94°C for 1 min 30°C for 1.5 min (3 min transition from 30°-72°C) 72°C for 3 min	35 cycles: 94°C for 1 min 62°C for 1 min 72°C for 3 min (Increase by 1 sec each cycle)	72°C 10 min

Table 7: Thermal cycling conditions for the original DOP-PCR protocol, as described in 1992 by Telenius et al. (12)

dcDOP-PCR Amplification

Samples (100µl total reaction volume) were amplified with the ABI GeneAmp® 9700 PCR System. After an initial 5-minute denaturation step at 95°C, non-specific amplification consisted of 12 cycles of (94°C for 1 minute, 30°C for 1.5 minutes, and 72°C for 3 minutes) with a 3-minute ramp to 72°C, followed by 35 cycles of specific amplification (94°C for 1 minute, 62°C for 1 minute, and 72°C for 2 minutes) with a 14-second increase in each subsequent cycle, and final extension for 7 minutes at 72°C (Table 8).

	Denaturation	Non-specific amplification (Low-stringency conditions)	Specific amplification (High-stringency conditions)	Final Extension
Dawson Cruz DOP-PCR (dcDOP-PCR)	95°C 5 min	12 cycles: 94°C for 1 min 30°C for 1.5 min (Ramp for 3min to 72°C) 72°C for 3 min	35 cycles: 94°C for 1 min 62°C for 1 min 72°C for 2 min (Increase by 14sec each cycle)	72°C 7 min

Table 8: Thermal cycling parameters for the dcDOP-PCR method, which increases the number of non-specific amplification cycles to twelve (as opposed to the five low-stringency cycles used in original DOP-PCR) (12, 23).

Sample Concentration after DOP-PCR

Following DOP-PCR amplification, all samples were concentrated using Amicon® Ultra-0.5 centrifugal filter units with Ultracel-10 membranes (Millipore, Billerica, MA). After pre-hydrating the membrane of the filter unit with 25µl of molecular grade H₂O, the entire volume of DOP-PCR product (100µl) and an additional 375µl of molecular grade water were added to the Amicon® (500µl maximum filter volume), followed by centrifugation at 14,000 x g for 20 minutes. The filtrate was carefully pipetted off and discarded. Molecular grade H₂O was added back to the filter (up to a total volume of 500µl), and the columns were centrifuged at

14,000 x g for 30 minutes (or until the volume was reduced to 25µl). The Amicon® filters then were inverted in new sterile tubes and centrifuged at 1000 x g to recover the concentrated DOP-PCR product.

Multiplex STR Amplification

Amplification of 16 STR loci was carried out using the AmpF/STR® Identifiler® Plus PCR Amplification Kit (Applied Biosystems, Cat.#4427368). 10µl of the concentrated DOP-PCR product were combined with 15µl of master mix (for a total reaction volume of 25µl). The master mix (per sample) consisted of 10µl of AmpF/STR® Identifiler® Plus Master Mix and 5µl of AmpF/STR® Identifiler® Plus Primer Set. Negative and positive controls were 10µl of TE⁻⁴ buffer and 10µl 9947A Control DNA (0.1ng/µl), respectively. PCR amplification was performed on the ABI GeneAmp® 9700 PCR System, with the following parameters: initial incubation at 95°C for 11 minutes; 28 cycles of (94°C for 20 seconds and 59°C for 3 minutes); final extension at 60°C for 10 minutes.

Post-PCR Purification and CE Analysis

Following STR amplification, the samples were purified using the Qiagen MinElute® Post-PCR Purification Kit (Qiagen Cat.#28004) according to the manufacturer's recommendations. Purified Identifiler® Plus-amplified DOP-PCR products were size-separated and detected on an ABI 3500xl Genetic Analyzer (Applied Biosystems, Foster City, CA) using 1µl PCR product, 8.7µl of Hi-Di™ Formamide, and 0.3µl of GeneScan™ 600 LIZ® Internal Lane Size Standard. 1µl of AmpF/STR Identifiler® Plus allelic ladder was included at least once per injection on the 96-well plate. All samples were denatured at 95°C for 5 minutes and then immediately cooled on ice for 5 minutes. Electrophoresis was performed on a 36-cm capillary array with POP-4™ polymer (Applied Biosystems, Cat.#4393715) using standard (default) injection time (10 seconds). The collected STR data were sized and typed with GeneMapper® ID-X Software Version 1.2 (Applied Biosystems, Foster City, CA).

III. Results and Discussion

Generation of Damaged/Compromised Samples

Many methods that have previously been used on “naked” DNA molecules to simulate *in situ* DNA damage had significantly less effect on native DNA. This was not surprising, given that native DNA is afforded some protection from damage when surrounded by the normal cellular milieu of proteins, lipids, carbohydrates, and other nucleic acids. For each of the methods employed in this study to degrade DNA, noticeable decreases in RFU peak heights and/or allele dropout (compared to non-damaged controls) were used as rough indicators that damage had occurred. It should be noted, though, that generation of significantly damaged samples was much more challenging than anticipated and required extensive periods of time and substantial effort to accomplish. However, this aspect was imperative to the principal goals of our study (i.e. to assess the efficacy of DNA repair and WGA on samples that realistically emulate those encountered in forensic casework).

Results of each of the respective damaging protocols are shown below. Based on these findings, the pool of degraded samples used for DNA repair and WGA studies were narrowed to three sample types: environmentally-damaged bloodstains, human skeletal remains, and bleach-damaged whole blood.

Oxidative Damage to DNA in Whole Human Blood via Fenton Reaction and Treatment with Potassium Permanganate (KMnO₄)

The Fenton reaction is a method commonly used to generate oxidative damage in naked DNA (2,3,8). With this method, a solution of hydrogen peroxide (H₂O₂) and an iron catalyst (FeCl₃) react to produce two hydroxyl radicals (-OH) that damage the DNA molecule. A 2009 study on DNA damage and repair used the Fenton reagent and potassium permanganate (KMnO₄) to successfully damage *naked* cell line DNA (2). In order to damage *native* DNA in whole blood (which presumably poses more challenges due to its protected state), our experiments involved a five-fold increase in concentration of each of the damaging agents used (Table 9). Additionally, the incubation periods for each of the reactions were increased from 20-120 minutes (with naked DNA) to up to 48 hours with native DNA targets.

Sample Type	Fenton Reaction	Potassium Permanganate
<i>Naked</i> DNA (cell-line)	Fe-EDTA (9mM-18mM) Hydrogen peroxide (30mM)	100mM KMnO ₄
<i>Native</i> DNA (whole blood)	Fe-EDTA (45mM-90mM) Hydrogen peroxide (150mM) *5-fold increase in concentration	500mM KMnO ₄ *5-fold increase in concentration

Table 9: Comparison of treatment of *naked* cell-line DNA vs. *native* DNA in whole human blood with the Fenton reagent and potassium permanganate.

As stated previously, in human cells DNA does not occur as a “naked” structure, and hence the same Fenton chemistry that generated oxidative damage in purified DNA may not do so to the same degree when DNA is complexed with other materials. Attempts to substantially damage DNA in whole human blood with Fenton reagents or potassium permanganate were not successful (i.e., damage here is defined as that which will impact STR typing results). Even when the concentration of the damaging agent and exposure times were increased five-fold (compared to conditions typically used with naked DNA samples), no allele dropout occurred. Small reductions in allele peak heights were observed, but not enough to affect the quality or interpretation of the STR profiles (Table 10).

It should be noted here that our Fenton reaction parameters were modeled after a 2009 study that successfully damaged *naked* DNA molecules using the concentrations described in Table 9. This 2009 study did not report the pH (or pH range) under which the Fenton reaction was carried out (2) and we did not measure it. The kinetics of Fenton chemistry reveals that the efficiency of the reaction is greatly affected by the pH of the solution. The optimal pH range for the Fenton reaction is between pH 3 and pH 6. At higher (more basic) pH levels, ferrous iron

catalytically decomposes H₂O₂ into oxygen and water, without the formation of the hydroxyl radicals that cause the intended damage (56,57). For this reason, any future studies utilizing Fenton reagents to generate *in vitro* DNA damage should closely monitor pH levels of the reactions.

Sample Genotype	Non-damaged Positive control	After treatment with Fenton reagents at 5X concentration for 12 hours		After treatment with Fenton reagents at 5X concentration for 48 hours	
		Fe-EDTA (45mM-90mM)	Hydrogen Peroxide (150mM)	Fe-EDTA (45mM-90mM)	Hydrogen Peroxide (150mM)
Allele	RFU	RFU	RFU	RFU	RFU
D8S1179	12	7755	6393		4490
	13	7660	5687		4992
D21S11	27	7943	4440		3631
	31	7166	3532		2874
D7S820	8	8325	3064		2424
	12	7900	3187		2596
CSF1P0	12	8653	8024		5792
D3S1358	16	8005	6395		5278
	17	7502	6472		5100
TH01	6	9570	8302		6725
D13S317	12	6518	6389		5064
	15	5987	5061		4126
D16S539	12	7248	6391		5160
	13	6878	5208		3696
D2S1338	17	7788	5977		3572
	23	7417	4900		3407
D19S433	14	8568	7729		6662
vWA	15	5422	5402		3298
	16	8488	5123		3177
TPOX	9	7687	6814		4815
	12	7295	4341		3799
D18S51	14	8368	8253		6815
Amel	X	9873	7593		6870
D5S818	11	7567	5633		3700
	12	7477	5223		4033
FGA	20	7264	4469		3618
	24	6891	4903		3019
Mean ± SD		7675 ± 949	5737 ± 1463		4398 ± 1326

Table 10: Oxidative damage to native DNA in a representative whole human blood sample after treatment with Fenton reagents for 12 hours and 48 hours, showing minimal reduction in RFU levels and no incidence of allele dropout (despite increasing the concentration of the reagents five-fold as compared to the concentrations used with naked DNA samples). Results obtained using another well-known oxidizing agent --- potassium permanganate (KMnO₄) --- were comparable (data not shown).

Depurination of DNA in Human Blood Samples

Depurination is an alteration of DNA in which the purine base (adenine or guanine) is cleaved from the deoxyribose sugar by hydrolysis of the beta-N-glycosidic bond between them. This action results in an abasic/apurinic (AP) site that is not recognized by the DNA polymerase

and thus stalls PCR amplification. High-heat and acidic pH levels (in combination) are common conditions under which depurination of DNA occurs. The same 2009 study that used the Fenton reaction and KMnO_4 to damage naked cell-line DNA also successfully utilized an acidic buffer (pH 4.8) and heat to depurinate the purified nucleic acid (2). Similar to the oxidative damage studies using Fenton reagents and potassium permanganate, our depurination experiments with native DNA involved increasing both the concentration of the buffer as well as the exposure times. The effects of this depurination buffer on both liquid (non-coagulated) and coagulated human blood also were explored.

The results shown in Tables 11-12 demonstrate that damage occurred in liquid blood samples more so than in the dried bloodstains (and in a much more consistent manner). Since most intracellular chemical reactions occur in an aqueous environment, it is expected that damage would occur more slowly in a dehydrated substrate. The results shown in Table 11 clearly illustrate that the ten-fold increase in buffer concentration, as well as significant increases in incubation times, are necessary to depurinate native DNA in human blood (compared to protocols previously used on naked templates). Differences in DNA damage in dehydrated versus hydrated blood may be an important variable to further investigate since evidentiary samples from crime scenes may be collected in either state (although samples are typically dried before packaging).

LIQUID WHOLE BLOOD						LIQUID WHOLE BLOOD					
After depurination in 1X buffer (pH 4.8) at 70°C						After depurination in 10X buffer (pH 4.8) at 70°C					
Sample Genotype	Non-damaged Positive control	48 hrs	96 hrs	120 hrs		Sample Genotype	Non-damaged Positive control	48 hrs	96 hrs	120 hrs	
Allele	RFU	RFU	RFU	RFU		Allele	RFU	RFU	RFU	RFU	
D8S1179	12	7655	3610	2255	2196	D8S1179	12	7655	406		Complete loss of STR profile
	13	7660	3482	2177	2034		13	7660	435		
D21S11	30	8943	1832	1181	1117	D21S11	30	8943	111		
	31	7164	1952	940	867		31	7164	128		
D7S820	8	8235	1498	663	554	D7S820	8	8235			
	11	7800	1738	604	662		11	7800			
CSF1P0	12	8563	3720	1942	2186	CSF1P0	12	8563	175		
D3S1358	16	9005	4567	3658	3554	D3S1358	16	9005	1100	180	
	17	8502	3341	2935	2637		17	8502	771		
TH01	9	9750	8470	4949	4456	TH01	9	9750	1815	117	
D13S317	11	6815	2711	1699	1519	D13S317	11	6815	114		
	13	5897	3010	1311	1144		13	5897	145		
D16S539	12	7842	2829	1756	1713	D16S539	12	7842	250		
	13	6875	2817	1685	1357		13	6875	120		
D2S1338	21	7768	2418	1370	1303	D2S1338	21	7768			
	24	7412	2436	1156	1101		24	7412			
D19S433	12	8628	6120	4873	4443	D19S433	12	8628	3013	590	
	15	6422	3238	1848	1275		15	6422			
vWA	17	8455	3068	1927	1620	vWA	17	8455	166		
	9	7285	2139	1594	1502		9	7285	243		
TPOX	11	8881	2359	1313	1035	TPOX	11	8881	239		
	D18S51	13	8634	4649	2506		1919	D18S51	13	8634	
Amel	X	8411	5773	4427	3955	Amel	X	8411	1308	570	
D5S818	11	7567	2560	1362	1607	D5S818	11	7567			
	12	7477	2503	1298	1016		12	7477			
FGA	19	7624	2083	1491	1203	FGA	19	7624	225		
	20	6891	1948	933	1244		20	6891			
Mean ± SD	7858 ± 884	3217 ± 1559	1995 ± 1195	1823 ± 1088		Mean ± SD	7858 ± 884	399 ± 688	54 ± 157		

Table 11: Depurination of DNA in a whole human (liquid) blood sample using 1X and 10X depurination buffers (pH 4.8) and after incubation on a heat block at 70°C for 48 hours, 96 hours, and 120 hours.

DRIED BLOODSTAIN					
After depurination in 1X buffer					
(pH 4.8) at 70°C					
Sample Genotype	Non-damaged Positive control	48 hrs	96 hrs	120 hrs	
Allele	RFU	RFU	RFU	RFU	
D8S1179	12	7655	3693	3374	2599
	13	7660	3729	2579	2085
D21S11	30	8943	2899	1900	1177
	31	7164	2846	1642	1374
D7S820	8	8235	1972	1243	1247
	11	7800	2373	1237	1137
CSF1P0	12	8563	5867	3454	2651
	16	9005	6372	3880	3344
D3S1358	17	8502	4363	3236	3034
	9	9750	8528	8112	5350
TH01	11	6815	4396	2719	2170
	13	5897	3648	2647	1831
D13S317	12	7842	3797	2798	2034
	13	6875	4050	2593	2520
D16S539	21	7768	4564	2431	1699
	24	7412	2915	1611	1685
D2S1338	12	8628	7525	6012	4642
	15	6422	4498	2572	2103
D19S433	17	8455	2630	2743	1933
	9	7285	3104	2396	1459
vWA	11	8881	2485	1937	1692
	13	8634	6292	3356	3123
TPOX	X	8411	6372	6336	5868
	11	7567	3028	2404	2308
D18S51	12	7477	2768	2049	2015
	19	7624	2953	1314	1419
Amel	20	6891	2837	1544	1374
	11	7567	3028	2404	2308
D5S818	12	7477	2768	2049	2015
	19	7624	2953	1314	1419
FGA	20	6891	2837	1544	1374

Mean ± SD 7858 ± 884 4093 ± 1690 2893 ± 1610 2366 ± 1219

DRIED BLOODSTAIN					
After depurination in 10X buffer					
(pH 4.8) at 70°C					
Sample Genotype	Non-damaged Positive control	48 hrs	96 hrs	120 hrs	
Allele	RFU	RFU	RFU	RFU	
D8S1179	12	7655	3340	2848	2805
	13	7660	2872	2421	2263
D21S11	30	8943	2264	1896	1947
	31	7164	1953	1677	1306
D7S820	8	8235	1441	1416	856
	11	7800	1288	1641	1198
CSF1P0	12	8563	4006	3288	2411
	16	9005	4623	4334	4035
D3S1358	17	8502	4916	3670	3098
	9	9750	8083	6156	5630
TH01	11	6815	3532	2816	2442
	13	5897	3326	1781	1051
D13S317	12	7842	2647	2714	2047
	13	6875	2864	2357	1603
D16S539	21	7768	2599	1977	1578
	24	7412	2422	1672	1051
D2S1338	12	8628	7789	6556	5637
	15	6422	3040	2560	2502
D19S433	17	8455	3449	2372	2332
	9	7285	2383	2353	2177
vWA	11	8881	2494	2417	1765
	13	8634	5326	3994	3840
TPOX	X	8411	6978	4588	4483
	11	7567	2574	2259	2175
D18S51	12	7477	1988	1846	2535
	19	7624	2057	1849	1563
Amel	20	6891	1698	1603	1460
	11	7567	3028	2404	2308
D5S818	12	7477	2768	2049	2015
	19	7624	2953	1314	1419
FGA	20	6891	2837	1544	1374

Mean ± SD 7858 ± 884 3406 ± 1815 2780 ± 1332 2437 ± 1287

Table 12: Depurination of DNA in a dried human bloodstain using 1X and 10X depurination buffers (pH 4.8) and after incubation on a heat block at 70°C for 48 hours, 96 hours, and 120 hours.

Oxidative Damage via Peroxide-based Stain Remover

Another protocol that was explored to assess its ability to generate oxidative damage in DNA involved Arm & Hammer’s OxiClean® Free Triple Power Stain Fighter, a popular laundry additive with claims to completely remove bloodstains from clothing. Blood is a protein-based stain that contains an enzyme called catalase which reportedly reacts with ingredients in this product to produce water and oxygen. According to the manufacturer, the oxygen attacks and breaks down the bloodstain. The chemical ingredients in OxiClean® include water, ethoxylated alcohols C12-15, hydrogen peroxide, sodium polyacrylate, alkylbenzenesulfonic acid C10-16, linear alkylbenzene sulfonate, tinopal, and sanolin blue dye (27). After a 30-minute incubation period at both room temperature and 56°C, only slight decreases in allele peak heights were observed (Table 13). Results shown in this table were representative of the pool of samples subjected to this treatment protocol. Even when the incubation period was extended to one hour (which exceeds the length of a typical wash cycle), reduction in RFU levels was minimal and no allele dropout occurred (data not shown).

Sample Genotype	Allele	Non-damaged	After treatment	Non-damaged	After treatment
		Positive control (room temp)	w/10% OxiClean® for 30 min (room temp)	Positive control (56°C)	w/10% OxiClean® for 30 min (56°C)
		RFU	RFU	RFU	RFU
D8S1179	12	6189	5628	3826	2625
	13	5491	4928	3314	2305
D21S11	27	5213	4172	2679	1664
	31	4553	3896	2272	1354
D7S820	8	3640	2935	1970	1131
	12	3253	2992	1875	1152
CSF1P0	12	8867	7480	4542	3196
D3S1358	16	6520	7254	4805	3859
	17	5595	5737	4174	3573
TH01	6	14589	12271	8443	6349
D13S317	12	6545	4711	3443	3012
	15	5734	5748	3632	2360
D16S539	12	6511	5498	3176	2220
	13	6052	5271	2949	2519
D2S1338	17	5789	4095	3043	2024
	23	5574	3924	2663	2107
D19S433	14	9736	8713	6148	4578
vWA	15	6635	4299	3456	2693
	16	5127	4189	2439	2311
TPOX	9	5425	4909	2856	2181
	12	4541	3830	2825	2102
D18S51	14	10506	7106	5349	3599
Amel	X	8583	6343	5174	3881
D5S818	11	4063	3758	3176	1906
	12	3782	4088	2228	1698
FGA	20	3807	3368	2408	1365
	24	3920	3047	1813	1442
Mean ± SD		6157 ± 2489	5192 ± 2044	3507 ± 1485	2563 ± 1174

A

B

Table 13: Oxidative damage to DNA in a representative sample of whole human blood after treatment with OxiClean® Free Triple Power Stain Fighter at A) room temperature and B) 56°C, respectively.

DNA Damage in Human Bloodstains via Environmental Exposure

In addition to evaluating previously-documented techniques that damage naked cell-line DNA via chemical means, it was important investigate the combined effects of UV radiation, temperature, and humidity on DNA. In this study, human bloodstains were exposed to all three of these environmental insults simultaneously, since authentic forensic samples are typically subjected to a *combination* of exogenous insults (and thus would likely contain a *variety* of different DNA lesions, rather than a single type).

Record high-temperature and low-precipitation conditions in Texas during the summer of 2011 provided harsh conditions for assessing the stability and survivability of DNA in bloodstains. Despite these conditions, DNA in the bloodstains that were placed on the roof remained fairly durable and resistant to damage, likely due to the dry conditions. After two full weeks of environmental exposure, a decrease in STR allele peak heights was observed for all samples, although the level of damage was not severe enough to prevent a full genetic profile from being obtained. For samples placed in UV-transparent Acrylite® OP-4 acrylic boxes, allele dropout was not observed until the 4-week and 8-week exposure times and, interestingly, the *degree* of damage and amount of allele dropout observed varied between samples despite the fact that they were all subjected to the exact same environmental conditions and for identical exposure times (Table 14).

There are a number of possible explanations for these observations. Blood is composed of plasma and cellular elements, including leukocytes, erythrocytes, and thrombocytes (platelets). Typically, plasma constitutes approximately 55% of blood volume; 45% of the volume is composed of erythrocytes; and the remaining 1% contains leukocytes and thrombocytes, but it is widely known that pathologic changes in specific blood cell concentrations may occur as a result of disease, infection, or injury (11). Although the volume of blood collected from each individual in this study was the same, variations in the quantity of leukocytes per sample (e.g. due to sampling variance) could account for the differences observed between bloodstains in terms of apparent DNA damage. In other words, the level of damage may actually be very similar between samples, but certain bloodstains may have initially contained more leukocytes (and hence more DNA), contributing to the illusion that one individual's DNA was more robust than another's. Additionally of interest is that physiologic differences in the concentration of cellular elements in blood do occur according to race, age, sex, and geographic location. For example, the leukocyte counts for Caucasians are higher by $0.5 \times 10^9/L$ than for African Americans (11).

	Sample Genotype	After 8-weeks environmental exposure in a UV-transparent Acrylite® OP-4 acrylic box			Sample Genotype	After 8-weeks environmental exposure in a UV-transparent Acrylite® OP-4 acrylic box	
		Positive control RFU	RFU			Positive control RFU	RFU
D8S1179	Allele 12	1970	1495	D8S1179	Allele 12	1995	
	Allele 13	2187	885		Allele 13	1830	261
D21S11	Allele 27	1718	367	D21S11	Allele 31	1150	
	Allele 31	1959			Allele 31	1412	
D7S820	Allele 8	1111	171	D7S820	Allele 12	1851	
	Allele 12	1230					
CSF1P0	Allele 12	3113	287	CSF1P0	Allele 10	1548	
					Allele 12	1527	
D3S1358	Allele 16	2618	1924	D3S1358	Allele 16	2078	485
	Allele 17	3406	1390		Allele 18	1807	210
					Allele 9	2920	
TH01	Allele 6	5415	2342	TH01	Allele 9.3	2631	162
					Allele 12	2135	
D13S317	Allele 12	2360	520	D13S317	Allele 13	2205	
	Allele 15	2299	423				
D16S539	Allele 12	2443	436	D16S539	Allele 11	2613	
	Allele 13	2371	369		Allele 12	2126	
D2S1338	Allele 17	1295	306	D2S1338	Allele 17	1636	
	Allele 23	1912	161		Allele 23	1920	
D19S433	Allele 14	3755	1968	D19S433	Allele 14	3501	477
vWA	Allele 15	1832	942	vWA	Allele 14	2059	
	Allele 16	1808	603		Allele 17	1740	
TPOX	Allele 9	1684	434	TPOX	Allele 8	1388	
	Allele 12	1638	322		Allele 11	1306	
D18S51	Allele 14	3324	332	D18S51	Allele 12	1549	
					Allele 16	1422	
Amel	Allele X	3663	2442	Amel	Allele X	1357	201
					Allele Y	1482	301
D5S818	Allele 11	1580	375	D5S818	Allele 11	1433	
	Allele 12	1688	365		Allele 12	1327	
FGA	Allele 20	1168	293	FGA	Allele 20	1188	
	Allele 24	1628	375		Allele 22	1247	
	Mean ± SD	2266 ± 979	781 ± 708		Mean ± SD	1813 ± 550	70 ± 142

Table 14: DNA damage in two different human bloodstains after environmental exposure for eight weeks in a UV-transparent Acrylite® OP-4 acrylic box. Results are representative of the variation in levels of damage that were observed amongst all experimental samples. Boxes containing no RFU data signify the occurrence of allele dropout at that locus.

Another explanation for the observed differences in DNA damage between bloodstains of different individuals involves the plasma component of blood. Although the principal component of plasma is water, it also contains dissolved ions, proteins, carbohydrates, fats, hormones, vitamins, and enzymes (11). It is possible that certain plasma constituents (cholesterol, for example) may absorb some of the UV radiation and provide a protective barrier of sorts to the DNA within the leukocytes of that particular bloodstain. Lastly, the difference in levels of DNA damage between bloodstains could simply be stochastic. It is reasonable to assume that random insults by chance will vary somewhat from sample to sample even though exposure conditions are similar. These findings further assert the importance of investigating how DNA damage occurs in its native state as opposed to as a naked molecule.

Oxidative Damage to DNA in Human Blood via Bleach Exposure

Household bleach (sodium hypochlorite, NaOCl) degrades DNA through oxidative damage and the production of chlorinated base products. Exposure of DNA to increasingly higher concentrations of NaOCl will eventually cause cleavage of the strands, breaking the DNA into smaller and smaller pieces, and eventually to individual bases (7). Although in a laboratory setting decontamination procedures are carried out with fairly dilute concentrations of 10% bleach (0.6% NaOCl), bleach also may be used by criminals at much higher concentrations at a crime scene in an effort to destroy DNA evidence. Bleach was explored as a damaging agent to generate samples for potential use in repair and whole genome amplification studies.

Results show that even after liquid (non-coagulated) blood samples were immersed in a 10% Clorox® solution (0.6% NaOCl) for 1-hour and 2-hour incubation periods, full STR profiles could still be obtained from the exposed blood (although continual decreases in allele peak heights indicated that some oxidative damage was occurring). When the bleach concentration was increased to 50% Clorox® (3% NaOCl), allele dropout was observed at completion of the 1-hour incubation period, followed by complete loss of the STR profile after 2 hours of immersion (Table 15).

Sample Genotype	Non-damaged Positive control	LIQUID BLOOD: After immersion in	
		10% Clorox® for 1 hour	10% Clorox® for 2 hours
Allele	RFU	RFU	RFU
D8S1179	12	8008	3726
	13	6050	3973
	27	4966	3083
D21S11	31	4741	2276
	8	4180	1977
D7S820	12	3009	1775
	12	8977	4839
CSF1P0	16	8240	4584
D3S1358	17	7018	4889
	6	14148	9013
TH01	12	7688	3332
	15	5205	3152
D13S317	12	6123	3708
D16S539	13	5346	3050
	17	4457	3614
D2S1338	23	5293	2825
	14	10463	5892
D19S433	15	7145	3219
	16	4756	3101
vWA	9	4327	2384
	12	3904	2271
TPOX	14	8653	4859
D18S51	X	9246	6353
Amel	11	4610	2141
	12	3314	2632
D5S818	20	3866	1852
	24	4080	2145
FGA			

Mean ± SD 6215 ± 2563 3580 ± 1630 1984 ± 1447

A

Table 15: **A)** DNA damage in liquid (non-coagulated) blood after immersion in a 10% Clorox® (0.6% sodium hypochlorite) bleach solution for 1-hour and 2-hour incubation periods, showing moderate decreases in allele peak heights but no allele dropout. **B)** DNA damage in liquid (non-coagulated) blood after immersion in a 50% Clorox® (3% sodium hypochlorite) bleach solution, showing allele dropout and complete loss of STR profile at completion of the 1-hour and 2-hour periods, respectively.

Sample Genotype	Non-damaged Positive control	LIQUID BLOOD: After immersion in	
		50% Clorox® for 1 hour	50% Clorox® for 2 hours
Allele	RFU	RFU	RFU
D8S1179	12	7755	113
	13	7660	147
	27	7943	107
D21S11	31	7166	
	8	8325	152
D7S820	12	7900	
	12	8653	284
CSF1P0	16	8005	374
D3S1358	17	7502	121
	6	9570	332
TH01	12	6518	220
	15	5987	115
D13S317	12	7248	316
D16S539	13	6878	386
	17	7788	
D2S1338	23	7417	390
	14	8568	284
D19S433	15	5422	285
	16	8488	273
vWA	9	7687	181
	12	7295	238
TPOX	14	8368	433
D18S51	X	7935	488
Amel	11	7567	123
	12	7477	110
D5S818	20	7264	115
	24	6891	148
FGA			

Mean ± SD 7603 ± 844 239 ± 118

Complete loss of STR profile

B

In addition to damaging liquid whole blood samples, the effect of bleach on coagulated blood was investigated. Although blood samples were allowed to clot in microcentrifuge tubes prior to the initiation of the damaging protocol, only small decreases in allele peak heights were observed after two hours of incubation in 50% Chlorox® solution (despite mechanical re-solubilization of the clot via vortexing after the bleach solution was added) (Table 16). In the process of clotting, blood separates into four distinct layers: a dark red (almost black) jellylike clot; a thin layer of oxygenated red cells; a layer of white cells and platelets; and a layer of yellowish serum (11). Completion of the clotting mechanism appears to interfere with the bleach solution's ability to cause oxidative DNA damage. The damage does appear to still be occurring (as evidenced by the decrease in allele peak heights), but at a significantly lower rate than in the case in which liquid (non-coagulated) blood was pipetted directly into the bleach solution.

Sample Genotype	COAGULATED BLOOD:		
	Non-damaged Positive control	After immersion in 50% Clorox® for 2 hours	
Allele	RFU	RFU	
D8S1179	12	8589	6987
	13	10000	6333
D21S11	27	7207	5066
	31	4937	4397
D7S820	8	3545	3209
	12	3345	2959
CSF1P0	12	9499	7848
D3S1358	16	9828	9336
	17	10220	7678
TH01	6	13377	12638
D13S317	12	7535	6780
	15	7635	5538
D16S539	12	7359	5491
	13	6009	6635
D2S1338	17	6181	5640
	23	5315	4194
D19S433	14	13806	11324
vWA	15	7696	5609
	16	6093	5223
TPOX	9	6113	4362
	12	5783	4768
D18S51	14	10012	8074
Amel	X	13206	11025
D5S818	11	5930	4487
	12	5703	5055
FGA	20	3425	3837
	24	3970	2926
Mean ± SD	7493 ± 2957	6201 ± 2534	

Table 16: DNA damage in coagulated human blood after immersion in a 50% Clorox® (0.6% sodium hypochlorite) bleach solution for 2 hours, showing considerably less damage than was observed with liquid, non-coagulated blood (despite mechanical resolubilization of the clot via vortexing)

These findings with bleach have additional value beyond a method to damage native DNA. The results indicate that current decontamination methods using bleach in the laboratory may not be as effective as believed (at least for DNA complexed with other materials). Further studies may be warranted to determine if native DNA contamination is neutralized with bleach.

Human Skeletal Remains

STR analysis of most of the bone-derived extracts revealed moderate-to-severe levels of degradation (and possibly inhibition), as evidenced by allele dropout at multiple loci and/or low RFU peak heights. Combined with the low quantification values obtained (most under 1ng/μl, Tables 17-18) and the fact that skeletal remains are exposed to environmental inhibitors (e.g. humic and fulvic acids in soil), the samples with partial or low-RFU STR profiles were determined to be good candidates for subsequent DNA repair and WGA experiments.

Bone Extraction Method				
Hi-Flow® (Generon)		Amicon® Ultra-4/ MinElute®		
Sample ID	Quantity (ng/μl)	Sample ID	Quantity (ng/μl)	
1	036.001.001	0.2440	036.001.002	0.2490
	036.002.002	0.2300	036.002.001	0.2080
2	037.001.001	0.0051	037.001.002	0.0056
	037.001.003	0.0077	037.002.001	0.0100
3	038.001.002	0.0030	038.001.001	0.0009
	038.002.001	0.0030	038.002.002	0.0016
4	039.002.001	0.0900	039.002.002	0.0420
	039.001.001	0.0898	039.001.002	0.0648
5	040.001.002	0.0000	040.001.001	0.0867
	040.002.001	0.1100	040.002.002	0.0704
6	041.001.001	0.0134	041.002.001	0.0069
	041.003.001	0.0209	041.003.002	0.0098
7	042.001.001	0.0761	042.001.002	0.0285
	042.002.002	0.0550	042.002.001	0.0615
8	044.001.002	0.0229	044.001.001	0.0034
	044.002.001	0.0016	044.002.002	0.0053
9	045.003.001	1.3500	045.001.001	2.1900
	045.002.001	0.0606	045.002.002	1.1200
10	046.001.002	0.0029	046.001.001	0.0036
	046.002.001	0.0000	046.001.003	0.0029
11	047.001.001	0.0474	047.001.002	0.0154
	047.002.002	0.0413	047.002.001	0.0295
12	048.001.003	0.0218	048.001.001	0.0145
	048.002.001	0.0157	048.001.002	0.0152
13	048.002.003	0.0095	048.002.002	0.0051
	049.001.002	0.0122	049.001.001	0.0144
14	032.001.003	0.0012	032.001.001	0.0000
	032.002.001	0.0000	032.002.002	0.0000
15	033.001.003	0.0000	033.001.001	0.0000
	033.002.001	0.0000	033.002.002	0.0004
16	034.001.002	0.0000	034.001.001	0.0000
	034.002.001	0.0022	034.002.002	0.0004
17	035.001.003	0.0013	035.001.001	0.0000
	035.002.001	0.0000	035.002.002	0.0008
18	028.001.004	0.0028	028.001.003	0.0082
	028.001.005	0.0058	028.001.006	0.0065
19	029.001.003	0.0203	029.001.004	0.0125
	029.001.005	0.0153	029.001.006	0.0159
20	030.001.003	0.0042	030.001.004	0.0045
	030.001.005	0.0049	030.001.006	0.0032

Table 17: Summary of DNA extractions (80) on the contemporary skeletal remains of 20 different individuals, with reported DNA quantities obtained (ng/μl) using two different extraction methods. In addition to the low quantities of DNA recovered, most of these samples produced partial or low-RFU STR profiles upon analysis, making them ideal candidates for DNA repair and whole genome amplification.

Bone Extraction Method					
Hi-Flow® (Generon)		Amicon® Ultra-4/MinElute®		Organic (PCIA)	
Sample ID	Quantity (ng/μl)	Sample ID	Quantity (ng/μl)	Sample ID	Quantity (ng/μl)
Tooth #1	0.0400	Tooth #2	0.0433	Femur 009.001	0.0291
Tooth #4	0.0458	Tooth #3	0.1220	Femur 010.001	0.0255
Femur 001.001	0.0184	Femur 001.002	0.0096	Femur 011.002	0.0450
Femur 002.002	0.0284	Femur 002.001	undetermined	Femur 012.002	0.0449
Femur 003.002	0.0214	Femur 003.001	0.0287	Tibia 003.001	0.0456
Femur 004.001	0.0074	Femur 004.002	0.0440	Tibia 012.001	0.0331
Femur 005.002	0.0299	Femur 005.001	0.0016	Tibia 017.002	0.0353
Femur 006.002	0.0313	Femur 006.001	0.0043		
Femur 007.001	0.0227	Femur 007.002	0.0442		
Femur 008.002	0.0100	Femur 008.001	0.0218		
Femur 010.002	undetermined	Tibia 008.002	0.0292		
Femur 011.001	0.0460	Tibia 009.002	0.0038		
Femur 012.001	0.0305	Tibia 011.002	0.0081		
Tibia 003.002	0.0291	Tibia 013.002	0.0296		
Tibia 008.001	0.0438	Tibia 014.001	undetermined		
Tibia 009.001	0.0228	Tibia 015.002	0.0323		
Tibia 011.001	0.0163	Tibia 016.001	0.0378		
Tibia 012.002	undetermined	Tibia 018.002	0.0173		
Tibia 013.001	0.0153				
Tibia 014.002	0.0372				
Tibia 015.001	0.0178				
Tibia 016.002	0.0263				
Tibia 017.001	undetermined				
Tibia 018.001	0.0221				

Table 18: Summary of DNA extractions on the exhumed historical (120-year-old) skeletal remains of a Civil War soldier, with reported DNA quantities obtained (ng/μl) using three different extraction methods. In addition to the low quantities of DNA recovered, all of these samples produced partial, low-RFU STR profiles upon analysis, making them ideal candidates for DNA repair and whole genome amplification studies. For samples with quantification values listed as “undetermined,” the AmpFISTR Quantifiler® Human DNA Quantification assay was unable to detect/amplify the 62-bp hTERT region in the extract (hence, for calculations in subsequent DNA repair and WGA experiments, the quantification values for these samples were assumed to be 0 ng/μl).

PreCR™ Repair of Compromised Samples

After identifying methods that were successful in causing damage to DNA in its native state, repair protocols were investigated to assess their ability to improve obtaining STR profiles from degraded or LCN samples. As shown in Figure 10, the manufacturer-recommended PreCR™ Repair protocol improved the performance of STR profiling of bleach-damaged DNA for all 16 loci amplified. Sodium hypochlorite (NaOCl) primarily generates oxidative damage in DNA. Hence, successful repair of the type of lesion induced in these samples was consistent with previous studies involving repair of singular, sequestered damage (2,4).

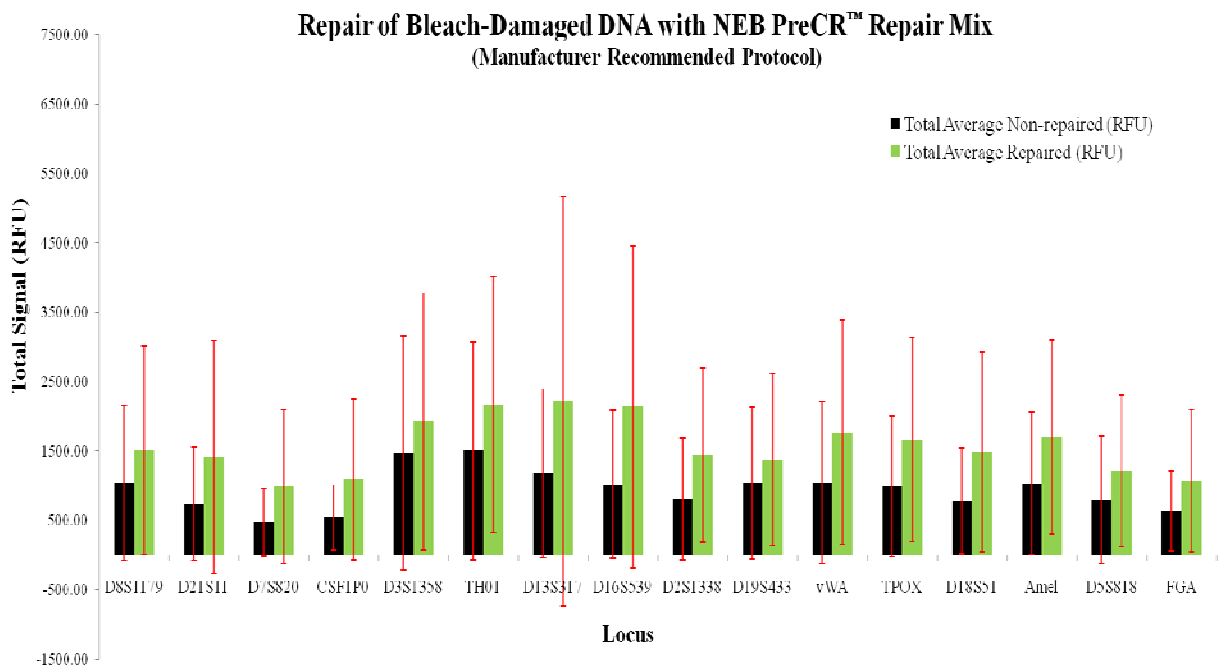


Figure 10: Average damage to DNA in whole human blood after immersion in a 50% Clorox® bleach solution (3% NaOCl) and average repair after treatment w/PreCR™ Repair Mix (according to the manufacturer’s recommendations). n = 40 blood samples (each repaired in duplicate, for a total of 80 repair reactions).

For some of the bleach-damaged samples, sufficient extract remained to perform the modified version of the PreCR™ Repair protocol. Twenty-five bleach-damaged samples were each repaired in duplicate, for a total of 50 modified repair reactions. Results from the modified protocol were directly compared with results generated with the manufacturer-recommended approach for the exact same samples (Figure 11). Congruent with a 2012 study on repair of UV-crosslinked DNA (4), the modified PreCR™ protocol outperformed the manufacturer-recommended approach in increasing allele peak heights for every locus examined with this bleach-damaged sample set. The repair modification may provide utility for casework because it eliminates the need to perform a separate repair reaction (which saves reagent costs and analyst time) and reduces the potential for contamination when transferring samples between tubes.

**Repair of Bleach-Damaged DNA with NEB PreCR™ Repair Mix:
Manufacturer Recommended Protocol vs. Modified Protocol**

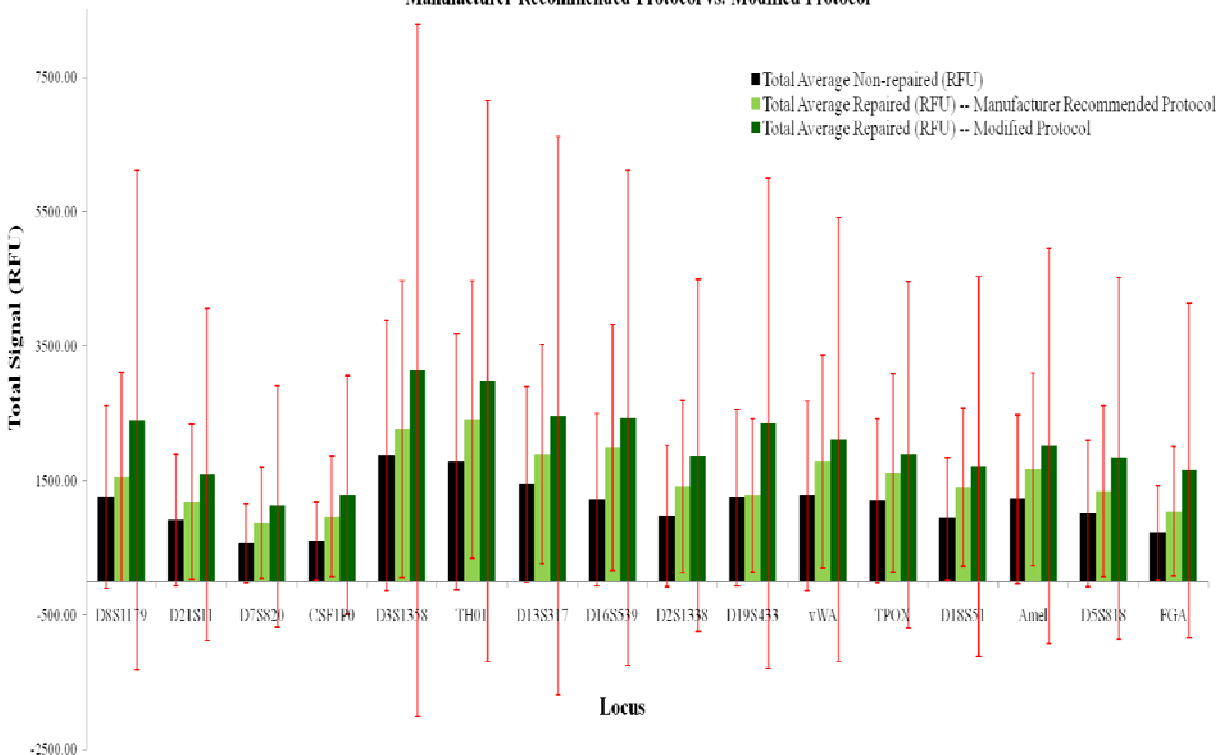


Figure 11: Comparison of repair of bleach-damaged DNA w/PreCR™ (manufacturer vs. modified protocol). n = 25 blood samples (each repaired in duplicate, for a total of 50 repair reactions)

The results show a consistent trend but are not significant. In part the variation is likely due to low level target sites and stochastic effects. Some of these effects may be due to variation in pipetting volumes. Ultimately, forensic samples may be damaged by multiple mechanisms resulting in a variety of lesions, and the quantity available for testing often is limited. Hence, it is our recommendation that the use of PreCR™ in casework should not be considered at this time due to its varied, unpredictable, and inconsistent results.

The manufacturer-recommended PreCR™ Repair protocol also improved STR profiles of environmentally-damaged DNA at the majority of loci examined, although to a lesser degree than with the bleach-damaged samples (Figure 12).

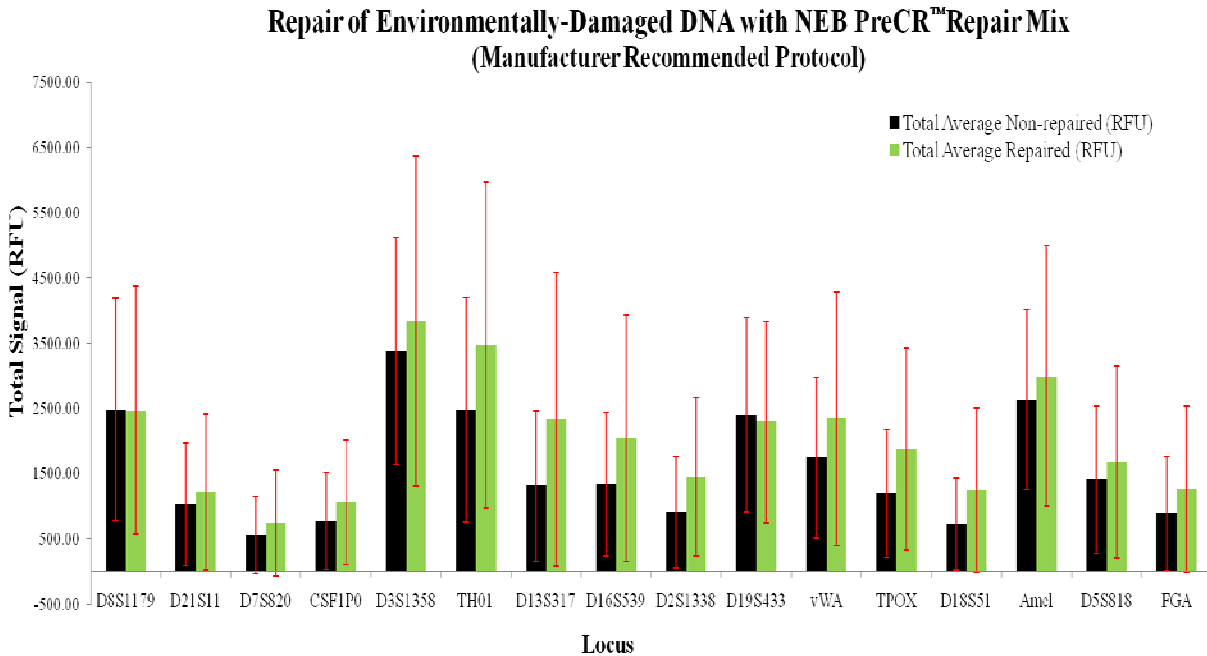


Figure 12: Average non-repaired DNA damage to environmentally-exposed bloodstains and average repair after treatment w/PreCR™ Repair Mix (according to the manufacturer’s recommendations). n = 75 bloodstains (each repaired in duplicate, for a total of 150 repair reactions).

For some of the environmentally-damaged samples, sufficient extract remained to perform the modified version of the PreCR™ Repair protocol. Thirty environmentally-damaged blood samples were repaired in duplicate, for a total of 60 modified repair reactions. Results from the modified protocol were directly compared with results generated with the manufacturer-recommended approach for the exact same samples (Figure 13). For this sample set, however, the repair assay did not improve the profile (i.e., increase allele peak heights) for the majority of loci (and in some cases resulted in lower RFU values), leaving its utility with environmentally-damaged samples in question. Additionally, in this case, the modified method did not surpass the manufacturer-recommended protocol in terms of increasing the total signal.

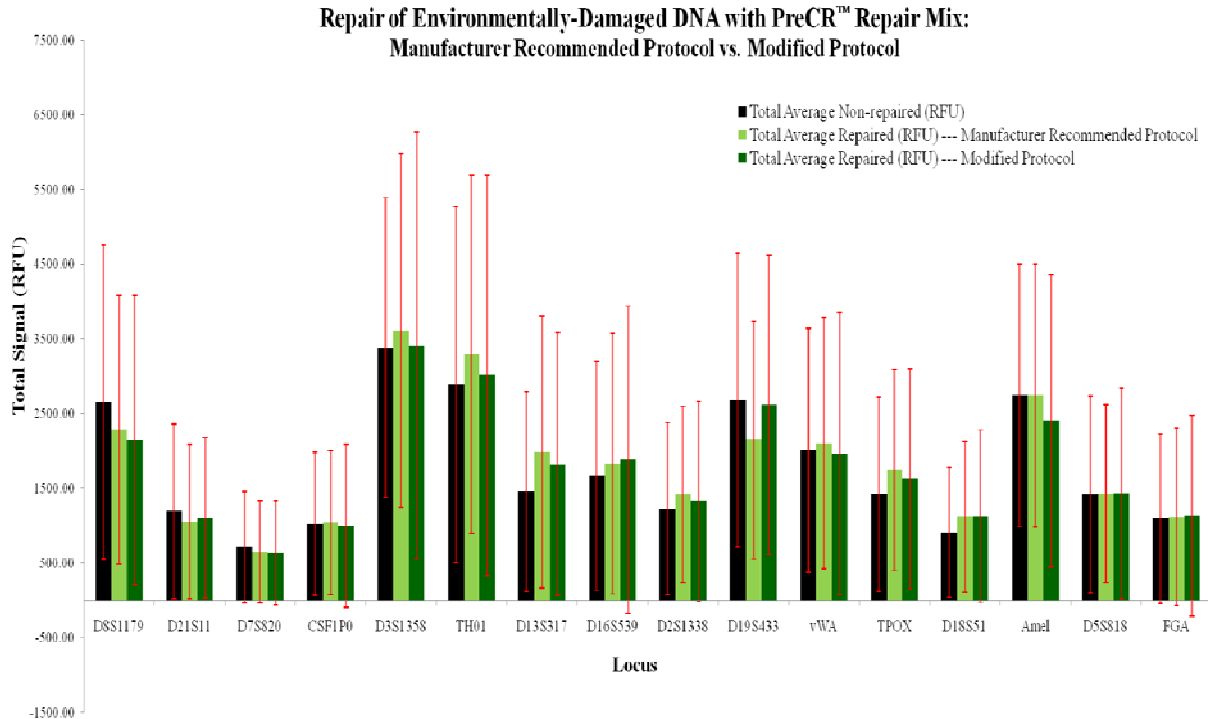


Figure 13: Comparison of repair of environmental damage (PreCR™ manufacturer vs. modified protocol). n = 30 bloodstains (each repaired in duplicate, for a total of 60 repair reactions).

Figures 14 and 15 represent the results for PreCR™ repair of degraded DNA from contemporary human skeletal remains. Fifty bone samples were repaired in duplicate using the manufacturer-recommended protocol (for a total of 100 repair reactions), while 30 bone samples were repaired in duplicate using the modified PreCR™ method (for a total of 60 modified repair reactions).

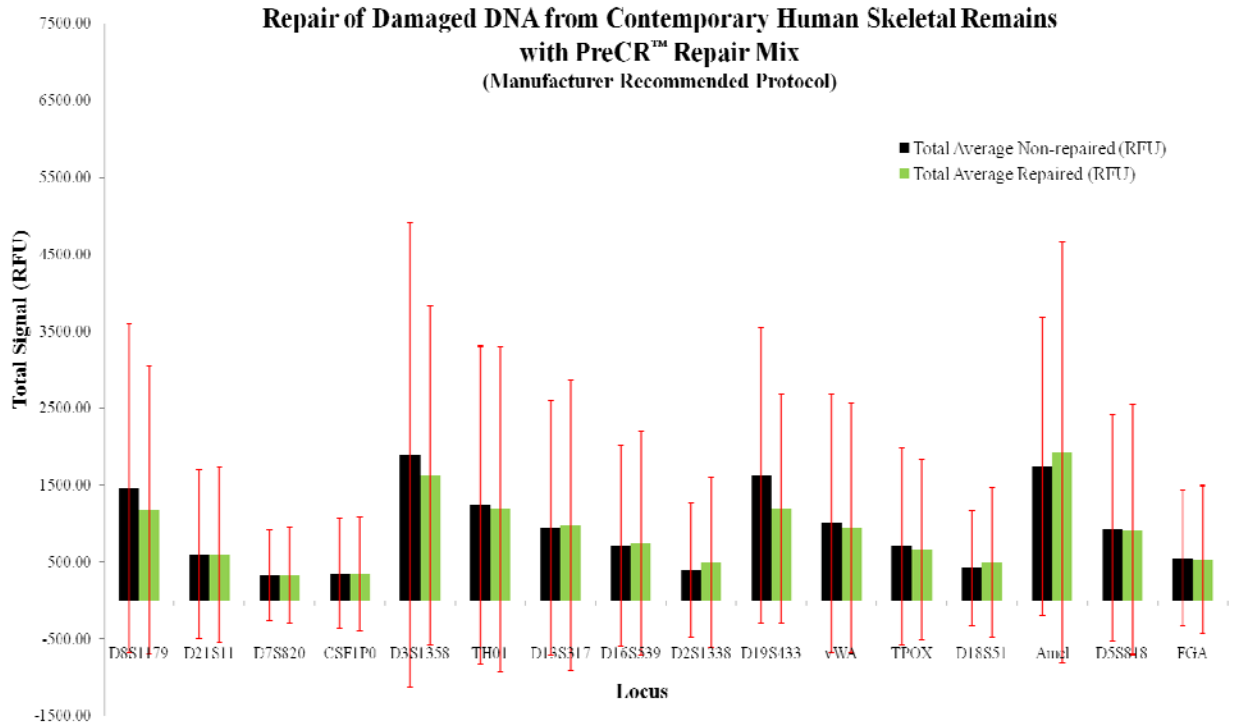


Figure 14: Average non-repaired DNA damage in contemporary human bone samples and average repair after treatment w/PreCR™ Repair Mix (according to the manufacturer’s recommendations). n = 50 bone samples (each repaired in duplicate, for a total of 100 repair reactions).

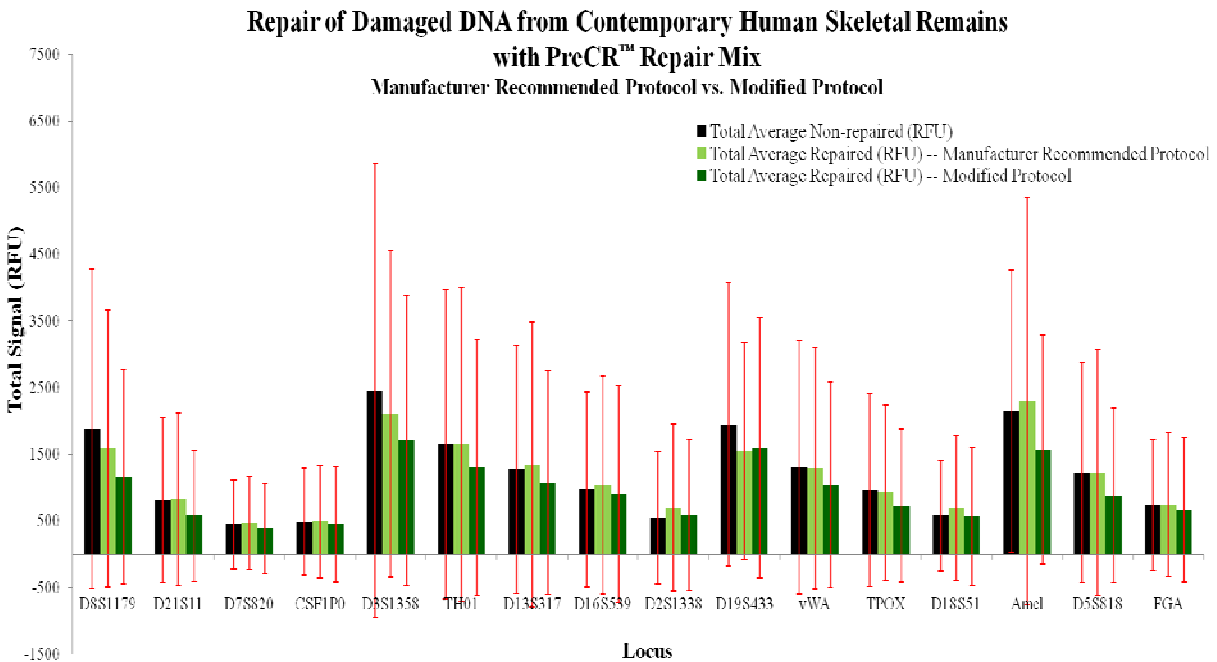


Figure 15: Comparison of repair of DNA damage in contemporary human bone w/PreCR™ Repair Mix (manufacturer vs. modified protocol). n = 30 bone samples (each repaired in duplicate, for a total of 60 repair reactions).

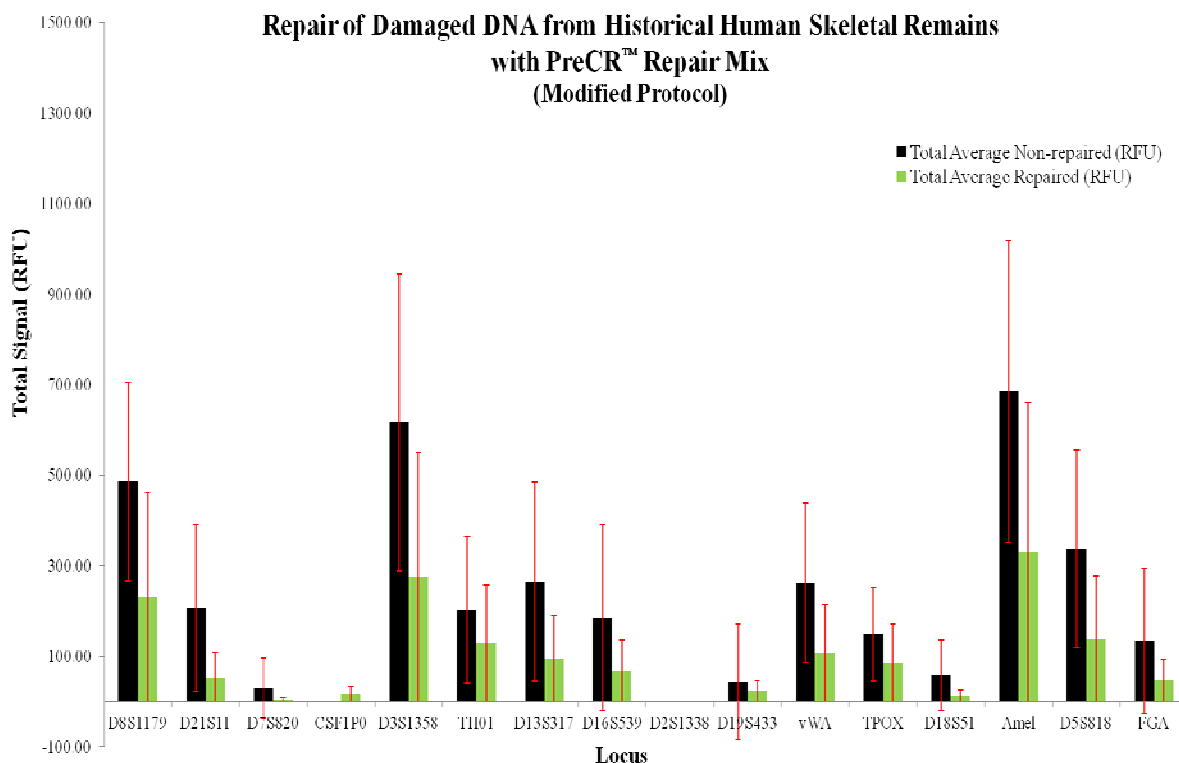


Figure 16: Average non-repaired DNA damage in historical human bone samples and average repair after treatment w/PreCR™ Repair Mix (modified protocol). Bones were 120 years old (n = 20).

Figures 14-16 reveal a reduction in total signal for the majority of loci examined in bone-derived DNA (for both the manufacturer-recommended and modified protocols, and for both the contemporary and historical skeletal remains). Skeletal samples likely contain a number of different types of lesions and thus present a substantially greater challenge in terms of DNA repair. One potential explanation for this “degradation effect” involves the complexity of damage in these samples combined with the fact that some of the PreCR™ enzymes require the damaged DNA to be in its double-stranded conformation. Although these enzymes can *recognize* damage in denatured strands, ssDNA lacks the complementary information necessary for the polymerization and ligation steps that occur during full repair of a lesion. Additionally, the presence of lesions directly adjacent to each other on opposite strands of dsDNA provides yet another possible explanation for the observed reduction in allele peak heights. In this scenario, if the two damaged bases are removed simultaneously, a double-strand break in the template would occur. Not only is highly-fragmented DNA difficult to repair, but polymerases would stall at these sites and inhibit PCR amplification. Lastly, the PreCR™ Repair Mix will not repair DNA-protein or DNA-DNA crosslinks present in a sample (28). Ultimately, if both strands of DNA in a forensic sample are damaged, there will be no template for repair. The scenarios under which the latter may occur are illustrated in Figure 17, providing a possible explanation for both the *lack* of repair in some damaged samples and the *variability* in the level of repair observed amongst environmentally-damaged samples from this study.

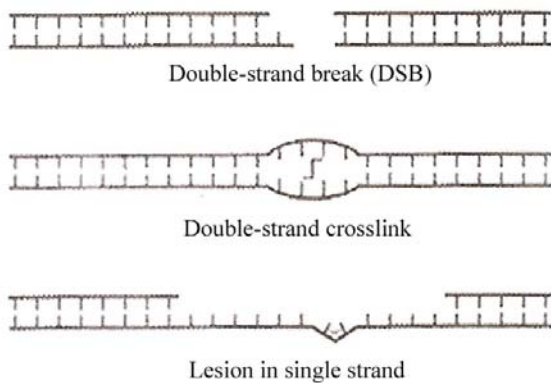


Figure 17: Illustration of scenarios in which both strands of a DNA template are damaged, leaving no template available for subsequent repair reactions with PreCR™

Additionally, as mentioned previously in the introduction of this report, damage to DNA in ancient or forensic samples typically arises from both endogenous and exogenous sources. Since ancient and forensic samples often have been exposed to environmental insults for extended periods of time, it is likely that the DNA contained within them possesses many of these more complex, bulky lesions (30,36). These types of lesions pose a greater challenge for DNA repair in general, but especially in the case of the *in vitro* PreCR™ assay. **DNA Repair: Implications for Forensic Casework**

Results to date indicate that the PreCR™ Repair assay holds some promise as an additional tool for improving STR typing of bleach-damaged DNA, although further studies are needed before its implementation into forensic casework could be considered. One important consideration is that UV-crosslinking and bleaching of laboratory workspaces, instruments, and plasticware are currently the standard practices for destroying exogenous/extraneous DNA molecules prior to DNA extraction or PCR amplification (47,48,49). A 2012 study demonstrated the effectiveness of PreCR™ in repairing naked DNA that has been damaged in the laboratory with a UV-crosslinker (4), and although the ability of PreCR™ to successfully improve bleach-damaged DNA profiles could be of great utility in cases involving crime scenes that have been cleaned with bleach by a perpetrator, these two research studies in combination reveal a complicating factor for the use of PreCR™ in casework. Since the PreCR™ Repair Mix can repair both UV-crosslinked and bleach-damaged DNA, it may also restore exogenous DNA that was intentionally destroyed by laboratory personnel during standard decontamination procedures.

Conversely, the repair assay did not significantly improve DNA profiles from environmentally-damaged bloodstains or bone (and in some cases resulted in lower RFU values for STR alleles), leaving its utility with these types of samples in question. Ultimately, the collective results from studies with environmentally-damaged bloodstains and skeletal remains suggest that the complexity and degree of damage dictates the efficacy of repair. Given that many forensic samples are significantly damaged and the quantity available for testing is often limited, the use of PreCR™ as a potential tool in casework is questionable due to its variable and unpredictable results. Additionally, aside from the need for additional research data and validation studies, quality control measures would need to be taken by the manufacturer if the PreCR™ Repair Mix were to be utilized in a probative forensic context. All of the PreCR™ quality control assays have been performed on *E. coli* DNA (not human substrates), and the product is not currently certified as being free of contaminating human DNA (28).

Degenerate-oligonucleotide-primed PCR (DOP-PCR)

Optimization with High-Quality DNA

Seven different DOP-PCR primers and two different variations in DOP-PCR thermal cycling parameters were tested. In particular, the efficacy of the original DOP-PCR method was compared with the 2009 Dawson Cruz protocol (which increased the number of low-stringency cycles from five to twelve) (23).

Amplification of high-quality cell-line DNA with each of the seven degenerate primers was performed to demonstrate that the reactions were working and to assess which primer(s) performed better. Ultimately, early investigations during this study demonstrated that the six modified DOP primers outperformed the original/traditional DOP primer (12) in terms of increased RFU levels, recovery of alleles, and number of artifacts observed (data not shown). For this reason, the study proceeded with focus on the modified primers. Two different input template amounts (100pg and 500pg) of female 9947A and male 007 control DNA were used for proof-of-concept prior to using the primers on damaged and LCN samples. All six primers improved the STR profiling of both 9947A and 007 templates, as shown in Tables 19-22. In these tables, the primer designations “dcDOP” and “abDOP” reflect modifications made to the original DOP primer by the Dawson Cruz lab (23) and our laboratory, respectively (and as described previously in the material and methods section of this report)

	D8S1179	D21S11	D7S820	CSF1PO	D3S1358	TH01	D13S317	D16S539					
9947A STR Profile	13	30	10	11	10	12	14	15	8	9.3	11	11	12
No WGA control (100pg)	424	150		175			327	206		184	266		247
10N dcDOP primer	8689	7306	833	640	3250	2480	1857	1659	4312	4316	10,643	2841	2196
12N(2) abDOP primer	6773	2546	1329	983	5217	1944	6577	4599	7470	11,059	3193	3675	1243
12N abDOP primer	2834	3907	583	1039	1926	2087	3547	3701	4007	3920	2916	803	2171
14N abDOP primer	2334	690	645	434	1219	1280	2607	3095	2639	4037	4287	1078	909
16N dcDOP primer	3747	3522	836	605	2912	1630	1080	1861	1157	3471	5414	1562	911
10N abDOP primer	1113	878	203		339	413	1425	999	975	1526	1510	853	688

	D2S1338	D19S433	vWA	TPOX	D18S51	Amel	D5S818	FGA					
9947A STR Profile	19	23	14	15	17	18	8	15	19	X	11	23	24
No WGA control (100pg)	193	225	154	255		359	447		203	188			
10N dcDOP primer	2064	2154	1553	560	19,508	19,459	2927	1053	1047	4902	8792	705	703
12N(2) abDOP primer	3316	3009	2369	2137	2737	3381	5472	2100	1040	12,097	2453	1704	2450
12N abDOP primer	1171	785	1726	1670	1829	1335	2613	560	1454	2583	2357	962	1130
14N abDOP primer	704	1582	1029	182	306	889	986	611	318	1842	2100	1272	510
16N dcDOP primer	902	419	820	881	4420	2709	1513	1133	930	4800	4519	586	1344
10N abDOP primer	583	354	822	667	817	484	836		362	960	1098	275	341

Table 19: Comparison of RFU peak heights after DOP-PCR of 100pg of high-quality control DNA (9947A) with six different degenerate primers.

	D8S1179	D21S11	D7S820	CSF1PO	D3S1358	TH01	D13S317	D16S539					
9947A STR Profile	13	30	10	11	10	12	14	15	8	9.3	11	11	12
No WGA control (500pg)	1855	1497	866	715	1090	752	1529	1475	1226	1289	2911	1826	1228
10N dcDOP primer	32,511	30,551	4240	4130	12,469	12,209	11,019	6510	1467	11,625	32,530	13,903	10,705
12N(2) abDOP primer	32,301	15,383	3399	4121	22,554	19,409	25,154	25,254	32,132	29,886	25,543	14,989	13,787
12N abDOP primer	32,696	16,293	7980	11,736	22,969	15,118	18,033	14,240	20,370	18,500	32,709	14,747	17,957
14N abDOP primer	14,002	9760	2406	2066	7352	6334	19,482	11,070	12,801	15,565	19,261	5455	6689
16N dcDOP primer	6970	5514	2066	1218	5989	5638	3563	3230	4620	4674	14,289	5281	2616
10N abDOP primer	13,925	8467	3400	3014	7723	15,035	10,003	8955	13,361	10,595	21,022	9074	7483

	D2S1338	D19S433	VWA	TPOX	D18S51	Amel	D5S818	FGA					
9947A STR Profile	19	23	14	15	17	18	8	15	19	X	11	23	24
No WGA control (500pg)	1458	1182	1075	1011	1377	1296	2098	669	875	1987	1825	834	976
10N dcDOP primer	6660	5783	9856	6648	8,601	32,115	9154	6114	6734	29,110	25,755	6613	7274
12N(2) abDOP primer	16,484	18,237	16,895	11,837	18,262	20,266	21,360	5835	6404	25,554	15,479	12,465	12,767
12N abDOP primer	9851	8057	12,174	10,881	20,856	20,011	15,368	11,069	8893	25,015	23,979	8136	5808
14N abDOP primer	5818	6103	9130	9519	7291	6703	9287	5391	3920	12,858	10,658	3498	3320
16N dcDOP primer	3043	3331	3321	2145	7708	6214	4564	2746	2286	9585	8614	1969	2392
10N abDOP primer	4455	5072	7768	5415	6759	8173	12,210	4318	5758	26,886	9584	3664	5021

Table 20: Comparison of RFU peak heights after DOP-PCR of 500pg of high-quality control DNA (9947A) with six different degenerate primers.

	D8S1179	D21S11	D7S820	CSF1PO	D3S1358	TH01	D13S317	D16S539							
Control DNA 007 STR Profile	12	13	28	31	7	12	11	12	15	16	7	9.3	11	9	10
No WGA control (100pg)		79		125			76	81				177	201	215	88
10N dcDOP primer	1966	3335	1429	445	732	601	3269	2799	900	1011	7998	2537	4290	613	707
12N(2) abDOP primer	1141	2014	701	471	384		2671	941	2382	2944	7997	2816	2161	1040	1138
12N abDOP primer	4990	4456	1306	1454	157	274	1201	354	2982	2573	7751	4285	8853	3949	3926
14N abDOP primer	2706	1112	2591	229	1076	330	1521	1375	2885	4505	6227	3507	2195	1827	3479
16N dcDOP primer	1237	469	1034	757	1046	366	2368	1310	2415	2342	5114	3457	5899	1467	1582
10N abDOP primer	684	552	240	623	223	180	999	712	711		326	163	807	1362	246
6N original DOP primer	851	2299	3768	715	311	339	1412	1792	3018	5354	6575	8727	6103	5952	2854

	D2S1338	D19S433	VWA	TPOX	D18S51	Amel	D5S818	FGA						
Control DNA 007 STR Profile	20	23	14	15	14	16	8	12	15	X	Y	11	24	26
No WGA control (100pg)	183	195				130	169	93		102		160	120	
10N dcDOP primer	350	1359	2005	521	3852	3207	773	1299	1084	616	3093	2895	668	552
12N(2) abDOP primer	975	1268	3383	2139	3512	742	2642	699	619	2500	2780	3073	1635	1395
12N abDOP primer	1237	2335	1940	1382	1801	2784	2353	787	620	1969	7877	3247	1518	1202
14N abDOP primer	1908	2872	2075	1554	4678	1422	1665	651	779	1970	871	3825	746	687
16N dcDOP primer	1493	2180	1432	2281	3226	1457	1149	985	614	1104	3181	3712	940	262
10N abDOP primer			526	520	321	613	603	574				324		275
6N original DOP primer	990	2885	1206	2641	2096	2813	3411	979	230	1042	7923	4286	536	939

Table 21: Comparison of RFU peak heights after DOP-PCR of 100pg of high-quality control DNA (007) with seven different degenerate primers.

	D8S1179		D21S11		D7S820		CSF1PO		D3S1358		TH01		D13S317		D16S539	
Control DNA 007 STR Profile	12	13	28	31	7	12	11	12	15	16	7	9.3	11	9	10	
No WGA control (500pg)	984	1058	824	573	777	534	880	853	1418	1436	1893	1410	2912	1337	1478	
10N dcDOP primer	16,734	22,371	5074	5988	2870	2275	7722	7927	10,678	8464	28,336	21,931	24,903	8054	4745	
12N(2) abDOP primer	19,601	18,100	6536	4953	3158	2007	12,029	14,296	23,670	19,023	28,194	14,221	24,033	17,310	10,561	
12N abDOP primer	22,439	15,181	11,436	4998	5646	7120	15,592	12,442	16,795	15,525	21,952	20,023	32,754	19,903	10,539	
14N abDOP primer	13,199	9360	7804	4036	2241	2612	12,234	10,086	29,102	22,962	26,897	32,022	16,100	8741	8224	
16N dcDOP primer	12,330	10,974	6804	6665	2807	5173	15,849	11,210	13,186	10,593	14,296	13,111	32,371	17,488	9442	
10N abDOP primer	9186	8801	8115	6046	4175	4896	9944	9894	14,772	12,409	20,532	18,086	31,316	21,234	10,052	
6N original DOP primer	13,420	7994	7426	14,210	3345	1546	10,719	12,398	7600	6521	18,553	26,248	27,172	8272	5970	

	D2S1338		D19S433		VWA		TPOX		D18S51		Amel		D5S818		FGA	
Control DNA 007 STR Profile	20	23	14	15	14	16	8	12	15	X	Y	11	24	26		
No WGA control (500pg)	1151	1476	1095	983	1134	1278	2204	983	817	913	1057	1583	807	617		
10N dcDOP primer	6254	8904	4825	7545	20,149	19,890	7229	4845	3896	9513	16,390	18,201	3799	2508		
12N(2) abDOP primer	11,781	10,818	13,586	11,438	15,291	20,961	18,093	5221	5027	23,092	12,586	15,683	9235	6562		
12N abDOP primer	12,007	11,555	11,134	10,870	14,881	20,503	15,863	7717	7499	21,267	24,002	27,394	6988	9970		
14N abDOP primer	9501	7081	11,732	9254	6339	12,731	16,805	4220	4697	8874	6668	12,530	4343	4033		
16N dcDOP primer	9420	11,078	9053	10,160	15,926	20,406	17,660	7099	7672	10,828	11,550	21,640	7157	2722		
10N abDOP primer	6937	6535	8168	8424	16,525	15,050	14,569	5717	5482	24,126	24,487	20,547	5930	6796		
6N original DOP primer	8474	4366	5199	5153	15,004	23,385	11,832	3886	2418	5152	6004	13,087	3966	3471		

Table 22: Comparison of RFU peak heights after DOP-PCR of 500pg of high-quality control DNA (007) with seven different degenerate primers.

Modified DOP-PCR with Compromised Samples

With high-quality DNA, the preliminary data indicated that the 10N dcDOP primer, the modified 12N abDOP primer, and the modified 12N(2) abDOP primer performed best in terms of increasing allele peak heights. Given these results, DOP-PCR with two of these new primers was performed on damaged DNA from a human bloodstain that had been environmentally-exposed for 24 weeks. The amount of template was varied to assess the range of input DNA needed to obtain optimal results. Although the 2009 Dawson Cruz study recommended that no more than 100pg of DNA be used in the DOP-PCR reaction (to ensure profile quality with minimal artifacts) (23), our results show that 100pg may not be enough template when dealing with degraded samples (Table 23). Degraded samples simply may contain lower intact template molecules, and in turn do not provide sufficient DNA for efficient binding of the degenerate primers and subsequent DOP-PCR. The latter presumption (and our results) are further supported by a 2003 study which found that, when amplifying low-copy and/or degraded DNA, WGA requires several hundred picograms of template DNA to be effective in dealing with stochastic selection of alleles (although this depends on the quality and specific characteristics of each sample, and mitigating these stochastic effects may not be possible in all cases) (50).

	D8S1179		D21S11		D7S820		CSF1PO	D3S1358		TH01		D13S317	D16S539
STR Profile from an Environmentally-Damaged Bloodstain (24-week exposure)	12	13	28	29	8	10	11	17	18	9	9.3	12	9
No WGA control (65.7pg)		105	61				67	189	98	89	9.3	520	234
10N dcDOP primer	363	466						578					382
12N(2) abDOP primer	206	208				398			607		560	539	294
No WGA control (328.5pg)	598	457	278	205			319	378	808	177	363	679	410
10N dcDOP primer	787	949	340	178				300	500	220	536	550	369
12N(2) abDOP primer	3148	955	779		392	632	444	2551	3450	2474	1946	2493	3143
No WGA control (657pg)	892	1139	574	417	302	193	711	1693	1614	1272	1436	1384	1370
10N dcDOP primer	1557	2983	810	1241	215	262	831	1749	3728	1111	1919	3668	1390
12N(2) abDOP primer	3937	4172	2061	2774	432	806	1199	9065	6947	4451	2881	6292	3640

	D2S1338		D19S433		VWA	TPOX	D18S51		Amel		D5S818		FGA	
STR Profile from an Environmentally-Damaged Bloodstain (24-week exposure)	22	23	14	16.2	18	8	11	15	16	X	Y	11	12	20
No WGA control (65.7pg)				120	18	96					167	102		123
10N dcDOP primer			211		454							356		
12N(2) abDOP primer		235	383	299	428			191	191			311		585
No WGA control (328.5pg)			428	312	665	283	272		196	720	471	262	355	326
10N dcDOP primer		264	382	545	895	375	448		553	522	209	588		
12N(2) abDOP primer	657	801	2466	922	2204	458	1072	202	320	2645	1628	1345	1782	1342
No WGA control (657pg)	510	559	1110	880	1882	802	792	438	310	991	869	952	767	1119
10N dcDOP primer	716	152	1863	2703	4165	1194	709		358	3060	3101	3758	1379	1019
12N(2) abDOP primer	725	355	4400	4556	6754	1743	1214	2784	345	5703	6154	1857	3126	2097

Table 23: DOP-PCR whole genome amplification of environmentally-damaged DNA in a bloodstain after 24 weeks of exposure: Comparison of RFU values obtained with the 10N dcDOP primer and 12N(2) abDOP primer for three different amounts of input DNA (65.7pg, 328.5pg, and 657pg).

As shown in Table 23, both the 10N and 12N(2) primers were generally effective at improving STR profiling of the damaged template, although they both performed better with a higher amount of input DNA (657pg) than previously recommended. In fact, some allele dropout was observed when less than 657pg of damaged template were added to the DOP-PCR. The electropherograms shown in Figures 18-19 further reveal that the previous assertion that addition of more than 100pg of DNA results in significant artifacts (making results uninterpretable) does not necessarily apply when the candidate template is substantially degraded prior to DOP-PCR.

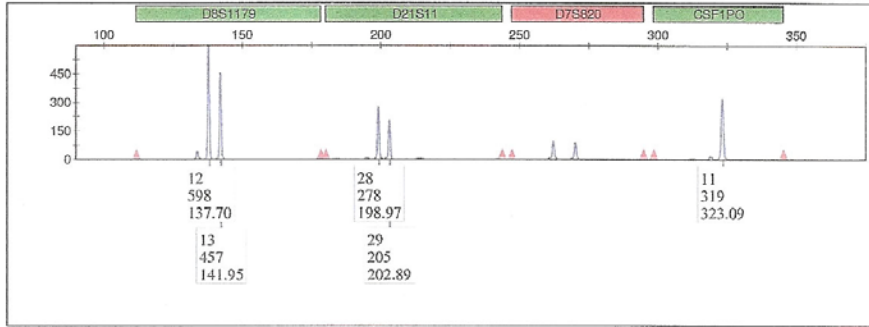


Figure 18A:
STR typing results for an environmentally-damaged bloodstain (Table 23) **prior to DOP-PCR**, with 328.5pg of input DNA.

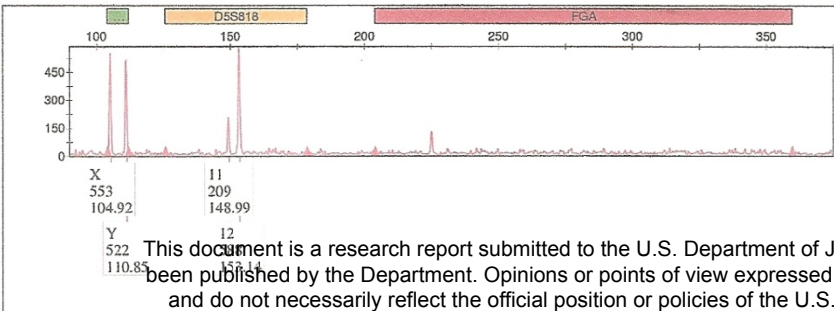
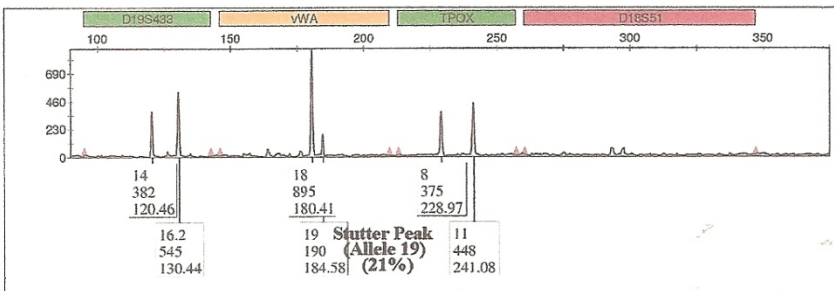
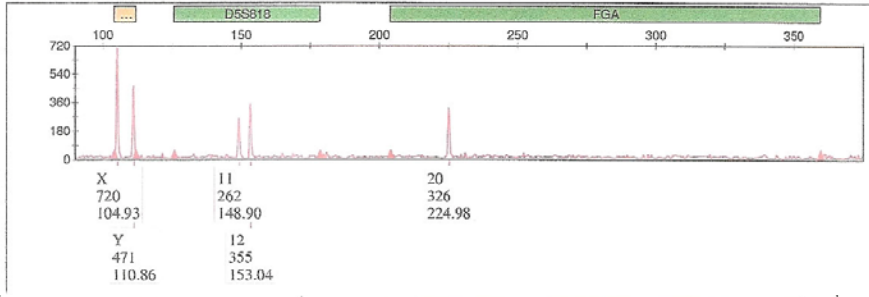
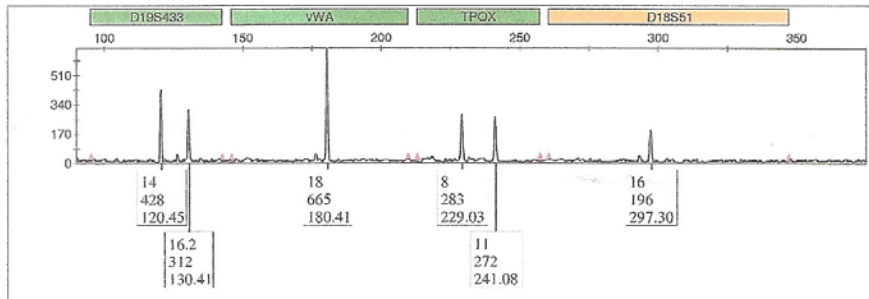
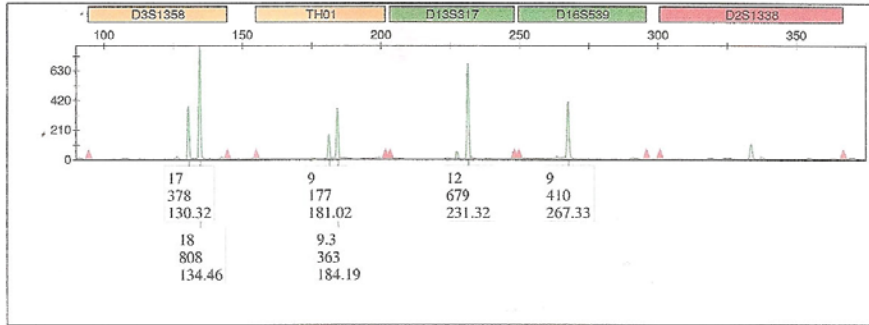


Figure 18B:
Electropherogram results

for DOP-PCR of an environmentally-damaged bloodstain with the **10N dcDOP primer** and 328.5pg of input DNA. These results demonstrate that input amounts greater than the previously-recommended “maximum” of 100pg do not produce substantial artifacts when the template is significantly degraded prior to the DOP-PCR reaction.

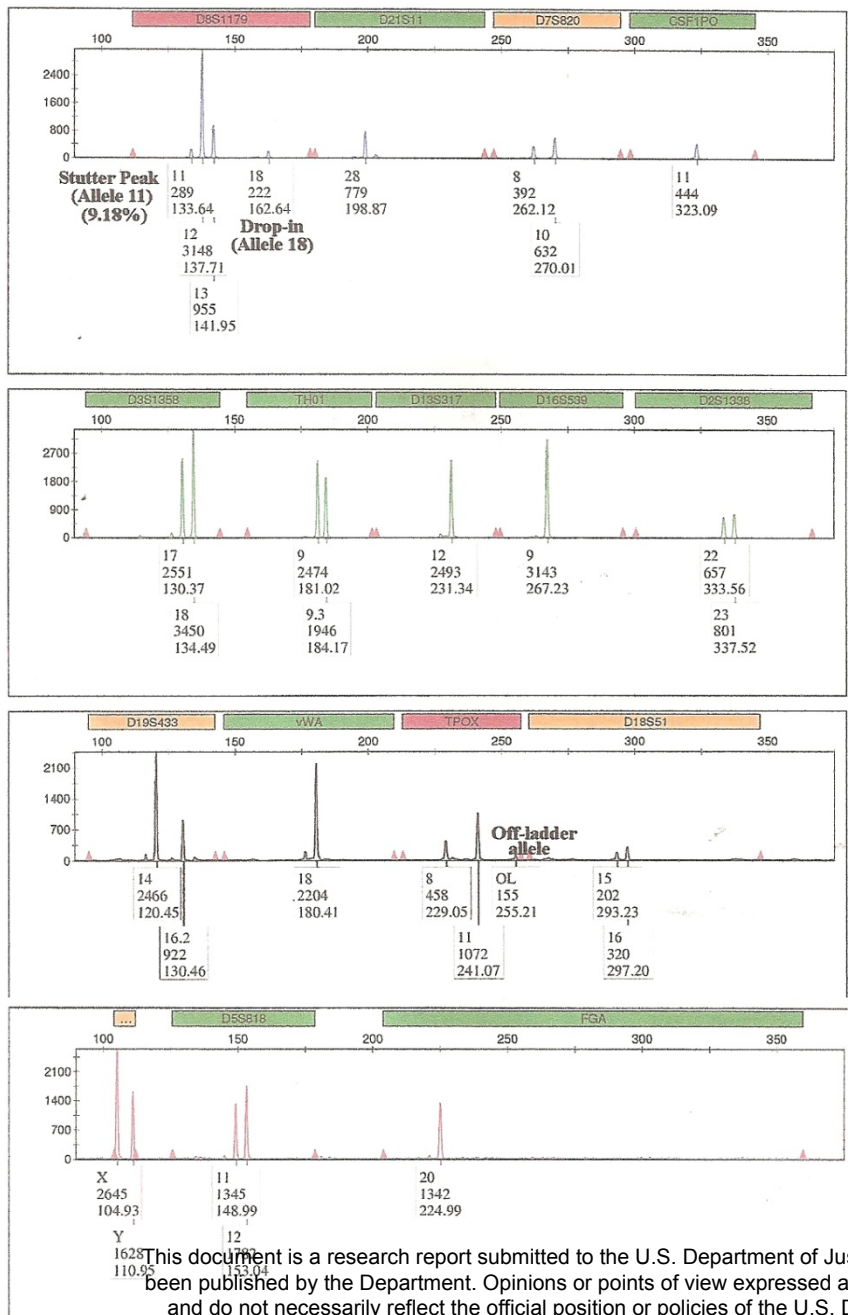
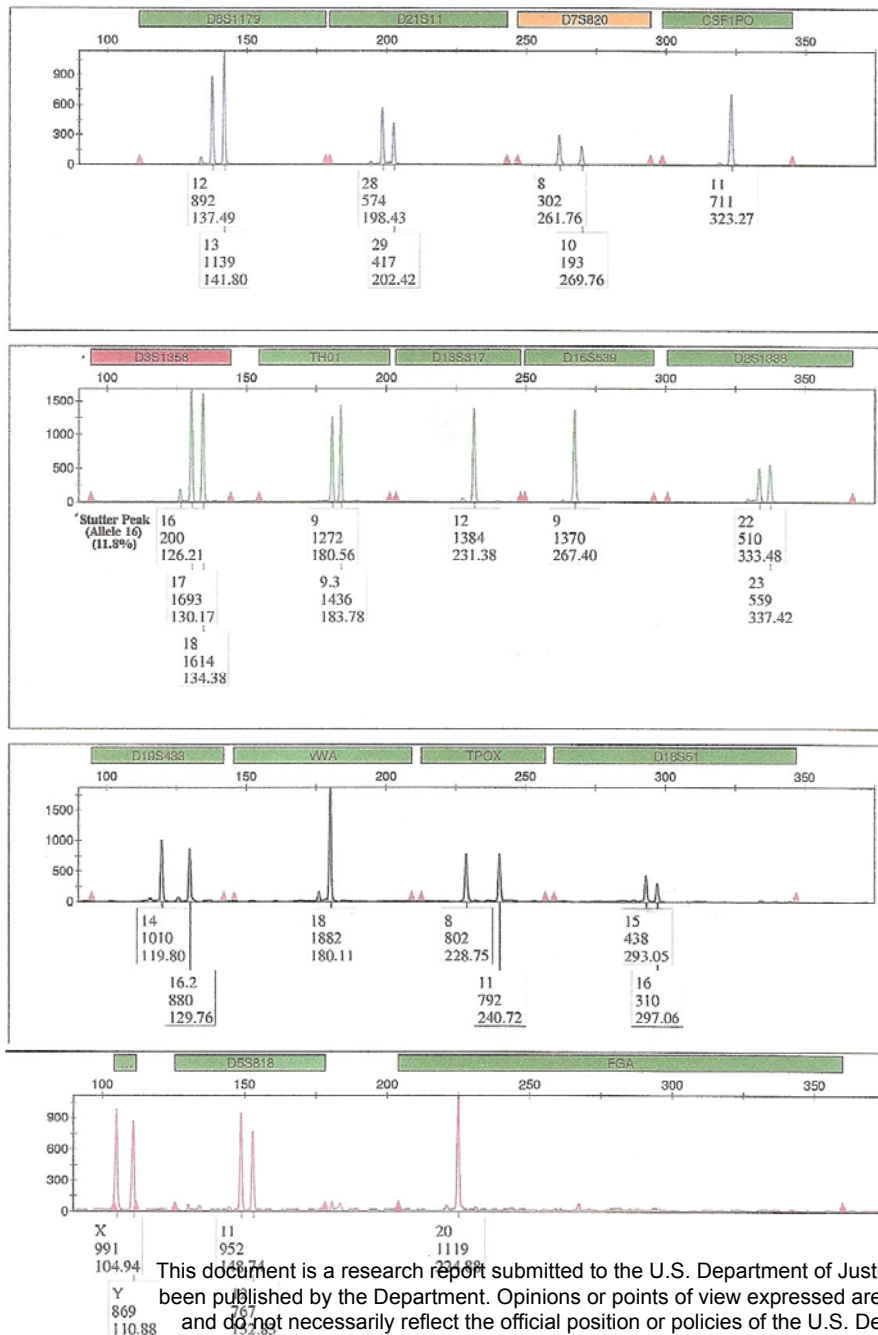


Figure 18C: Electropherogram results for DOP-PCR of an environmentally-damaged bloodstain with the **12N(2) abDOP primer** and 328.5pg of input DNA. Even with three times the previously-recommended input amount, only three artifacts were observed (one stutter peak, a drop-in allele, and one off-ladder allele), as labeled in the

image). Note the higher allele peak heights compared with Figure 18B.



Interestingly, when the input template was increased to 657pg, the 10N dcDOP primer did generate a substantial number of artifacts, but the 12N(2) abDOP primer still produced an electropherogram with minimal artifacts (with the same quantity of input DNA) (Figures 19B and 19C). Figure 19A shows STR typing results from this blood sample (Table 23) prior to DOP-PCR.

Figure 19A:

STR typing results for an environmentally-damaged bloodstain (Table 23) **prior to DOP-PCR**, with 657pg of input DNA.

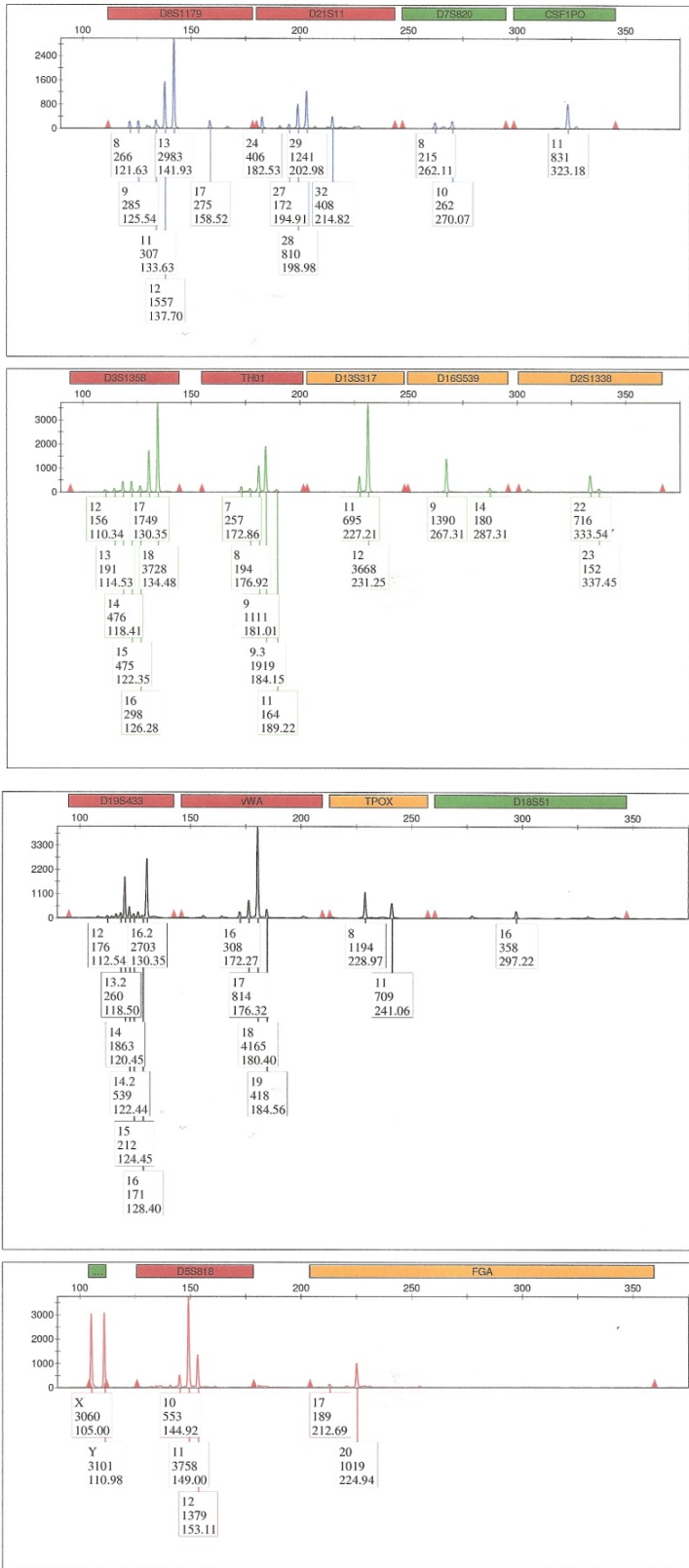


Figure 19B: Electropherogram results for DOP-PCR of an environmentally-damaged bloodstain with the **10N dcDOP primer** and 657pg of input DNA. Substantial artifacts are present (e.g. stutter peaks, drop-in alleles), which would make interpretation of this profile more difficult.

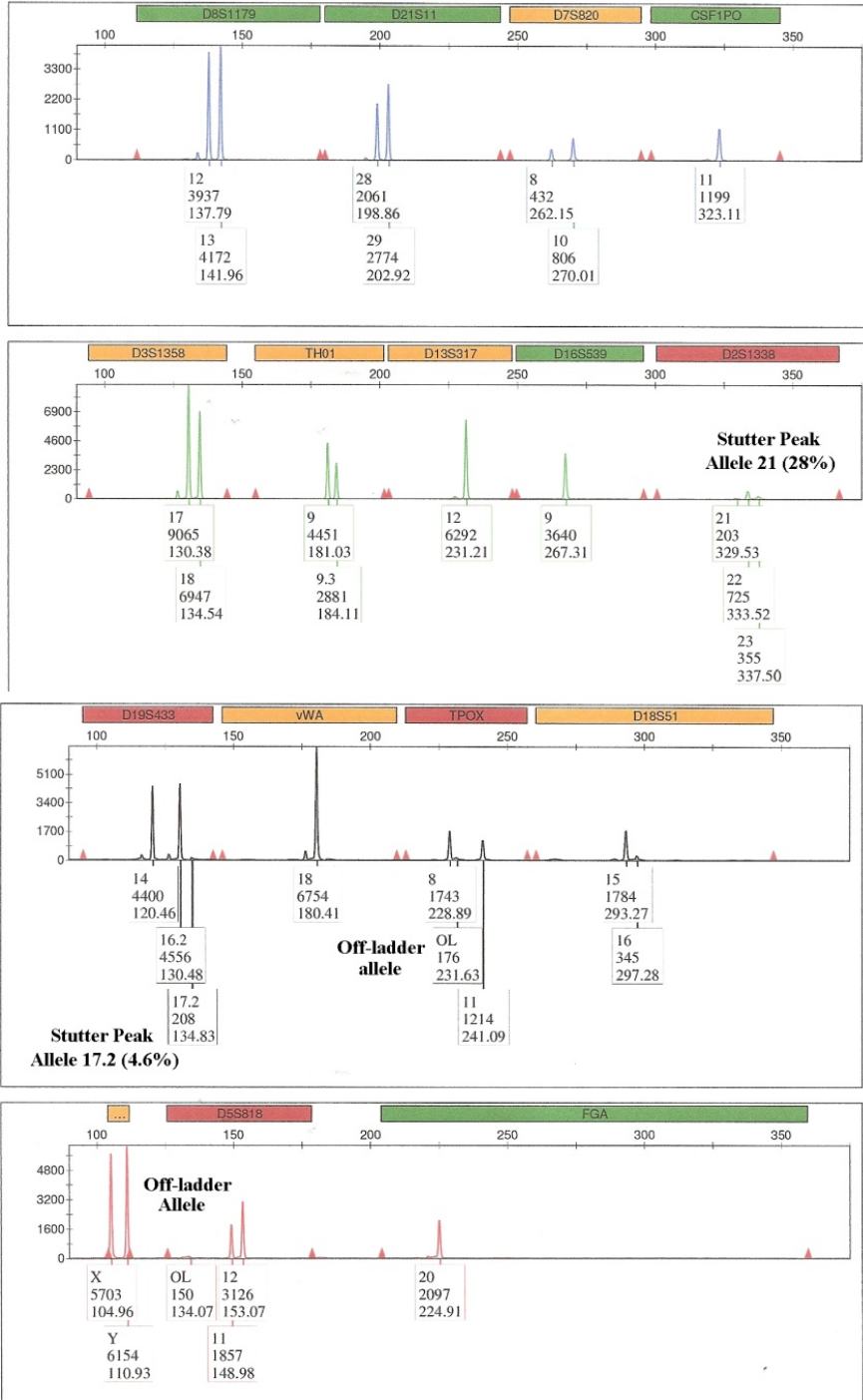


Figure 19C: Electropherogram results for DOP-PCR of an environmentally-damaged bloodstain with the **12N(2) abDOP primer** and 657pg of input DNA. This sample displays only a few artifacts and is thus better quality than the results obtained when the 10N dcDOP primer was used with the same sample and an equivalent quantity of input DNA (Figure 19B).

Table 24 shows results of another environmentally-damaged bloodstain that was amplified with the 10N dcDOP primer and 12N(2) abDOP primer. Since the maximum volume of extract that can be added to the Identifiler® Plus PCR amplification reaction is 10µl, the “before DOP-PCR” quantity listed in the table (728pg) represents the amount of DNA used in pre-DOP-PCR genotyping (10µl × 0.0728 ng/µl). Given that initial STR typing yielded a partial profile with low RFU levels (Figure 20A), a full 1ng of input template DNA was used for the subsequent DOP-PCR reactions.

	D8S1179		D21S11		D7S820		CSF1PO	D3S1358		TH01		D13S317	D16S539
STR Profile from an Environmentally-Damaged Bloodstain (24-week exposure)	12	13	28	29	8	10	11	17	18	9	9.3	12	9
Before DOP-PCR (728pg)	245	299	147	69				312	642	96	91	371	226
10N dcDOP primer	1928	1703		310	177	176	242	3008	2640	1257	382	1485	847
12N(2) abDOP primer	1585	677	653	502				1239	1458	1321	1534	1181	973

	D2S1338	D19S433	VWA	TPOX	D18S51		Amel	D5S818	FGA					
STR Profile from an Environmentally-Damaged Bloodstain (24-week exposure)	22	23	14	16.2	18	8	11	15	16	X	Y	11	12	20
Before DOP-PCR (728pg)			185	267	373	158	120	112	124	291	332	336	143	215
10N dcDOP primer	190		1865	1063	1735		415			2471	3104	1632	885	939
12N(2) abDOP primer			2681	1667	754	400	875	316	167	1424	2224	913		600

Table 24: DOP-PCR whole genome amplification of environmentally-damaged DNA in a bloodstain after 24 weeks of exposure: Comparison of RFU peak heights obtained with the 10N dcDOP primer and 12N(2) abDOP primer (1ng total input template DNA).

The electropherograms shown in Figures 20B-20C reveal DOP-PCR results with each primer when a full 1ng (1000pg) of damaged template was used during WGA. Stutter peaks were observed at a few loci with both primers, although these artifacts are generally interpretable and could potentially be accounted for if 1) replicate DOP-PCR reactions were carried out on the same sample and/or 2) if the stochastic interpretation threshold were raised.

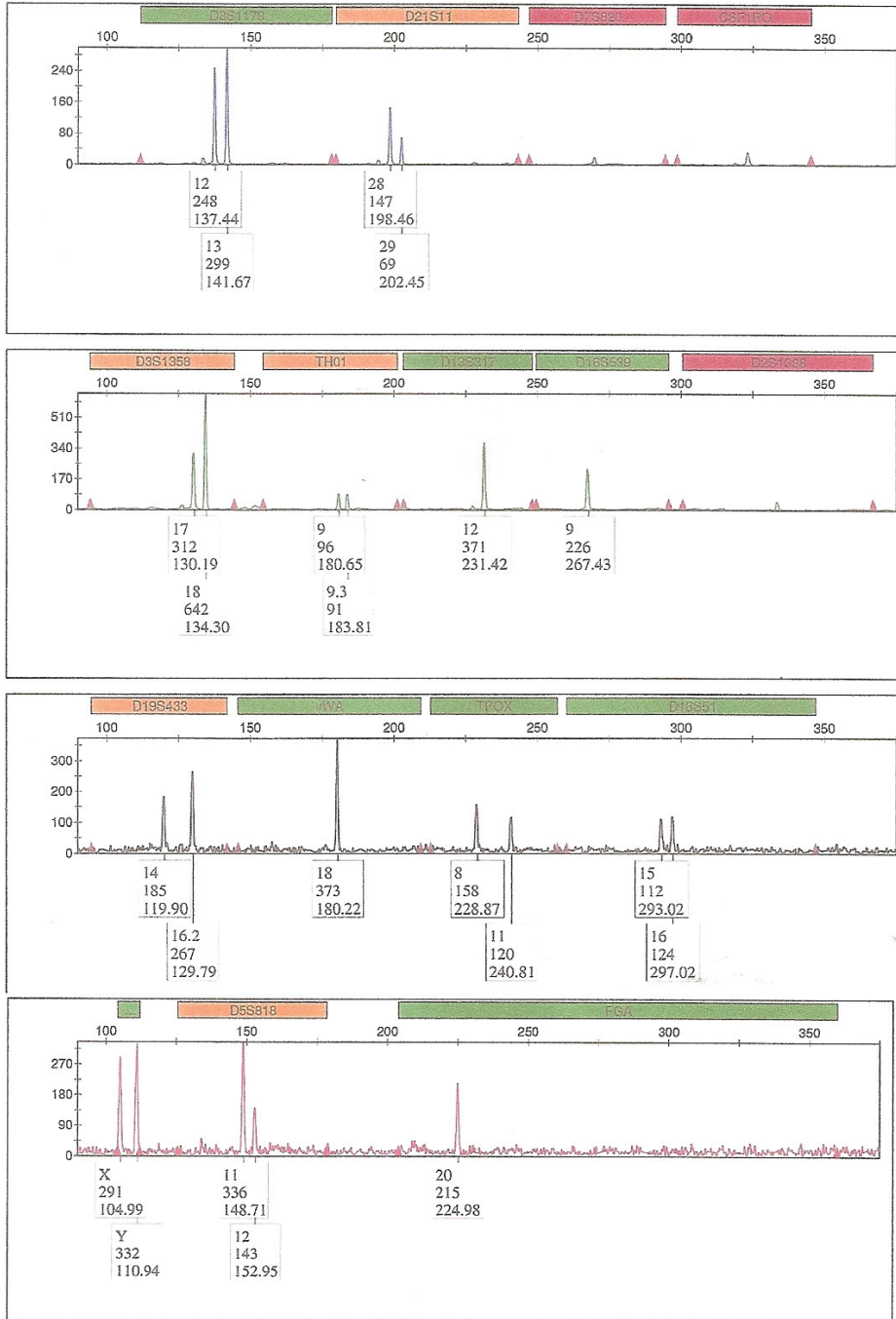


Figure 20A: STR typing results for an environmentally-damaged bloodstain (Table 24) **prior to DOP-PCR**, with 728pg of input DNA.

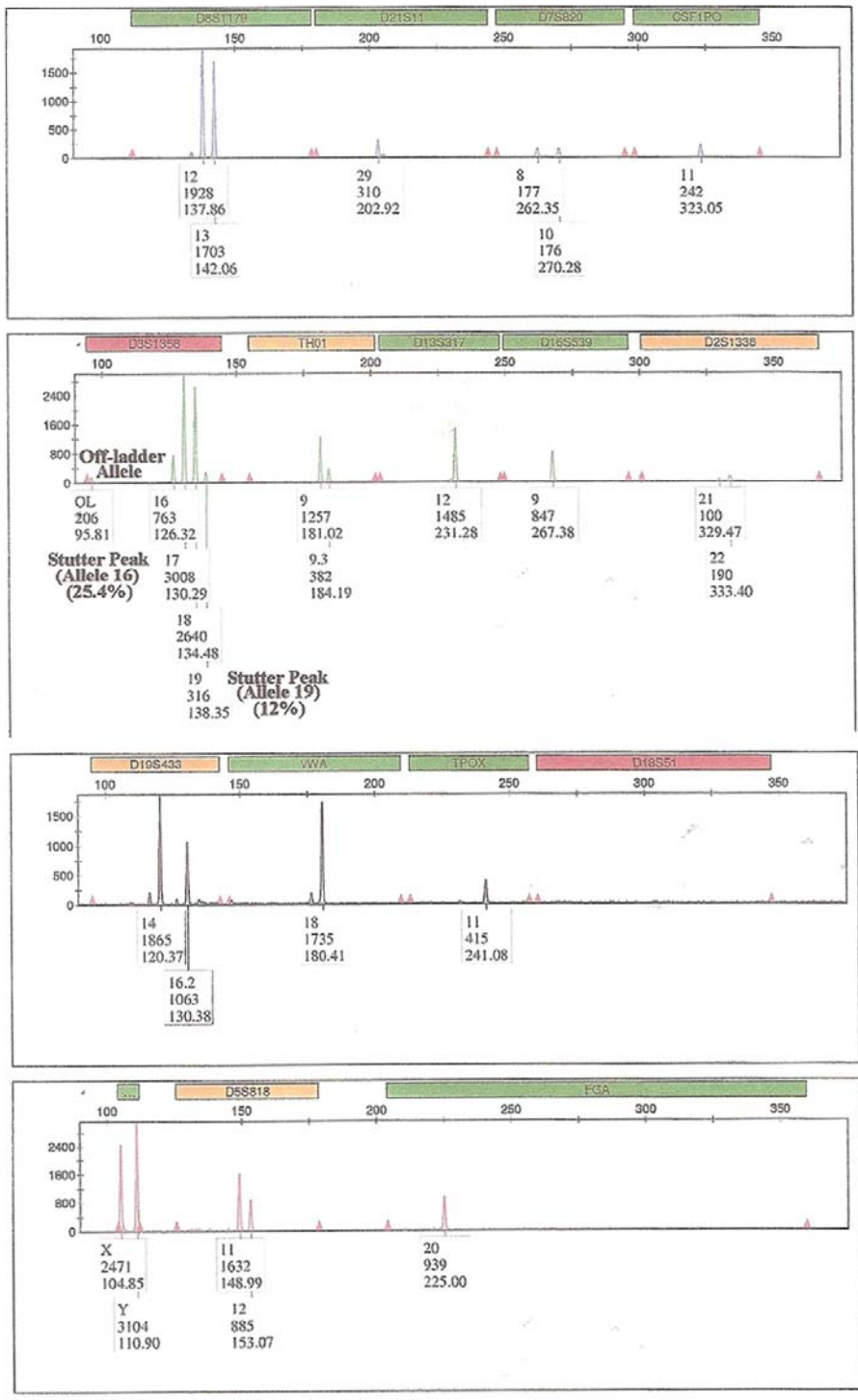


Figure 20B: Electropherogram results for DOP-PCR of an environmentally-damaged bloodstain with the **10N dcDOP primer** and 1 ng of input DNA. Two stutter peaks and an off-ladder allele are observed at locus D3S1358, but the profile does not exhibit excessive or uninterpretable artifacts, even with 1ng of input template.

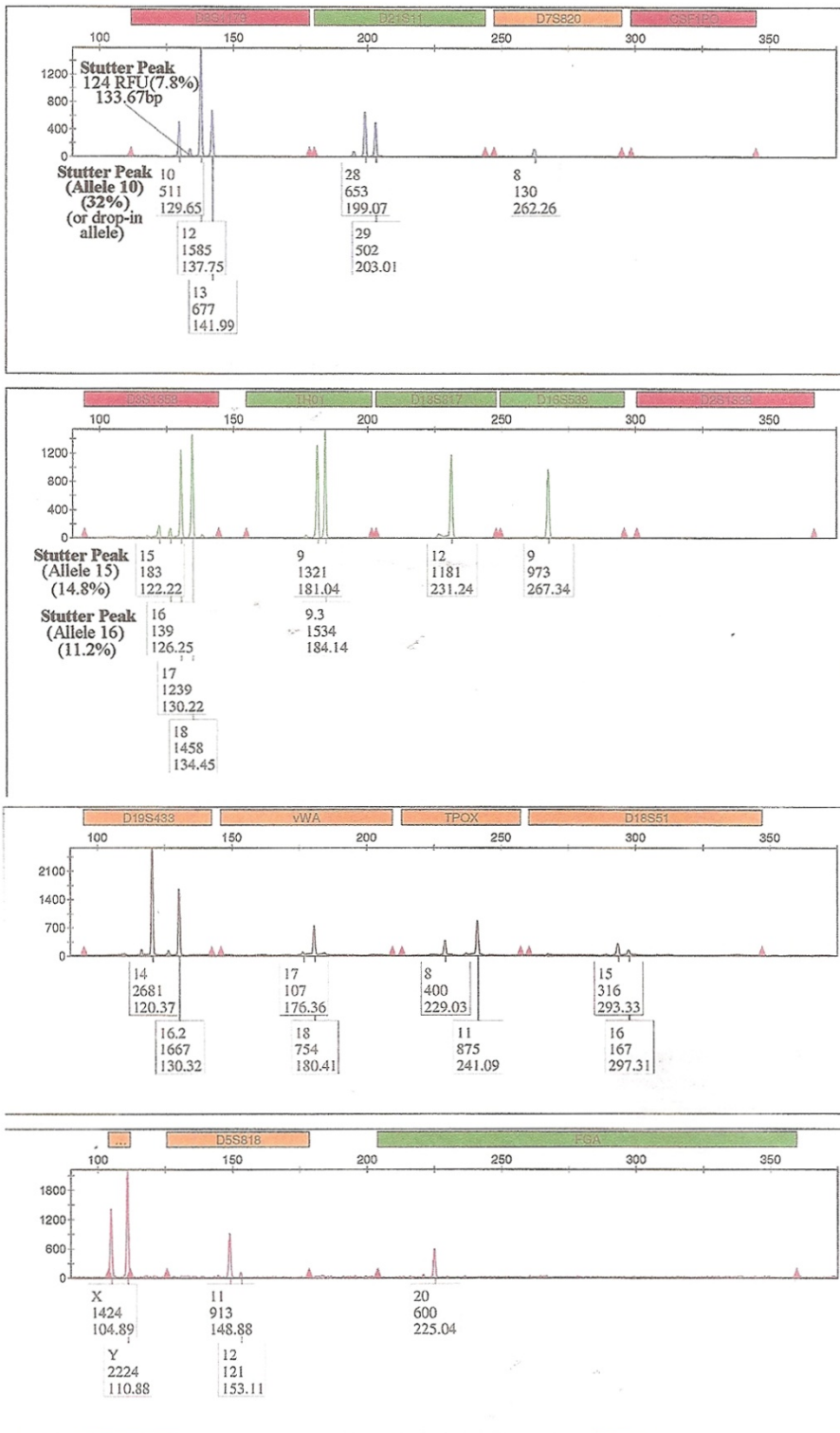


Figure 20C: Electropherogram results for DOP-PCR of an environmentally-damaged bloodstain with the **12N(2) abDOP primer** and 1ng of input DNA. Stutter peaks are observed at both D8S1179 and D3S1358 loci, but the profile does not exhibit excessive or uninterpretable artifacts, even with 1ng of input template.

In yet another example (Table 25), pre-WGA genotyping of an environmentally-damaged bloodstain yielded a partial, low RFU profile. Again, since the maximum volume of extract that can be added to the Identifiler® Plus PCR amplification reaction is 10µl, the “before DOP-PCR” quantity listed in the table (107pg) represents the amount of DNA used in pre-DOP-PCR genotyping (10µl × 0.0107 ng/µl). Since this initial STR typing yielded a partial profile with low RFU levels (Figure 21A), a full 1ng of input template DNA was used for the subsequent DOP-PCR reactions. DOP-PCR results using the 10N dcDOP and 12N(2) abDOP primers are shown in Figures 21B and 21C. Still consistent with the previously-described results, some artifacts are observed, but they are not excessive and could potentially be accounted for if 1) replicate DOP-PCR reactions were carried out on the same sample and/or 2) if the stochastic interpretation threshold were raised.

	D8S1179		D21S11		D7S820		CSF1PO		D3S1358		THO1		D13S317		D16S539	
STR Profile from an Environmentally-Damaged Bloodstain (24-week exposure)	11	14	30.2	32.2	10	11	9	13	14	18	7	9.3	11	12	9	12
Before DOP-PCR (107pg)	68								200	226	152					
10N dcDOP primer	2942	3446	1005	1140	183	407	338	323	5320	4783	2437	2529	1396	523	1165	459
12N(2) abDOP primer	697	3085	492	191	291	283	369	360	6405	3910	3630	2838	664	330	783	844

	D2S1338		D19S433		vWA		TPOX		D18S51		Amel		D5S818		FGA	
STR Profile from an Environmentally-Damaged Bloodstain (24-week exposure)	23	25	14	16	16	19	8	15	19	X	12	21	23			
Before DOP-PCR (107pg)			66	144			118			178	72	54				
10N dcDOP primer	166	247	3048	3198	2195	1348	1830	592		8150	3122	676	196			
12N(2) abDOP primer		327	4706	4981	1198	2637	3765	399	390	10,018	3234	426	486			

Table 25: DOP-PCR WGA of environmentally-damaged DNA from a bloodstain after 24 weeks of exposure: Comparison of RFU peak heights obtained with the 10N dcDOP primer and 12N(2) abDOP primer (1ng total input template DNA).

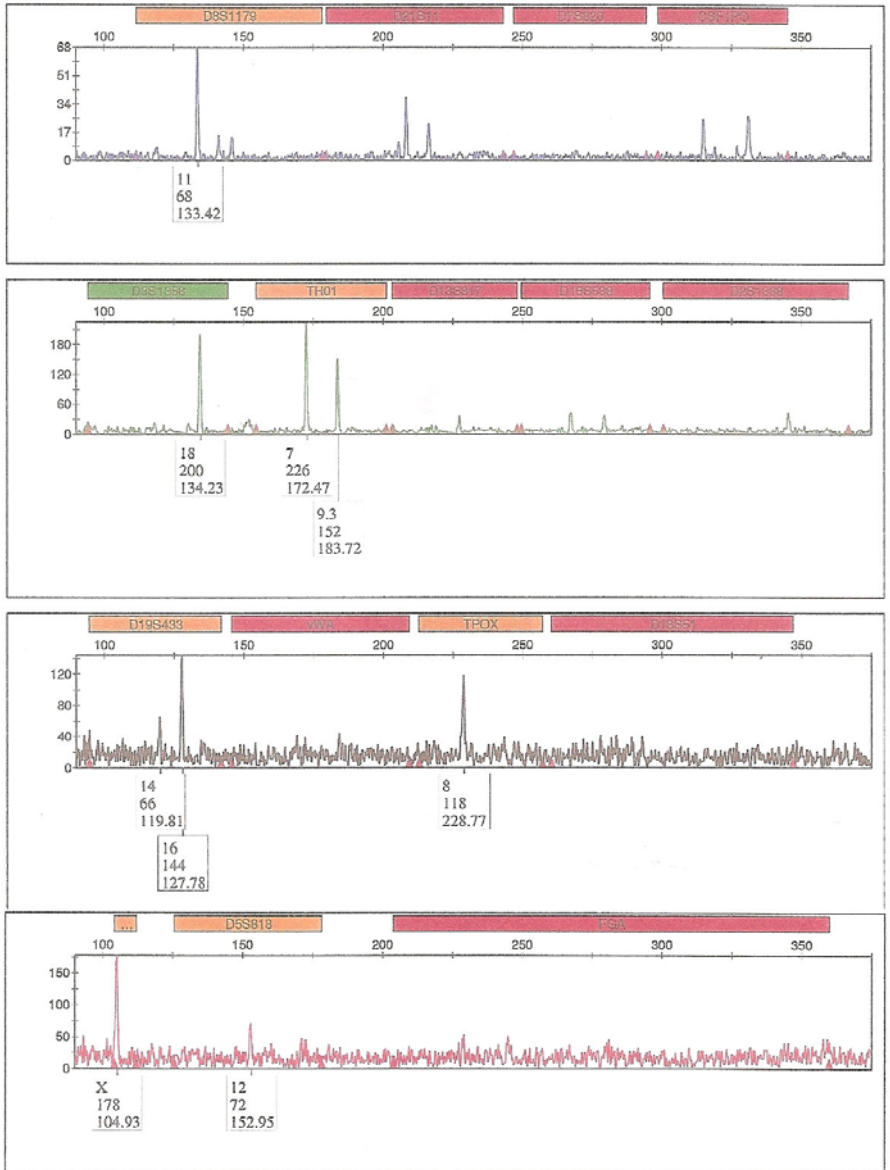


Figure 21A: STR typing results for an environmentally-damaged bloodstain (Table 25) prior to DOP-PCR, with 107pg of input DNA.

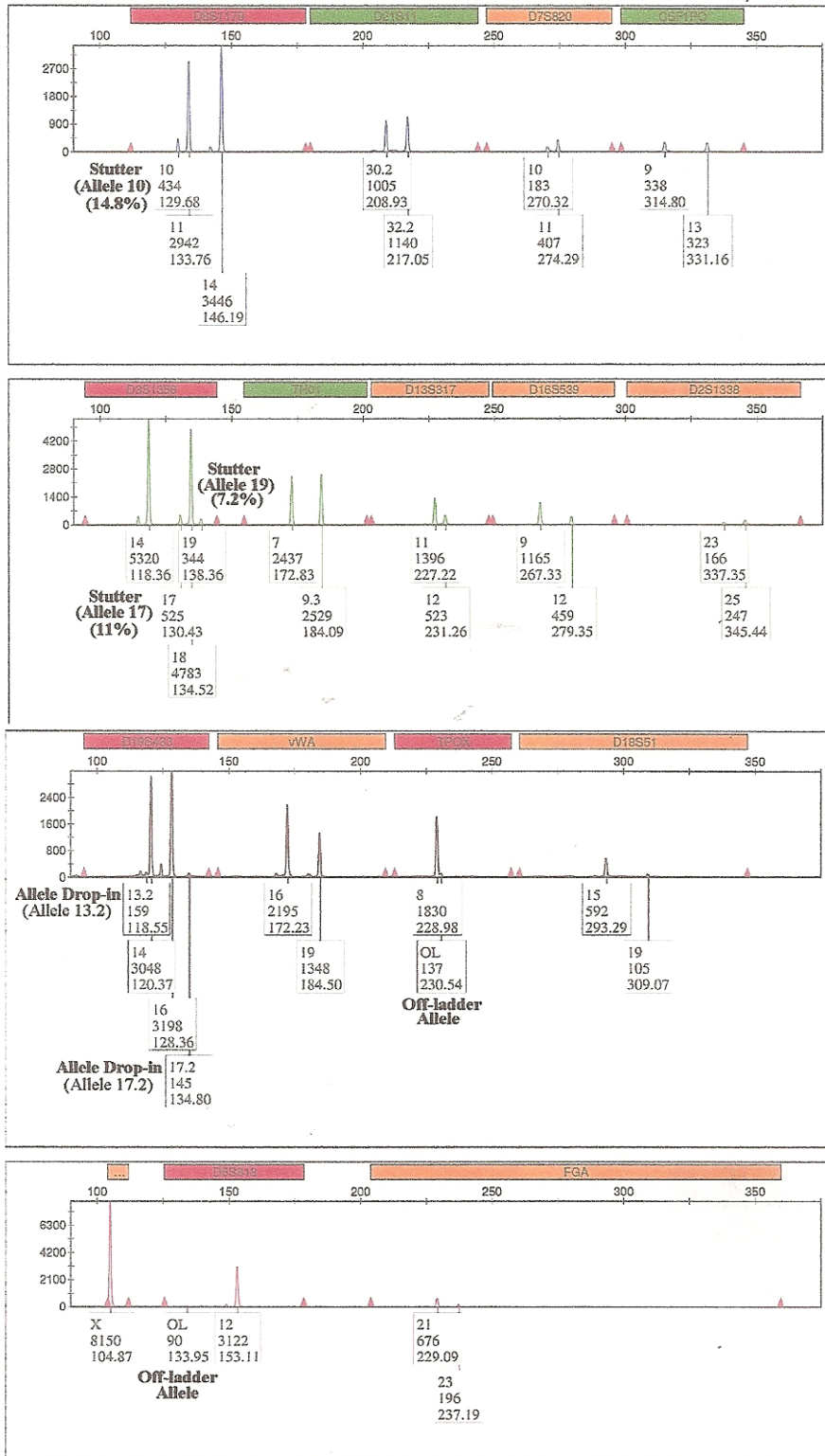


Figure 21B: Electropherogram results for DOP-PCR of an environmentally-damaged bloodstain with the 10N dcDOP primer and 1ng of input DNA. Multiple stutter peaks, two off-ladder alleles, and two drop-in alleles are observed.

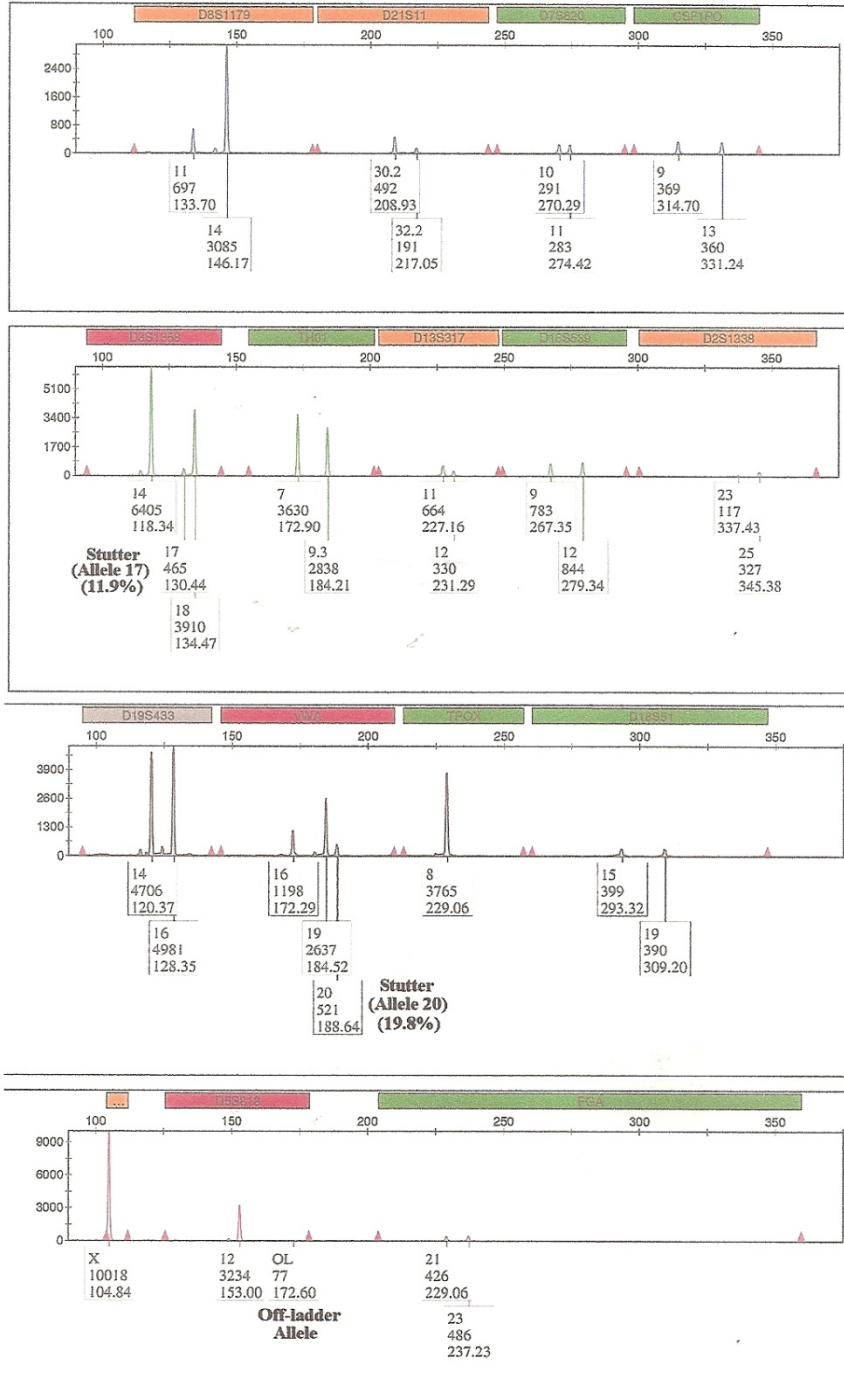


Figure 21C: Electropherogram results for DOP-PCR of an environmentally-damaged bloodstain with the **12N(2) abDOP primer** and 1ng of input DNA. This sample displays only a few artifacts and is thus better quality than the results obtained when the 10N dcDOP primer was used with the same sample and an equivalent quantity of input DNA (Figure 21B).

In addition to environmentally-damaged bloodstains, DOP-PCR reactions also were carried out on damaged DNA from human skeletal remains. Table 26 shows an example of DOP-PCR results (using three different primers) with degraded DNA from a contemporary human bone. With this particular sample, 413pg of initial input DNA yielded a very low RFU profile when amplified with the Identifiler® Plus PCR amplification kit (10µl × 0.0413 ng/µl) (Figure 22A). For this reason, 1000pg (1ng) of DNA was used in the subsequent DOP-PCR reactions in an attempt to provide sufficient template for the degenerate primers and to try to mitigate stochastic sampling during WGA. Interestingly, with this sample, very few stochastic artifacts appeared in any of the resulting electropherograms (Figures 22B-22D). Furthermore, both the 12N abDOP and 12N(2) abDOP primers outperformed the 10N dcDOP primer (in terms of increased RFU peak heights) at nearly every locus examined.

	D8S1179	D21S11	D7S820	CSF1PO	D3S1358	TH01	D13S317	D16S539							
STR Profile from Contemporary Skeletal Remains (Environmental Damage: Bone 047.002.002)	13	14	31	10	11	10	12	15	16	6	7	12	13	10	12
Before DOP-PCR (413pg)	90	148	256	59	80	366	422	126	133	300	80	89			
10N dcDOP primer	1987	783	3049	212	267	269	226	1189	1270	1399	1228	709	2003	371	1874
12N abDOP primer	2673	3519	1423	507	371	385		1931	1861	1146	2059	1621	1059	2003	861
12N(2) abDOP primer	3200	1552	2249		290		1703	1162	1788	930	1904	1348	1157	770	682

	D2S1338	D19S433	VWA	TPOX	D18S51	Amel	D5S818	FGA							
STR Profile from Contemporary Skeletal Remains (Environmental Damage: Bone 047.002.002)	22	23	13.2	14	16	8	11	15	17	X	Y	12	13	19	25
Before DOP-PCR (413pg)	82	98	119	60	516	123	147	64	157	210	75	101			
10N dcDOP primer	578		1033	944	1614	632	254	271	798	1391	477	1325	328	480	
12N abDOP primer		347	593	1426	2377	753	1136	458	158	2003	1487	1259	1710	1275	479
12N(2) abDOP primer	306	1758	1132	1195	2964	857	1809	836	750	2178	2388	905	2324	1313	501

Table 26: DOP-PCR WGA of degraded DNA from an environmentally-damaged contemporary human bone sample: Comparison of RFU peak heights obtained using three different degenerate primers [10N dcDOP, 12N abDOP, and 12N(2) abDOP] and with 1000pg (1ng) total input DNA.

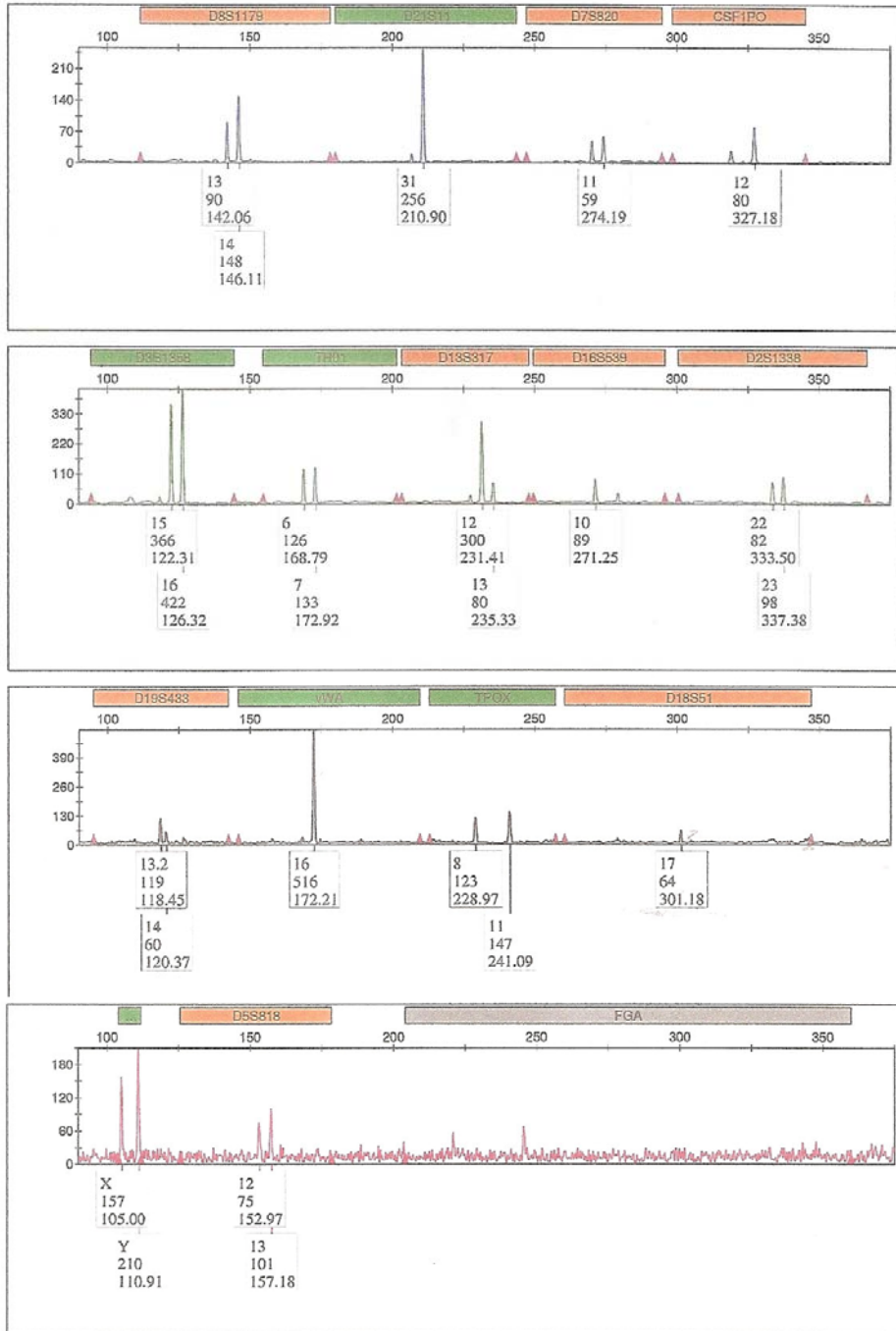


Figure 22A: STR typing results for environmentally-damaged DNA from a contemporary human bone sample (Table 26) prior to DOP-PCR, with 413pg of input DNA.

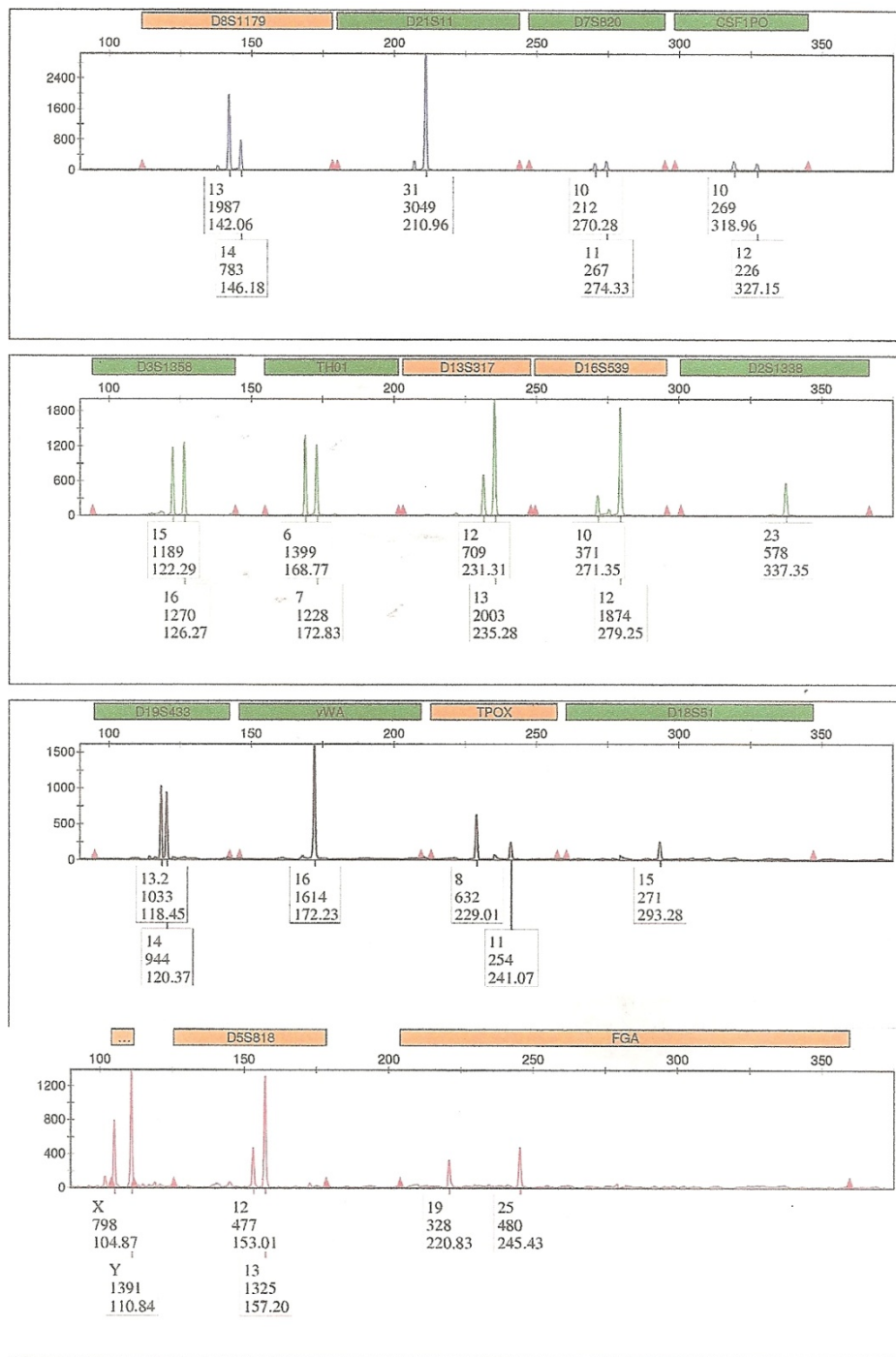


Figure 22B: Electropherogram results for DOP-PCR of environmentally-damaged DNA from a contemporary human bone sample with the **10N dcDOP primer** and 1ng of input DNA. No stochastic artifact peaks were observed.

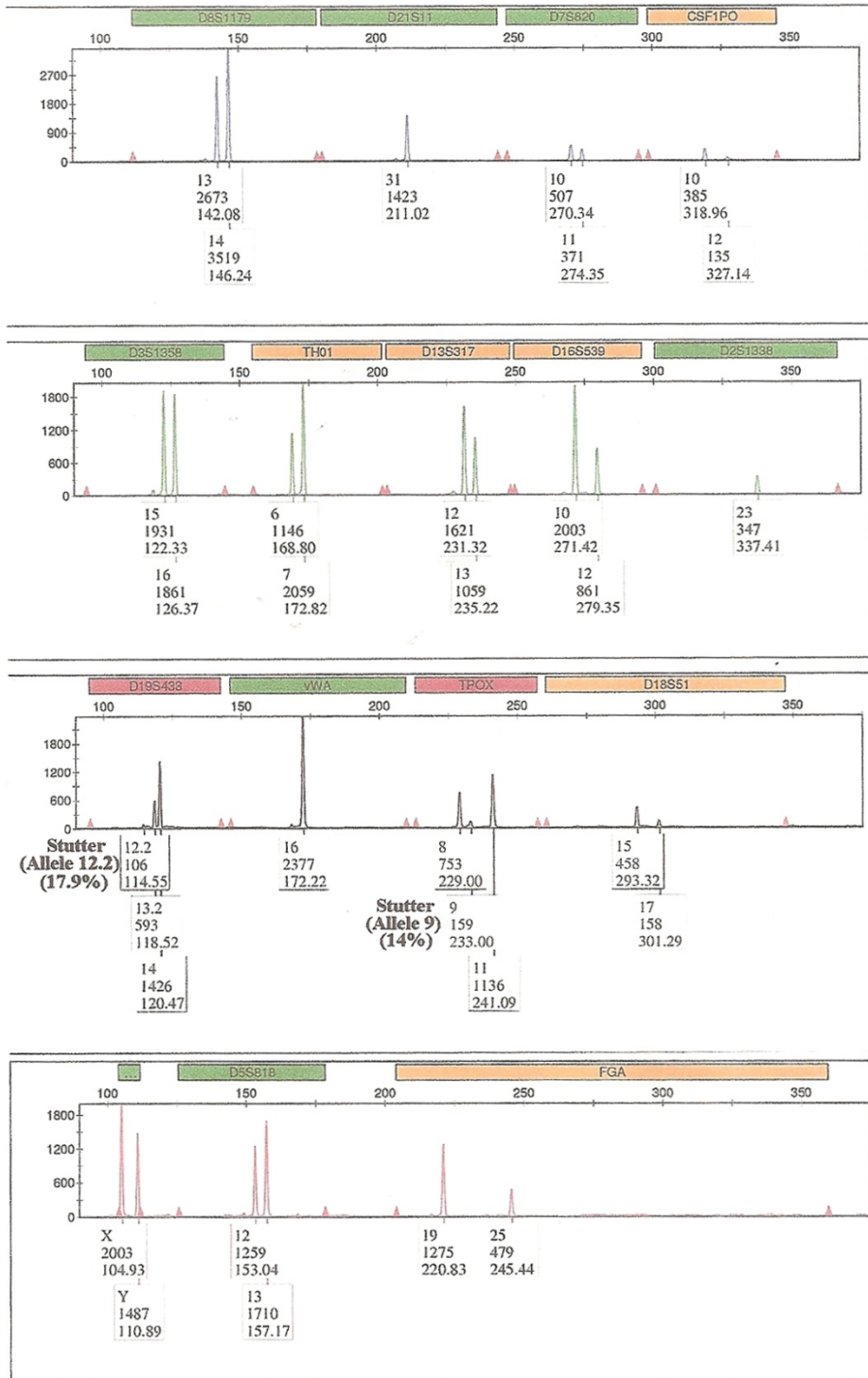


Figure 22C: Electropherogram results for DOP-PCR of environmentally-damaged DNA from a contemporary human bone sample with the **12N abDOP primer** and 1ng of input DNA. Two stutter peaks were observed (17.9% and 14%, respectively). DOP-PCR with this primer outperformed the 10N dcDOP primer (in terms of increased RFU peak heights) at virtually every locus examined (see Table 26).

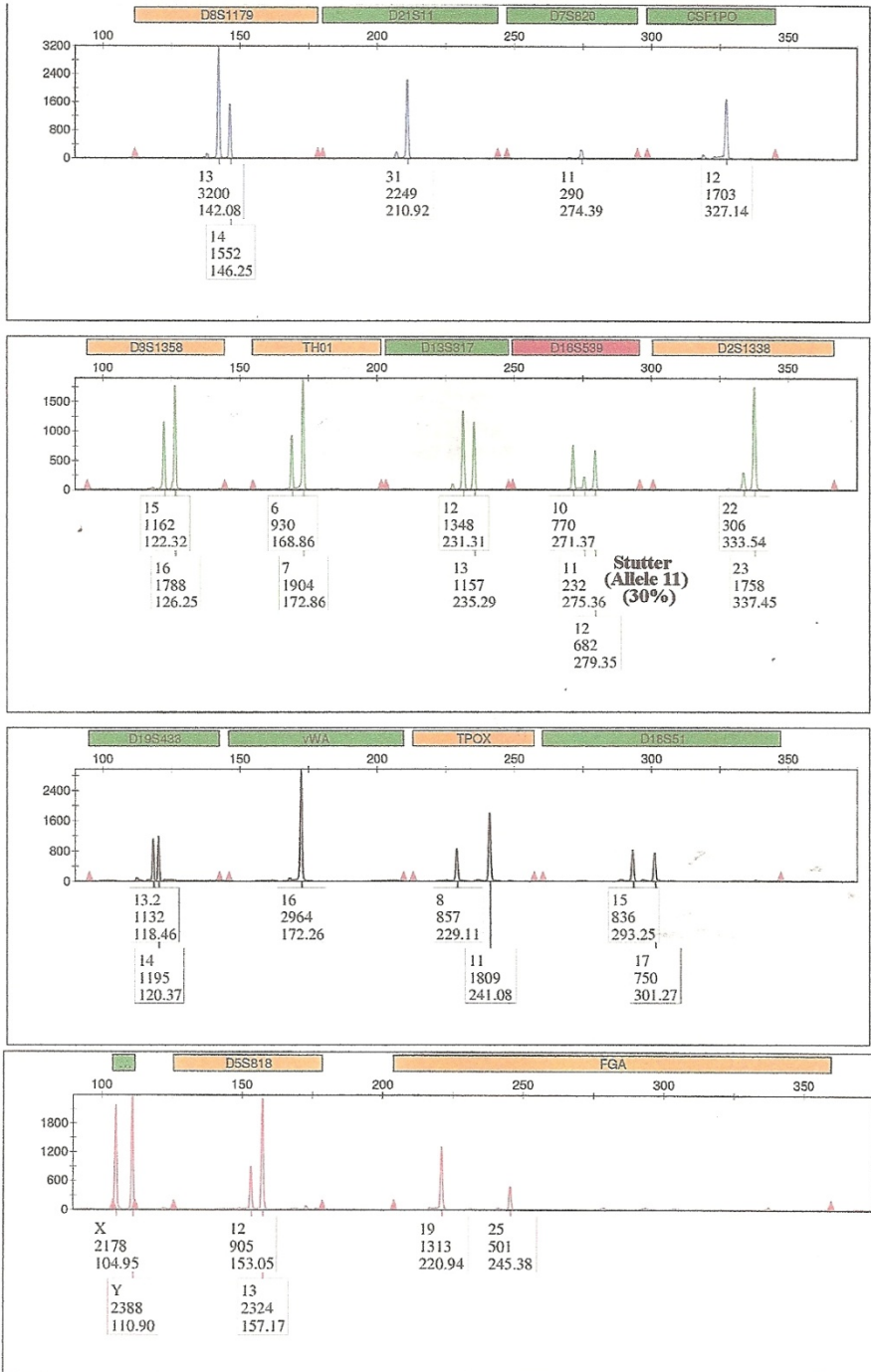


Figure 22D: Electropherogram results for DOP-PCR of environmentally-damaged DNA from a contemporary human bone sample with the **12N(2) abDOP primer** and 1ng of input DNA. Only one stutter peak was observed, despite adding ten times the previously-recommended maximum of 100pg template. DOP-PCR with this primer (as well as with the 12N abDOP primer, Figure 22C) outperformed the 10N dcDOP primer (in terms of increased RFU peak heights) at virtually every locus examined (see Table 26).

A set of historical skeletal remains (120-year-old Civil War bones) also were subjected to WGA with the three modified DOP-PCR primers. It should be noted that no single extract from these remains yielded a full STR profile when initially examined (i.e. prior to WGA). Fifty different bone sections (tibiae, femora, and teeth) were extracted via three different methods, amplified with the AmpFISTR Identifiler® Plus PCR amplification kit, and the results were compiled to generate a consensus profile (Table 27).

Sample ID	D8S1179	D21S11	D7S820	CSF1PO	D3S1338	TH01	D13S317	D16S539	D2S1338	D19S433	vWA	TPOX	D18S51	AMEL	D5S818	FGA
Tooth #1_Hi-Flow-E1	13	32			17,18	9	12	9		12,16	14			X,Y	11,12	19
Tooth #1_Hi-Flow-E2	13				18					12	14			Y		
Tooth #2_AFDIL-E1	13	28			17,18	6,9	11,12	9,11		12,16	14,20	11	17	X,Y	11,12	20
Tooth #3_AFDIL-E1	13	28,32			17,18	6				12,16				X,Y	11,12	20
Tooth #4_Hi-Flow-E1	13				17,18					12,16	20			X,Y	11,12	19
Tooth #4_Hi-Flow-E2	13				17					12,16				X,Y	11	
R.femur 001.001_Hi-Flow-E1	13	32			17		11	11			14,20			X,Y		
R.femur 001.001_Hi-Flow-E2	13				6						11					
R.femur 001.002_AFDIL-E1	13	28,32			17,18	6	11,12	9,11		14,20	8,11	15		X,Y	11,12	19,20
R.femur 001.002_AFDIL-E2														X		
R.femur 002.001_AFDIL-E1	13				17									X,Y		
R.femur 002.002_Hi-Flow-E1	13	28,32			17,18	6,9	11,12	9,11		14,20	11	17		X,Y	11,12	19,20
R.femur 002.002_Hi-Flow-E2	13				17,18	6		9						X,Y		
R.femur 003.001_AFDIL-E1	13	28,32			17,18	6,9	11,12	9		20			15	X,Y	11,12	19,20
R.femur 003.002_Hi-Flow-E1	13				17,18					14,20				X,Y		
R.femur 004.001_Hi-Flow-E1	13	28			17,18	9	11,12			20	11	15		X,Y	11,12	
R.femur 004.002_AFDIL-E1	13	32			17,18	6	12			14	11	17		X,Y	11,12	19,20
R.femur 005.001_AFDIL-E1	13	28			17,18	6				20	11			X,Y	11,12	
R.femur 005.002_Hi-Flow-E1	13	28			17,18	6,9	11	9		16	14	11		X,Y	11,12	
R.femur 005.002_Hi-Flow-E2	13				6,9		9				11	15		X	11,12	
R.femur 006.001_AFDIL-E1	13				17	6,9	11	9			20	11		X,Y		
R.femur 006.002_Hi-Flow-E1	13	28,32	9,11		17,18	6,9	11,12	9,11		12	14,20	11	15	X,Y	11,12	19,20
R.femur 007.001_Hi-Flow-E1	13	28,32			17,18	6,9	11,12	9,11		12	14	11	17	X,Y	11,12	19,20
R.femur 007.002_AFDIL-E1	13	28	9,11		17,18	6,9	11,12	9		14,20	11	15,17		X,Y	11,12	19,20
R.femur 008.001_AFDIL-E1	13	32			17,18	6	12	9,11		14,20	11			X,Y	11,12	19,20
R.femur 008.002_Hi-Flow-E1	13	28			17,18					12	11			X,Y	11,12	
R.femur 009.001_Organic-E1	13	28			17,18	9	11,12	9		12,16	14	11		X,Y	11,12	19,20
R.femur 010.001_Organic-E1	13				17,18		12			12,16	14	11		X	11	
R.femur 010.002_Hi-Flow-E1										14						
R.femur 011.001_Hi-Flow-E1	13	28	11		17,18	6,9	12	11		12,16	14,20			X,Y	11,12	19
R.femur 011.002_Organic-E1	13	28			17,18	6,9	11,12	9,11		12,16	14,20	11		X,Y	11,12	19,20
R.femur 012.001_Hi-Flow-E1	13	28			17,18	6	11,12			12,16	14,20	11		X,Y	11	19,20
R.femur 012.002_Organic-E1	13	28,32		9	17,18	6,9	11,12	9,11	17,19	12,16	14,20	11		X,Y	11,12	19,20
Tibia 003.001_Organic-E1	13	32		9	17,18	6,9	11,12	9,11		12,16	20	11		X,Y	11,12	19
Tibia 003.002_Hi-Flow-E1	13				17,18	9	11,12	11		14,20	11			X,Y	11,12	20
Tibia 008.001_Hi-Flow-E1	13	28,32	9,11		17,18	6,9	11,12	9,11		14,20	11	17		X,Y	11,12	19,20
Tibia 008.001_Hi-Flow-E2	13				17	6,9	11,12			14,20	11			X,Y		19
Tibia 008.002_AFDIL-E1	13	28,32	9,11		17,18	6,9	11,12	9,11		14,20	11	15,17		X,Y	11,12	19
Tibia 009.001_Hi-Flow-E1	13	28,32			17,18	6,9	11,12	9		14,20	11	17		X,Y	11,12	
Tibia 009.001_Hi-Flow-E2	13				17,18	9	12	9		12	14,20	11		Y	11,12	
Tibia 009.002_AFDIL-E1	13	32			17,18		12	9						X,Y	12	19
Tibia 011.001_Hi-Flow-E1	13	28			17,18	6,9	11,12	9,11		12	14	11		X,Y	11,12	19
Tibia 011.001_Hi-Flow-E2	13				17,18	9								X,Y	11	19
Tibia 011.002_AFDIL-E1	13	28,32	9,11		17,18	6,9	11,12	9		14,20	11	17		X,Y	11,12	19
Tibia 012.001_Organic-E1	13		9		17,18	6,9	11	9		12,16	14,20	11	15	X,Y	11,12	
Tibia 012.002_Hi-Flow-E1	13				17,18		11							X		
Tibia 013.001_Hi-Flow-E1	13				17,18			9,11			14	11		X,Y	11	
Tibia 013.002_AFDIL-E1	13	28,32			17,18	6	11,12	11		14,20	11	15		X,Y	11,12	19
Tibia 014.001_AFDIL-E1	13				17,18	6				20				X,Y	11,12	
Tibia 014.002_Hi-Flow-E1	13	28,32	11		17,18	6,9	11,12	9,11		12,16	14,20	11		X,Y	11,12	19,20
Tibia 014.002_Hi-Flow-E2	13				17,18	9	12	9		16	20	11	17	X,Y	11	19
Tibia 015.001_Hi-Flow-E1	13	32			17,18		11,12	9		12	14,20	11		X,Y	11,12	19,20
Tibia 015.002_AFDIL-E1	13	28,32	9,11		17,18	6,9	11,12	9,11		12	14,20	11	17	X,Y	11,12	19,20
Tibia 016.001_AFDIL-E1	13	28,32	9,11		17,18	6,9	11,12	9,11		14,20	11	15,17		X,Y	11,12	19,20
Tibia 016.002_Hi-Flow-E1	13	28,32	9		17,18	6,9	11,12	9,11		12	14,20	11	15,17	X,Y	11,20	19,20
Tibia 017.001_Hi-Flow-E1	13				17		12			12				X		19
Tibia 017.002_Organic-E1	13	28,32	9,11	12	17,18	6,9	11,12	9,11		12,16	14,20	11	15,17	X,Y	11,12	19,20
Tibia 018.001_Hi-Flow-E1	13	28	11		17,18	6	11,12	9,11		14,20	11	15,17		X,Y	11,12	19,20
Tibia 018.001_Hi-Flow-E2	13				17	6,9	11			12	11				11,12	
Tibia 018.002_AFDIL-E1	13	28,32			17,18	6,9	11,12	9,11		14,20	11			X,Y	11,12	19
Consensus STR Profile	13,13	28,32	9,11		17,18	6,9	11,12	9,11		12,16	14,20		15,17	X,Y	11,12	19,20

Table 27: STR typing results for 120-year-old historical skeletal remains

Table 28 and Figure 23A show DOP-PCR results using 489pg of input template DNA from these remains. A higher quantity of DNA (e.g., 1ng) would have been preferable, but sufficient volume of extract was not available to carry out the comparison DOP-PCR reactions using each of the three modified primers. Using 1ng of input template likely would have further improved the STR typing results. However, even when less than 1ng was used for the DOP-PCR reaction, the RFU values at most loci increased and several alleles that had previously dropped out of the profile were recovered. More importantly, the majority of the alleles that were recovered as a result of DOP-PCR were consistent with the alleles in the compiled consensus profile (see Table 27 and Figures 23B-23D).

	D8S1179	D21S11	D7S820	CSF1PO	D3S1358	TH01	D13S317	D16S539								
120-year-old Skeletal Remains: Consensus STR Profile	13	28	32	9	11	9	12	17	18	6	9	11	12	9	11	
Femur 005.001 AFDIL-E1 (No WGA)	746	78							440	346	77					
10N dcDOP primer	1944	224	422		328				1090	1950	886	627	880	681	475	225
12N abDOP primer	854	245	500	99	252		91	2748	2539	1690	689	649	318	474	237	
12N(2) abDOP primer	1212	613	276	115	333			943	792	133	460	208	321	577	349	

	D2S1338	D19S433	vWA	TPOX	D18S51	Amel	D5S818	FGA								
120-year-old Skeletal Remains: Consensus STR Profile		12	16	14	20	8	11	15	17	X	Y	11	12	19	20	
Femur 005.001 AFDIL-E1 (No WGA)					191		252			460	631	212	137			
10N dcDOP primer			1198	338		147		462		454	1800	1117	680	493	117	266
12N abDOP primer			776	362	744	461		305	148	166	1022	1998	683	675	268	362
12N(2) abDOP primer			526	108	516	338		608		86	1356	968	392	508	85	112

Table 28: DOP-PCR WGA of degraded DNA from 120-year-old historical human skeletal remains (femur): Comparison of RFU peak heights obtained with the 10N dcDOP primer, 12N abDOP primer, and 12N(2) abDOP primer. Amount of DNA added to DOP-PCR reaction was 489pg. Numbers in red represent original RFU values prior to subjecting the sample to DOP-PCR.

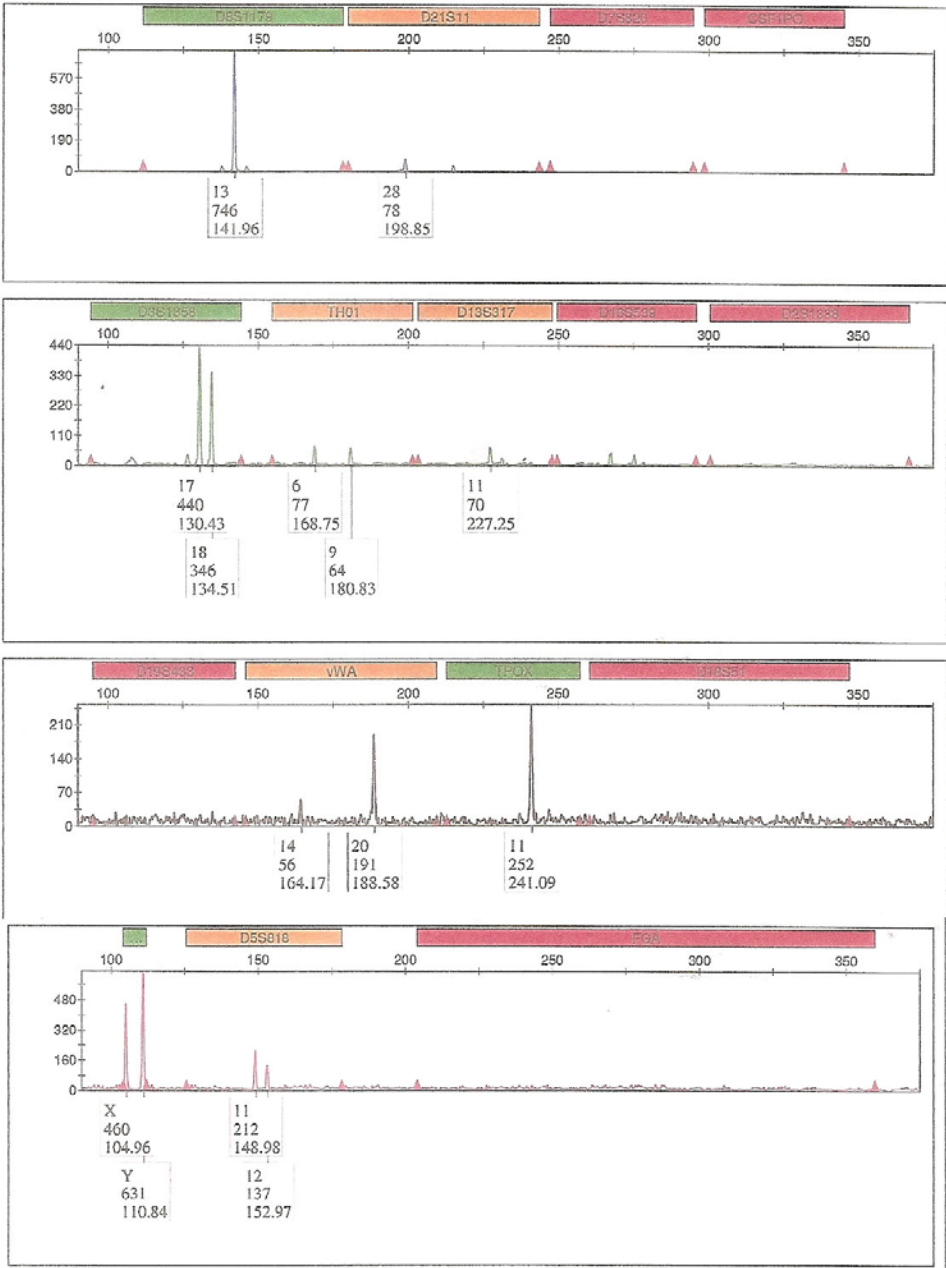


Figure 23A: STR typing results for degraded DNA from 120-year-old historical human skeletal remains (femur) prior to DOP-PCR, with 489pg of input DNA (Table 28).

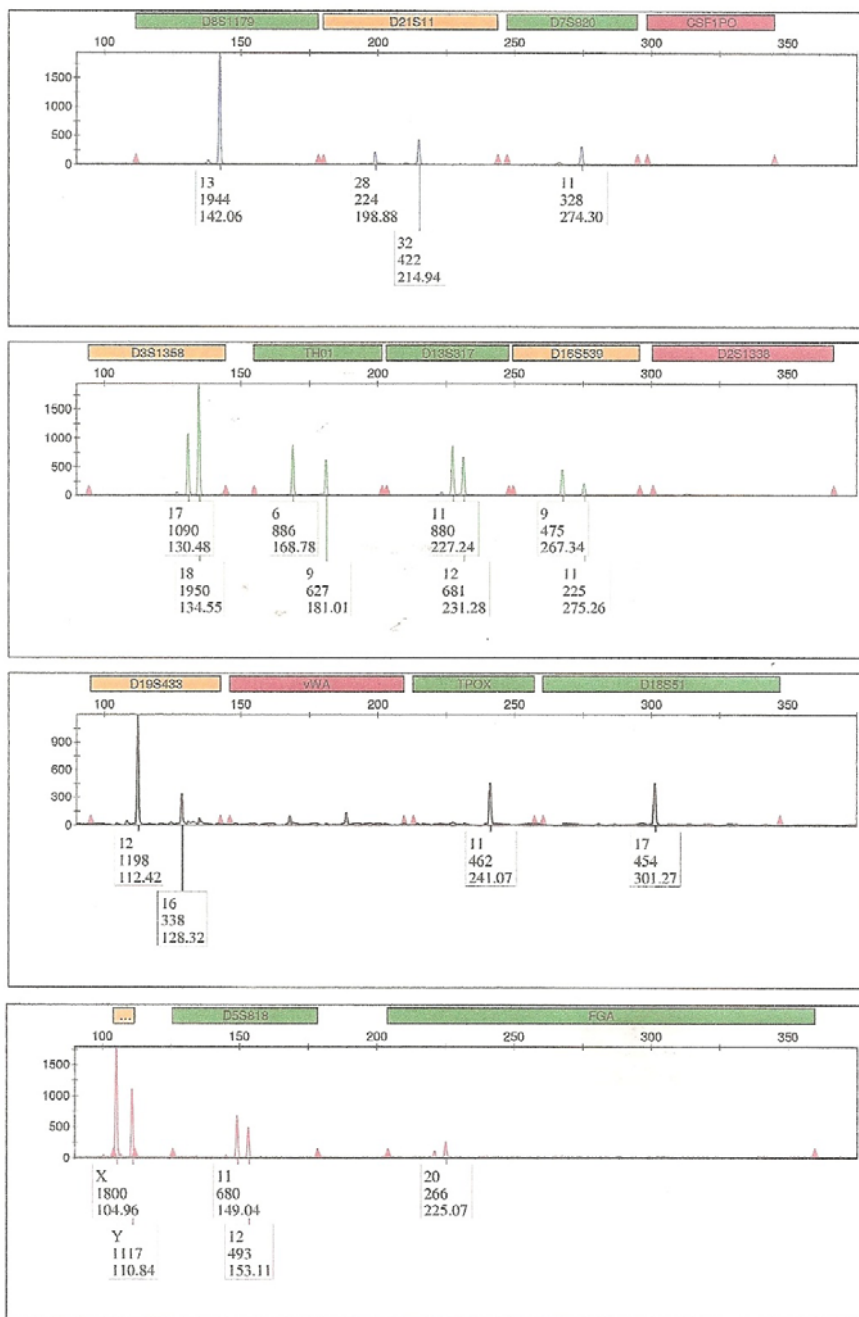


Figure 23B: Electropherogram results for DOP-PCR WGA of degraded DNA from 120-year-old historical human skeletal remains (femur) with the **10N dcDOP primer**. Amount of DNA added to DOP-PCR reaction was 489pg. No artifact peaks were observed, and recovered alleles were consistent with the previously-constructed consensus profile (Table 27).

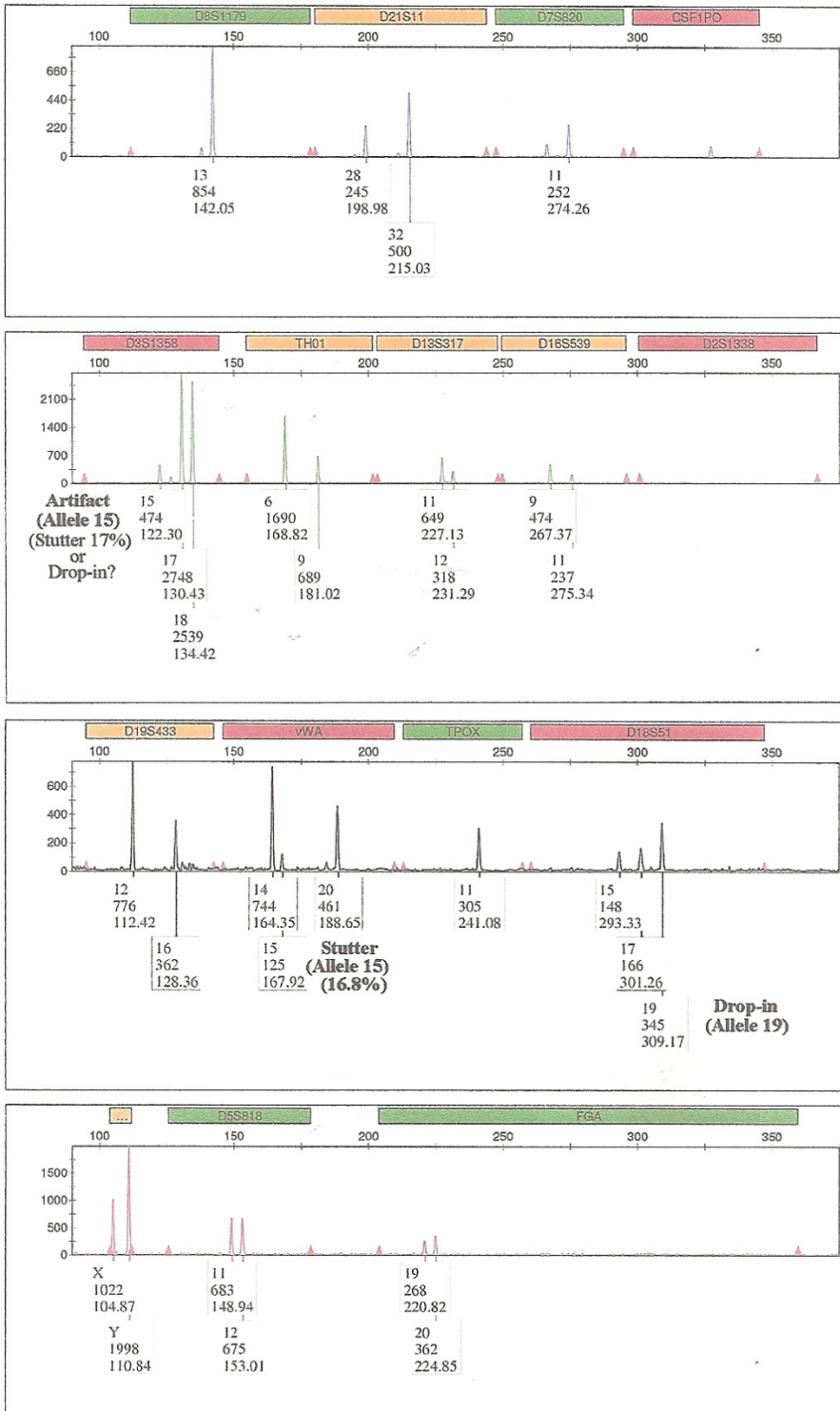


Figure 23C: Electropherogram results for DOP-PCR of degraded DNA from 120-year-old historical human skeletal remains (femur) with the 12N abDOP primer. Amount of DNA added to DOP-PCR reaction was 489pg. A few artifact peaks were observed, including a drop-in allele (allele 19) at the D18S51 locus that had not previously been observed in any of the 50 samples used to construct the consensus profile (Table 27).

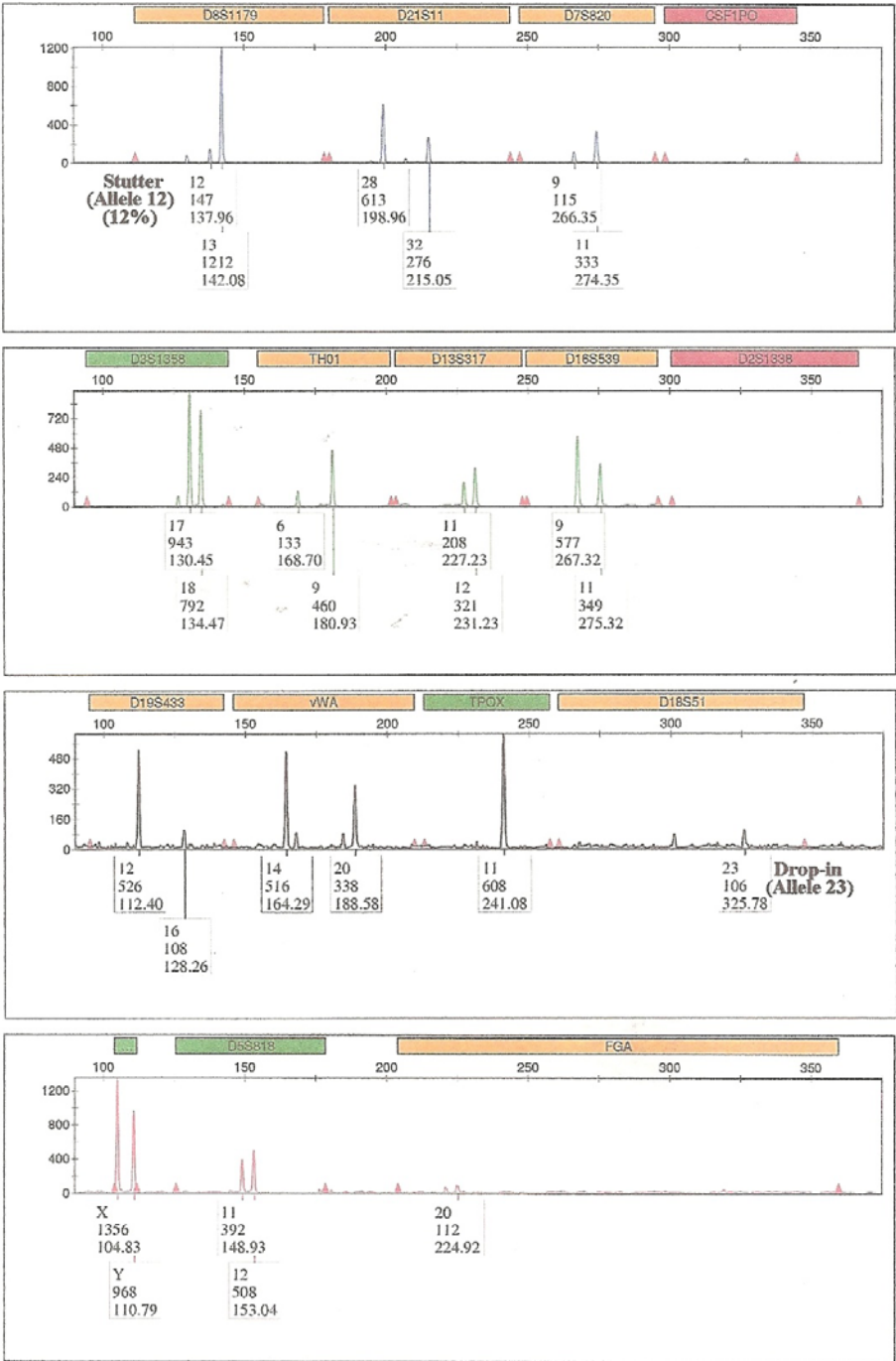


Figure 23D: Electropherogram results for DOP-PCR of degraded DNA from 120-year-old historical human skeletal remains (femur) with **the12N(2) abDOP primer**. Amount of DNA added to DOP-PCR reaction was 489pg. A few artifact peaks were observed, including a drop-in allele (allele 23) at the D18S51 locus that had not previously been observed in any of the 50 samples used to generate the consensus profile (Table 27).

Table 29 (below) depicts DOP-PCR results of another 120-year-old historical bone (tibia). As was mentioned previously with the sample described in Table 28, a higher quantity of input template DNA (e.g. 1ng) would have been preferable, but sufficient volume of extract was not available to carry out the comparison DOP-PCR reactions using each of the three modified primers. Again, using 1ng of input template likely would have further improved the STR typing results. However, even when less than 1ng was used for the DOP-PCR reaction, the RFU values at most loci increased and several alleles that had previously dropped out of the profile were recovered (similar to the results with the femur sample in Table 28). Once again, the majority of the alleles that were recovered as a result of DOP-PCR were consistent with the alleles in the compiled consensus profile (electropherograms not shown).

	D8S1179	D21S11	D7S820	CSF1PO	D3S1358	TH01	D13S317	D16S539							
120-year-old Skeletal Remains: Consensus STR Profile	13	28	32	9	11	9	12	17	18	6	9	11	12	9	11
Tibia 018.002 AFDIL-E1 (No WGA)	723	231	89					449	200	89	92	138	180	87	178
10N dcDOP primer	1433	344		103	199			801		590	383	673	433		
12N abdOP primer	2275	142	122	119	127			781	700	547	532		242	725	341
12N(2) abdOP primer	1568	218	209	399	99			755	498	336	293	353			146

	D2S1338	D19S433	VWA	TPOX	D18S51	Amel	D5S818	FGA								
120-year-old Skeletal Remains: Consensus STR Profile		12	16	14	20	8	11	15	17	X	Y	11	12	19	20	
Tibia 018.002 AFDIL-E1 (No WGA)				172	192		88			567	333	110	170	181		
10N dcDOP primer			365		441	188		979		214	1380	225	250	351	387	462
12N abdOP primer			158		443	162		501		341	1303	810	432	415	286	263
12N(2) abdOP primer			128	170	548	252		372		271	1630	1448	403	320	221	120

Table 29: DOP-PCR WGA of degraded DNA from 120-year-old historical skeletal remains (tibia): Comparison of RFU peak heights obtained with the 10N dcDOP primer, 12N abdOP primer, and 12N(2) abdOP primer. Amount of DNA added to DOP-PCR reaction was 519 pg. Numbers in red represent original RFU values prior to subjecting the sample to DOP-PCR.

DOP-PCR: Implications for Forensic Casework

The redesign of DOP-PCR primers was hypothesized to improve typing success of degraded DNA and the data support that prediction. The original primer (and 10N dcDOP primer) contained a restriction site because cloning of fragments was desired in the original study. Thus, the restriction site in itself does not contribute to the amplification success and can be removed. If removed, then there is more flexibility in primer design. In addition, the original primer (i.e. 3' end of the primer) design will identify on average a site in the genome approximately every 4000 bases. Thus, the original primer could be effective for relatively intact DNA; however, forensic samples may be degraded and such long fragments may not be available for DOP-PCR. The newly designed primers are designed to sit on average approximately every 256 bases and thus could amplify shorter fragments.

The methods employed in the studies herein increased the sensitivity of detection of DNA typing. However, as with any samples with low amounts of template DNA that are subjected to increased sensitivity of detection analyses, exaggerated stochastic effects were observed. These effects manifested as heterozygote allele peak height imbalance, allele dropout, and increased stutter. Also, allele drop-in was observed. These properties are inherent in low template or LCN typing assays and are not novel observations. Thus no new artifacts were observed. Such effects, however, will impact the ability to interpret results and apply reliable statistical assessments. They are random and may not be observed consistently from multiple aliquots of the same sample with the levels of DNA and sampling variance inherent in such systems. Statistical models that incorporate uncertain events (e.g., peak area/height, drop-in, dropout, stutter etc.) have been proposed to assess the probability of observed results (for example see 46). Studies to quantify the uncertain events effectively are needed to employ a statistical model.

IV. Conclusions

Forensic samples can experience destructive taphonomic conditions, and thus have often endured extensive microbial and environmental insults. Consequently, the DNA in these environmentally-damaged samples frequently contains multiple complex lesions and may be highly fragmented. Previous studies on repairing DNA focused primarily on damaging extracted or naked DNA. We focused on damaging DNA in its native state. To do so entailed extensive studies on conditions to damage DNA while it is still complexed with other cellular molecules. Conditions are described in this report on how to damage such DNA and these can serve as a guide for others who desire to study DNA damage and repair.

The PreCR™ Repair Mix appeared to be challenged by myriad states of DNA damage that may be encountered in forensically-relevant samples. Considering that the amount of sample available in forensic cases is often limited, using 10-20µl of this valuable extract for PreCR™ repair seems to be premature for casework applications, given the assay's varied results. However, additional strategies do exist for potentially improving STR profiles of degraded and/or low-copy templates. Our assessment is that the unpredictable and variable results obtained in our PreCR™ DNA repair experiments indicate that it is more prudent to focus on amplifying existing *intact* template in low-copy or degraded samples as opposed to trying to repair damage.

We were successful in using a modified DOP-PCR to improve STR profiling of damaged DNA from environmentally-exposed bloodstains and skeletal remains. Rather than a prior recommendation not to exceed 100pg of input DNA (23) because of observed excessive artifacts, our results, with different primer design, indicated that up to 1ng of template can be added without production of excessive artifacts in the resultant electropherograms (especially when the candidate samples are severely degraded and have previously produced very low-RFU peak heights or partial profiles). However, the same stochastic and contamination effects observed with LCN typing were observed in the amplified samples. Future investigations might involve comparing results obtained from these DOP-PCR studies to a 2008 Cold Spring Harbor protocol (which involves “re-charging” the low-stringency PCR product with additional reagents before proceeding with high-stringency thermal cycling). It has been purported that addition of a newly-prepared master mix of PCR reagents to the low-stringency WGA product is necessary to provide sufficient resources for subsequent high-stringency cycles (i.e., because some of these reagents may have been depleted/exhausted during the first 5 cycles, thereby limiting the amount of product that can be produced in the second phase of DOP-PCR) (20).

Another potential strategy that could help mitigate and account for the stochastic effects observed in DOP-PCR of degraded and LCN templates is to perform independent replicate amplifications of each sample. Performing replicate DOP-PCR reactions could assist in the generation of a consensus STR genotype, and would help compensate and account for alleles that may drop in or out of the profile. This recommendation, however, assumes that sufficient template/extract is available for replicate DOP-PCR reactions. Lastly, large sample studies will be needed to estimate, if feasible, the rates of drop-in, dropout, and increased stutter if a statistical model is to be applied to WGA treated samples.

In late 2012, Zong et al (60) described a novel WGA method termed Multiple Annealing and Looping-Based Amplification Cycles (MALBAC). The methodology is based on quasi-linear preamplification to reduce the bias often associated with nonlinear amplification. Their results with MALBAC demonstrate successful amplification of picogram quantities of DNA. However, DNA fragment sizes in the 10-100kb in size are required as starting templates for MALBAC reaction (60). Since these fragment sizes are substantially larger than those typically encountered in degraded samples, MALBAC is not likely a candidate for use in forensic casework. But the fact that it showed promise for minute quantities of DNA may suggest some specialized applications.

V. References

1. Hall, A. and J. Ballantyne (2004). Characterization of UVC-induced DNA damage in bloodstains: forensic implications. *Anal Bioanal Chem* 380(1): 72-83.
2. Nelson, J. (2009). *Repair of Damaged DNA for Forensic Analysis*. National Institute of Justice.
3. Marrone, A. and J. Ballantyne (2009). Changes in dry state hemoglobin over time do not increase the potential for oxidative DNA damage in dried blood. *PLoS One* 4(4): e5110.
4. Diegoli et al. (2012). An optimized protocol for forensic application of the PreCR Repair Mix to multiplex STR amplification of UV-damaged DNA. *Forensic Science International* 6(4):498-503.
5. Foran, D. R. (2006). Relative degradation of nuclear and mitochondrial DNA: an experimental approach. *Journal of Forensic Science* 51(4): 766-770.
6. CYRO (2001). Technical Data Acrylite OP-4 Acrylic Sheet. Parsippany, NJ, CYRO Industries.
7. Kemp B.M. and D.G. Smith (2005). Use of bleach to eliminate contaminating DNA from the surface of bones and teeth. *Forensic Science International* 154(1):53-61.
8. Mello Filho, A. C., M. E. Hoffmann, et al. (1984). Cell killing and DNA damage by hydrogen peroxide are mediated by intracellular iron. *Biochem J* 218(1): 273-275.
9. Tuchinda et al. (2006). Photoprotection by window glass, automobile glass, and sunglasses. *Journal of American Academy of Dermatology* 54(5):845-854.
10. Loreille et al. (2010). Integrated DNA and fingerprint analyses in the identification of 60-year-old mummified human remains discovered in an Alaskan glacier. *Journal of Forensic Science* 55(3):813-818.
11. McKenzie, S.B. and J.L. Williams (2010). Clinical Laboratory Hematology, Second Edition (Elizabeth Zeibig, Ed.). New Jersey: Pearson Education, Inc.
12. Telenius et al. (1992). Degenerate oligonucleotide-primed PCR: General amplification of target DNA by a single degenerate primer. *Genomics* 13:718-725.
13. Cheung, V.G. and S.F. Nelson (1996). Whole genome amplification using a degenerate oligonucleotide primer allows hundreds of genotypes to be performed on less than one nanogram of genomic DNA. *Proceedings of the National Academy of Sciences USA* 93:14676-14679.

14. Esteban, J.A. et al. (1993). Fidelity of ϕ 29 DNA polymerase. *Journal of Biological Chemistry* 268:2719-2726.
15. Nelson, J.R. et al. (2002). Establishment of an error rate of only 3×10^{-6} for the MDA reaction. *BioTechniques* Supplement: 44-47.
16. Dean, F.B. et al. (2002). Demonstration of low amplification bias of MDA compared with other WGA methods. *Proceedings of the National Academy of Sciences USA* 99:5261-5266.
17. Hughes et al. (2005). The use of whole genome amplification in the study of human disease. *Progress in Biophysics and Molecular Biology* 88:173-189.
18. Struan et al. (2002). SNP genotyping on a genome-wide amplified DOP-PCR template. *Nucleic Acids Research* 30(22):e125.
19. Kiss et al. (2002). Optimisation of the degenerate oligonucleotide primed PCR (DOP-PCR) for capillary thermocycler. *Biomolecular Engineering* 19:31-34.
20. Arneson et al. (2008). Whole genome amplification by degenerate oligonucleotide primed PCR (DOP-PCR). *Cold Spring Harbor Protocols* 3(1):1-5.
21. Hughes, S. and R. Lasken (2005). Whole Genome Amplification. Oxfordshire, England: Scion Publishing Ltd.
22. Bonnette et al. (2009). dcDegenerate oligonucleotide primed PCR for multilocus, genome-wide analysis from limited quantities of DNA. *Diag Mol Pathol* 18(3):165-175.
23. Dawson Cruz, T. (2009). *Development and optimization of a whole genome amplification method for accurate multiplex STR genotyping of compromised forensic casework samples*. National Institute of Justice.
24. Zheng et al. (2011). Whole genome amplification in preimplantation genetic diagnosis. *Journal of Biomedicine and Biotechnology* 12(1):1-11.
25. Williams, G. (2011). Forensic applications of whole genome amplification. *International Journal of Criminal Investigation* 1(3):123-135.
26. Westen AA, Nagel JH, Benschop CC, Weiler NE, de Jong BJ, Sijen T. Higher capillary electrophoresis injection settings as an efficient approach to increase the sensitivity of STR typing. *J Forensic Sci.* 2009 54(3):591-8.
27. Church and Dwight Product Ingredient Disclosure for OxiClean® Free Triple Power Stain Fighter (Product Code: ING-1608). <http://www.armandhammer.com>
28. PreCR™ Repair Mix Product Information. <https://www.neb.com>

29. Miyakoshi, J. and M.Yoshuda (2000). Exposure to strong magnetic field at power frequency potentiates X-ray-induced DNA strand breaks. *Journal of Radiation Research* 41: 293-302.
30. Geacintov, N.E. and S. Broyde (2010). The Chemical Biology of DNA Damage. Weinhein, Germany: Wiley-VCH Publishing.
31. Valko et al. (2007). Free radicals and antioxidants in normal physiological functions and human disease. *International Journal of Biochemistry and Cell Biology* 39:44-84.
32. Shafirovich, V. and N.E. Geacintov (2010). "Role of free radical reactions in the formation of DNA damage." In The Chemical Biology of DNA Damage. Weinhein, Germany: Wiley-VCH Publishing:81-104.
33. Onori et al. (2006). Post-mortem DNA damage: A comparative study of STRs and SNPs typing efficiency in simulated forensic samples. *International Congress Series* 1288:510-512.
34. Jun, S. (2010). DNA chemical damage and its detection. *International Journal of Chemistry* 2(2):261-265.
35. Lindahl, T. and B. Nyberg (1972). Rate of depurination of native deoxyribonucleic acid. *Biochemistry* 11:3610-3618.
36. Friedberg et al. (2006). DNA Repair and Mutagenesis. Washington D.C.: ASM Press.
37. De Gruijl, F. and H. Rebel (2008). Early events in UV carcinogenesis: DNA damage, target cells, and mutant p53 foci. *Journal of Photochemistry and Photobiology* 84:382-387.
38. Golenberg et al. (1996). Effect of highly fragmented DNA on PCR. *Nucleic Acids Research* 24(24):5026-5033.
39. Yang, W. (2008). Structure and mechanism for DNA lesion recognition. *Cell Research* 18:184-197.
40. Lindahl, T. (1993). Instability and decay of the primary structure of DNA. *Nature* 362:709-715.
41. Hitomi et al. (2007). The intricate structural chemistry of base excision repair machinery: Implications for DNA damage recognition, removal, and repair. *DNA Repair* 6:410-428.
42. Gillet, L.C. and O.D. Scharer (2006). Molecular mechanisms of mammalian global genome nucleotide excision repair. *Chem Rev* 106:253-276.

43. Cadet et al. (2005). Ultraviolet radiation-mediated damage to cellular DNA. *Mutation Research* 571:3-17.
44. Cooke et al. (2003). Oxidative DNA damage: mechanisms, mutation, and disease. *The FASEB Journal* 17:1195-1214.
45. Sedgwick, B. (2004). Repairing DNA-methylation damage. *National Review of Molecular Cell Biology* 5:148-157.
46. Balding D.J., and J. Buckleton (2009). Interpreting low template DNA profiles. *Forensic Science International Genetics* 4:1-10.
47. Prince, A.M. and L. Andrus (1992). PCR: How to kill unwanted DNA. *Biotechniques* 12:358-360.
48. Kwok, S. and R. Higuchi (1989). Avoiding false positives with PCR. *Nature* 339:237-238.
49. Tamariz et al. (2006). The application of ultraviolet irradiation to exogenous sources of DNA in plasticware and water for the amplification of low copy number DNA. *Journal of Forensic Sciences* 51:790-794.
50. Lasken, R.S. and M. Egholm (2003). Whole genome amplification: Abundant supplies of DNA from precious samples or clinical specimens. *Trends in Biotechnology* 21:531-535.
51. Biological effects of radiation: Direct and Indirect Action of Ionizing Radiation on DNA. http://curriculum.cna.ca/curriculum/cna_bio_effects_rad/direct_indirect_eng.asp?bc=Direct and Indirect Action of Ionizing Radiation on DNA&pid=Direct and Indirect Action of Ionizing Radiation on DNA
52. dSpacer (abasic furan) oligo modification from Gene Link. http://www.genelink.com/newsite/products/mod_detail.asp?modid=28
53. Hurley, L.H. (2002). DNA and its associated processes as targets for cancer therapy. *Nature Reviews Cancer* 2:188-200.
54. Mutation mechanisms. <http://www.web-books.com/MoBio/Free/Ch7F.htm>
55. Margolin et al. (2006). Paradoxical hotspots for guanine oxidation by a chemical mediator of inflammation, *Nature Chemical Biology* 2:365-366.
56. Kremer, M.L. (2003). The Fenton reaction: Dependence of the rate on pH. *Journal of Physical Chemistry* 107(11): 1734-1741.

57. Jung et al. (2009). Effect of pH on Fenton and Fenton-like oxidation. *Environmental Technology* **30**(2): 183-190.
58. Luo, Y., Henle, E.S., and S. Linn (1996). Oxidative damage to DNA constituents by iron-mediated Fenton reactions. *Journal of Biological Chemistry* **271**: 21167-21176.
59. Quantifiler® Kits User Manual (2012).
http://tools.invitrogen.com/content/sfs/manuals/cms_041395.pdf
60. Zong, C., Lu, S., Chapman, A.R., and X.S. Xie (2012). Genome-wide detection of single nucleotide and copy number variations of a single human cell. *Science* **338**(6114): 1622-1626.

VI. Dissemination of Research Findings

Presentations

Promega 22nd International Symposium on Human Identification

October 2011 (National Harbor, MD)

- Poster presentation: “Assessing the Role of DNA Repair in Forensically Revelant Samples.” A.Ambers, R.Benjamin, M.Turnbough, and B.Budowle

National Institute of Justice (NIJ) Annual Conference

June 2012 (Arlington, VA)

- Poster presentation: “Assessing the Role of DNA Repair in Forensically Revelant Samples.” A.Ambers, R.Benjamin, M.Turnbough, and B.Budowle

Promega 23rd International Symposium on Human Identification

October 2012 (Nashville, TN)

- Poster presentation: “Assessing the Role of DNA Repair and Whole Genome Amplification (WGA) in Forensically Revelant Samples.” A.Ambers, R.Benjamin, M.Turnbough, and B.Budowle

American Academy of Forensic Sciences (AAFS) 65th Annual Scientific Meeting

NIJ Grantees Meeting, February 2013 (Washington D.C.)

- Oral presentation: “Assessing the Role of DNA Repair and Whole Genome Amplification (WGA) in Forensically Relevant Samples.” A.Ambers and B.Budowle

American Academy of Forensic Sciences (AAFS)

NIJ Grantees Live Webinar: Current Forensic Research Seminar Series

“Tarnished Gold Standard: Limited Quantity and Degraded DNA, Part I”

(Three separate webinars: May 7, 14, and 16, 2013)

- Webinar oral presentation: “Addressing Quality and Quantity: the Role of DNA Repair and Whole Genome Amplification (WGA) in Forensically Relevant Samples.” A.Ambers and B.Budowle

Publications

Manuscripts covering the following topics are in progress

- “Assessment of the Role of DNA Repair in Forensically Relevant Samples”
- “Improved DOP-PCR for Amplification of Degraded DNA in Environmentally-damaged bloodstains and Human Skeletal Remains”

VII. Participating Scientists and Collaborations

Scientists

Bruce Budowle, Ph.D. (grant PI)
Director, Institute of Applied Genetics
Dept. of Forensic and Investigative Genetics
University of North Texas Health Science Center
Fort Worth, Texas

Angie Ambers, M.A., M.S.
Institute of Applied Genetics
Dept. of Forensic and Investigative Genetics
University of North Texas Health Science Center
Fort Worth, Texas

Jonathan L. King
Institute of Applied Genetics
University of North Texas Health Science Center
Fort Worth, Texas

Collaborators

Harrell Gill-King, Ph.D.
Laboratory of Forensic Anthropology
Dept. of Biological Sciences
University of North Texas
Denton, Texas

Dennis Dirkmaat, Ph.D.
Mercyhurst Archaeological Institute
Dept. of Applied Forensic Sciences
Mercyhurst College
Erie, Pennsylvania

Robert C. Benjamin, Ph.D.
Associate Professor
Department of Biological Sciences
University of North Texas
Denton, Texas

Generon Ltd.
12 Rawcliffe House, Howarth Rd.
Maidenhead
Berkshire, U.K.

Meredith Turnbough, Ph.D.
Assistant Research Professor
Department of Biology
Arizona State University
Phoenix, Arizona